

KRATKA NAVODILA

SHORT INSTRUCTION

Celotna doktorska disertacija, vključno s prilogami, naj ne bi obsegala več kot 200 strani.

Vsako glavno poglavje se mora pričeti na lihi strani.

Poglavja si morajo slediti v zaporedju, predpisanem s predlogo.

V kolikor so v delo vključeni algoritmi in/ali slike in/ali tabele, so kazala zanje obvezna.

Pri navajanju virov in literature je potrebno upoštevati pravila, opisana v dokumentu Navajanje virov.doc.

V prilogi je obvezno naštet lastne objave iz disertacije.

Complete doctoral dissertation including appendices should not exceed 200 pages.

Each main chapter should begin on an odd page.

The chapters should follow as prescribed in the template.

When the work contains algorithms and/or figures and/or tables their indexes are obligatory.

The references should consider the rules as described in the document Citation style.doc.

Publications of the candidate from the dissertation must be listed in appendix.

NE BRIŠI

DON'T DELETE

AGRON MILLAKU

**EFFECT OF INGESTED NANOFIBERS AND
NANOPARTICLES ON DIGESTIVE GLAND
EPITHELIUM OF A MODEL TEST ORGANISM**

Doctoral Dissertation

**UČINEK ZAUŽITIH NANOVLAKEN IN
NANODELCEV NA EPITELIJ PREBAVNEGA
SISTEMA PRESKUSNEGA ORGANIZMA**

Doktorska disertacija

Supervisor: Matjaz Torkar, Assist. Prof. Dr

Co-Supervisor: Damjana Drobne, Prof. Dr

2010

MEDNARODNA PODIPLOMSKA ŠOLA JOŽEFA STEFANA
JOŽEF STEFAN INTERNATIONAL POSTGRADUATE SCHOOL
Ljubljana, Slovenia



Index (Format: Table of Contents)

Abstract	VII
Povzetek	IX
Abbreviations	XI
1 Introduction	1
1.1 General information.....	1
1.1.1. Nanomaterials.....	1
1.1.2 Nanomaterials and application	2
1.1.3 Nanomaterials and environment.....	3
1.1.3.1 Test of effect of nanomaterials.....	5
1.1.3.2 Research of potential effects.....	6
2 Aims and Hypothesis	7
3 Materials and Methods	9
3.1 Materials.....	9
3.1.1 Test organism.....	9
3.1.2 Food preparation.....	10
3.1.3 Experiment design.....	10
3.1.4 Nanofibers and nanoparticle tested.....	11
3.2 Method.....	13
3.2.1. Biological sample prepared for SEM.....	13
3.2.1.1 Fixation.....	13
3.2.1.2 Glutaraldehyde.....	14
3.2.1.3 Formaldehyde.....	14
3.2.1.4 Osmium tetroxide.....	14
3.2.1.5 Acetone.....	14
3.2.1.6 Critical point dry.....	14
3.2.1.7 Sputter coating.....	15
3.2.2 SEM investigates.....	15
3.2.2.1 SEM (Field Emission Scanning Electron Microscopy JEOL-JMS-6500 F).....	15
3.2.3 Samples preparation.....	16
3.2.4 Chemical analyze.....	23
4 Results	25
5 Discusion	25
6 Conclusions	83
7 Acknowledgements	84

8 References	85
Index of Figures	89
Index of Tables	92
Appendix 1: Publications	93
Appendix 2: Personal bibliography from the period 2008-2010	93

Abstract

Engineered nanofibers and nanoparticles are recognized as capable of inducing cellular perturbations according to the oxidative stress paradigm or by interacting directly with biological membranes. A number of authors in their investigations with the nanofibres and nanoparticles has reported the ability of nanofibers and nanoparticle to cause the different damage on the structure and function of the cells, tissues and organisms. The cell membrane, mitochondria and cell nucleus are considered as major cell compartments relevant for possible nanoparticle-induced toxicity. When nanofibers and nanoparticles interact with cell membranes, they cause defects such as physical disruptions, formation of holes and thinned regions. It was reported that cationic nano-objects pass through cell membranes by generating transient holes, a process undoubtedly associated with cytotoxicity. It is known that a range of nanofibres and nanoparticle affects in *in vitro* exposed systems the phagocytic ability of the cells.

Examples include the cytotoxicity to rat lung alveolar macrophages, human dermal fibroblast and human lung carcinoma cells, hepatic injury in mice, pathologic changes of gills in fish, decreasing of production and activity in some enzymes such as catalaza and glutathione-S- transferaza etc.

In many articles was proved that nanofibers and nanoparticle can negative impact to cells, tissues and organisms. Some of the effects were observed also in the aquatics environments.

The aim of this study was to test the effect of nanofibres and nanoparticles, ingested with food on test organism. After the study we will be able to answer in some questions:

- a) Do ingested nanofibers or nanoparticle cause morphological defaces of gland cell epithelium cells like: shape changes of cells, changes of the cells size, loss of microvilli, loss of lipid droplets etc:
- b) After how long these interactions will be detected, which is the minimal dose and exposed time that can affects in the cells morphology or in the digestive system.

For this study we used the *Porcellio scaber Latreille*,(1809, Isopoda, Crustaceae) as a test organism. Terrestrial isopods were already used in testing effects of ingested nanofibers and nanoparticles in many researches.

The animals were collected from the different unpolluted areas near Ljubljana city. Animals were collected in gardens under concrete blocks, pieces of decaying wood, and other organic wastes. The animals from each location were kept in separate glass tanks containing soil and leaf litter from their natural environment and at high relative humidity for the acclimatization.

The hepatopancreas of control and exposed group of animals after the dissection were prepared for SEM by the standard protocol for biological samples. Biological samples prepared for SEM need to be fixed and dried because of the high vacuum in the specimen chamber; they need to be additionally covered by gold conductive nanolayer to ensure good contrast of the images. Due to very high resolution of FEG-SEM it is expected that possible morphological changes in cell structures caused by nanofibres and nanoparticles will be observed and explained. A Field Emission Gun Scanning Electron Microscope (FEG-SEM) provides high spatial resolution and can operate at low accelerating voltage which makes it indispensable for biological examination.

Data obtained from the experiment with nanofibers have shown that nanofibers interact with digestive gland epithelial cells. They can cause a different changes in the structure of the surface epithelium such are: interaction with the membranes, penetration in the cells, makes a hole ect. Data obtained from the experiment with nanoparticles have shown that nanoparticles have caused morphological changes on surface microvilli of cells.

Studying the interaction between nanofibres and nanoparticles with cells in *in vivo* experiment could significantly contribute to the science and understanding of bio-nano interactions. Allso the dose and the

time of exposed will be very significant to certain the limit value of this material in some products. This knowledge will contribute to assess the safety aspect of nanomaterials and use of them in the human life. In this case the interactions were detected and documented. A further bio-nanointeraction studies as well as toxicity studies will be needed to be sure for the potential of nanofiber and nanoparticles to interact and cause changes in different organisms.

Povzetek

Za inženirska nanovlakna in nanodelce se predpostavlja, da lahko povzročajo celične motnje skladno s paradigmo oksidativnega stresa ali z neposredno interakcijo s celično membrano. Številni avtorji v svojih raziskavah nanovlaken in nanodelcev poročajo o zmožnostih nanovlaken in nanodelcev, da povzročajo različne poškodbe na strukturi in pri delovanju celic, tkiv in organizmov. Celične membrane, mitohondrij in celična jedra so glavna področja primerna za toksičnost, ki jo povzročijo nanodelci. Interakcija nanovlaken in nanodelcev s celičnimi membranami, povzroča poškodbe kot so telesne motnje, nastanek lukenj in stanjšana področja. Poroča se, da kationski nanodelci prehajajo skozi celične membrane s povzročanjem prehodnih odprtin, to je process, ki je nedvomno povezan s citotoksičnostjo. Poznano je, da določena nanovlakna in nanodelci vplivajo na fagocitično sposobnost celic pri v živo izpostavljenih sistemih.

Primeri vključujejo citotoksičnost na alveolarne makrofage v pljučih podgan, fibroblastov v človeški koži, rakaste celice v človeških pljučih, poškodbe jeter pri miših, patološke spremembe v škrgah rib, zmanjšanje nastajanja in aktivnosti nekaterih encimov, kot sta katalaza in glutationskih-S-transferaz, itd.

V številnih člankih je dokazano, da nanovlakna in nanodelci lahko negativno vplivajo na celice, tkiva in organizme. Nekateri učinki so opaženi tudi v okolju vodnih športov.

Namen te študije je bil preskusiti vpliv s hrano zaužitih nanovlaken in nanodelcev na preskusne organizme. Študij naj bi dal odgovore na nekatera vprašanja:

- a) Ali zaužita nanovlakna in nanodelci lahko povzročijo morfološke spremembe epitelnih celic prebavnega sistema, kot na primer: sprememba oblike celic, sprememba velikosti celic, odsotnost microvilijev, odsotnost kapljic maščob itd.
- b) Po kakšnem času bodo te interakcije odkrite, katera sta minimalna doza in čas izpostavljenosti, ki vplivata na morfologijo celic v prebavnem sistemu.

Za te preiskave smo kot preskusni organizem uporabili *Porcellio scaber Latreille*, (1809, Isopoda, Crustaceae). Kopenski enakonožci so že bili uporabljeni v številnih raziskavah za preskus učinkov zaužitih nanovlaken in nanodelcev.

Preskusne živali so bile iz različnih še neonesnaženih delov iz okolice Ljubljane. Živali so bile zbrane v vrtovih pod kosi opeke, pod kosi razpadajočega lesa in pod drugimi organskimi odpadki. Za aklimatizacijo so bile živali iz vsake lokacije zadržane v ločenih steklenih posodah, kjer je bila zemlja in stelja iz listja iz njihovega naravnega okolja ter visoka vlažnost.

Prebavne cevi kontrolnih in izpostavljenih živali, po razkosanju, so bile pripravljene po običajnih postopkih za biološke vzorce, za SEM preiskave. Biološki vzorci, pripravljene za SEM, morajo biti fiksirani in posušeni zaradi visokega vakuuma v komori za vzorec; dodatno morajo biti prekriti s prevodnim nanoslojem iz zlata, da se zagotovi dober kontrast posnetkov. Zaradi visoke ločljivosti FEG-SEM se pričakuje, da bo mogoče opaziti in razložiti morebitne spremembe morfologije celičnih struktur, povzročenih z nanovlakni in nanodelci.

Vrstični mikroskop s Field Emission izvorom elektronov (FEG-SEM) omogoča visoko prostorsko ločljivost ter lahko deluje pri nizki pospeševalni napetosti, kar je nujno za preiskave bioloških vzorcev.

Podatki dobljeni iz preskusov z nanovlakni so pokazali, da nanovlakna učinkujejo na epitelne celice prebavnega sistema. V strukturi epitelija lahko povzročajo različne spremembe, kot so: interakcija z membrano, penetracija v celice, povzročanje lukenj itd. Podatki iz preskusov z nanodelci so pokazali, da nanodelci povzročajo morfološke spremembe površinskih mikrovilijev celic.

Študij interakcije med nanovlakni, nanodelci in celicami pri *in vivo* preskusu lahko občutno prispeva k

znanosti in razumevanju bio-nano interakcij. Za določanje mejne vsebnosti teh snovi v različnih proizvodih sta pomembna količina in čas izpostave. To znanje bo omogočilo oceno mejne vsebnosti za uporabo nanomaterialov v človeškem življenju.

V tem primeru so bili odkriti in dokumentirani medsebojni vplivi. Za ugotovitev potenciala nanovlaken in nanodelcev, njihovega učinkovanja in povzročanja sprememb v različnih organizmih, so potrebna nadaljnja proučevanja bio-nano interakcije, kot tudi preiskave toksičnosti.

Abbreviations

SEM	=	Scanning Electron Microscopy.
FEG- SEM	=	Field Emission Gun Scanning Electron Microscope
TEM	=	Transmission Electro Microscopy
AES	=	Auger electron spectroscopy
ICP-OES	=	Inductively coupled plasma optical emission spectrometry
IMT	=	Institute of Metals and Technology
JSI	=	Josef Stefan Institute
WD	=	Working distance.
SEI	=	Secondary Electron Image
EDX	=	Energy dispersive X-ray spectroscopy
EDS	=	Energy dispersive spectroscopy
OTOTO	=	Osmium Tetroxide//Thiocarbohydrazide/Osmium Tetroxide//Thiocarbohydrazide/Osmium Tetroxide
kV	=	Accelerating Voltage
X100	=	Magnification
µm	=	micrometer
nm	=	nanometer
Ps	=	Porceilo Scaber L.
K	=	Control animals
A	=	Osmium preparation
B	=	OTOTO preparation
NMs	=	Nanomaterials
CNT	=	Carbon Nano Tube
NDs	=	Nanodiamonds
MCNT	=	Multi walled Carbon nanotubes
SCNT	=	Single walled Carbon nanotubes
TDG	=	Technical guidance document on the risk assessment
EPA	=	Environmental Protection Agency (USA)
EC	=	European Community
IMT	=	Institute of Metals and Technology
WO _x	=	Different tungsten oxides
Ag	=	Silver
HMDS	=	hexamethyldisilazane
Psi	=	pound per square inch
K°	=	Kelvin scale
C°	=	Celsius scale
MEMS	=	Microelectromechanical system

1. Introduction

1.1 General introduction

1.1.1 Nanomaterials

Nanomaterials (NMs) are defined as materials that have structural features with at least one dimension of 100 nm or less, and include nanofilms and nanocoatings (<100 nm) in one dimension, nanotubes and nanowires (<100 nm) in two dimensions and NMs (<100 nm) in three dimensions (Tiede et al, 2008). Nanomaterials can be differing in size, shape, composition and origin, and they can comprise organic or inorganic, crystalline or amorphous particles. They can be found as single particles, aggregates and powders or dispersed in a matrix, over colloids, suspensions and emulsions, nanolayers and films, and coated or stabilized as fullerenes and their derivatives (Jiang et al, 2009).

Physicist Richard P. Feynman was first who talked about the concept of nanoscience in 1959 in his key lecture at the annual meeting of the American Physical Society, and the term nanotechnology was coined in 1974 by Japanese researcher Nario Taniguchi to mean »precision machining with tolerance of a micrometer or less«. It refers to engineering on the molecular and atomic levels

Nanomaterials can be classified in two main groups: (i) natural and (ii) anthropogenic. The anthropogenic NMs can be incidental and engineered.

Natural nanomaterials are those that can occur naturally and may have been in the environment for millions of years (e.g. fullerenes has been detected in geological deposits from the Cretaceous-Tertiary boundary (Becker et al, 1994) . In addition, in a melt sample from an ice core dated as being about 10,000 years old, carbon nanotubes (CNTs) and fullerenes were detected in Greenland (Murr et al, 2004). Nanodiamonds (NDs) have been also found in the Younger Dryas Boundary Sediment Layer in North America (Kennet et al, 2009) . Nanomaterials can be further separated based on their chemical composition in to carbon-containing and inorganic nanoparticle.

Anthropogenic incidental nanomaterials are produced unintentionally during many industrial processes, or a consequence of engine pollution (e.g., welding fume and diesel emission particulates are sources of incidental NMs).

Finally, engineered nanomaterials and nanostructures are produced intentionally and differ because they are fabricated from the “bottom up”. During the past decade, interest in nanomaterials has risen dramatically because of their exceptional physico-chemical properties. Nanomaterials are characterized by large surface area- to-volume ratios, with about 40– 50% of the atoms being on the surface; this results in greater reactivity, compared with bulk materials, or quantum effects. They are used in many industrial areas (e.g., materials science, personal-care products and electronics) and will provide a promising technology in many other areas as medicine, aerospace, military defence, electronic etc.

Classification of nanomaterials (NMs) for commercial purposes include metals NMs, metal-oxide nanopowders, semiconductors and alloys, carbon-based NMs (CNMs) (e.g., fullerenes) and nanorods (CNTs and nanowires). In addition, nanolayers are the subject of the most important topics within nanotechnology. Through nanoscale engineering of surfaces and layers, a vast range of functionalities and new physical effects (e.g. magnetoelectronic or optical) can be achieved. Furthermore, nanoscale design of surfaces and layers is often necessary to optimize interfaces between different material classes (e.g., compound semiconductors on silicon wafers) to obtain the special desired properties.

1.1.2 Nanomaterials and application

Nanotechnologies are technologies of the future. Nanotechnology is defined as the understanding and control of matter at dimensions of roughly 1 to 100 nm, where unique physical properties make novel applications possible (EPA). Novel properties of engineered nanoparticles offer infinite possibilities in their

application. Advantages in nanotechnology in structural engineering, electronics, optics, consumer products, alternative energy, soil and water remediation, medical uses as therapeutic, diagnostic, or drug delivery devices, are likely to significantly benefit the society and the economy.

Since the discovery of carbon nanotubes (CNTs) in 1991, the global market for CNTs reached approximately \$12 million in 2002, \$ 26.2 million in 2008 and is growing to \$ 274.05million in 2009 (Future Markets, Inc. 2010). The reach of market for nanomaterials in year 2009 is present in the figure one published by Future Market.Inc. As can be seen the main markets for these nanomaterials are semiconductors, electronics and energy. The market for carbon nanotubes (CNTs), nanofibers, fullerenes and POSS and graphene grew at an annual rate of 30% per year up to 2008. However the market slowed down due to the global recession but picked up again in the fourth quarter of 2009, driven by demand from the semiconductors, electronics and energy markets. These will continue to be the main application markets through to 2015, when the market for these nanomaterials will account for an estimated US\$ 2.912million in revenues,as is shown in figure nr.2 (Future Markets, Inc. 2010).

The area in which nanomaterials has a big application are: semiconductors and electronics, energy, automobile, environment and water, medical and biotechnology, military and defence, , aerospace and aviation, telecommunications, sporting goods and plastics.

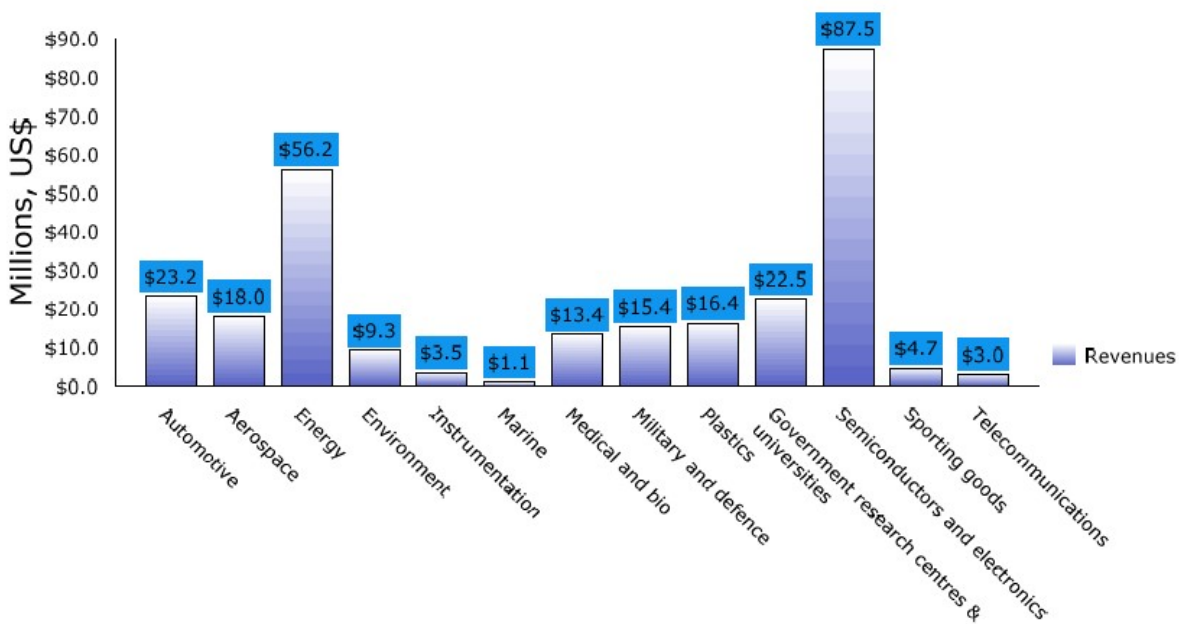


Figure 1: Main markets for carbon nanotubes, carbon nanofibers, fullerenes, POSS and graphene, by revenues, 2009. Presentetd by Future Markets Inc.

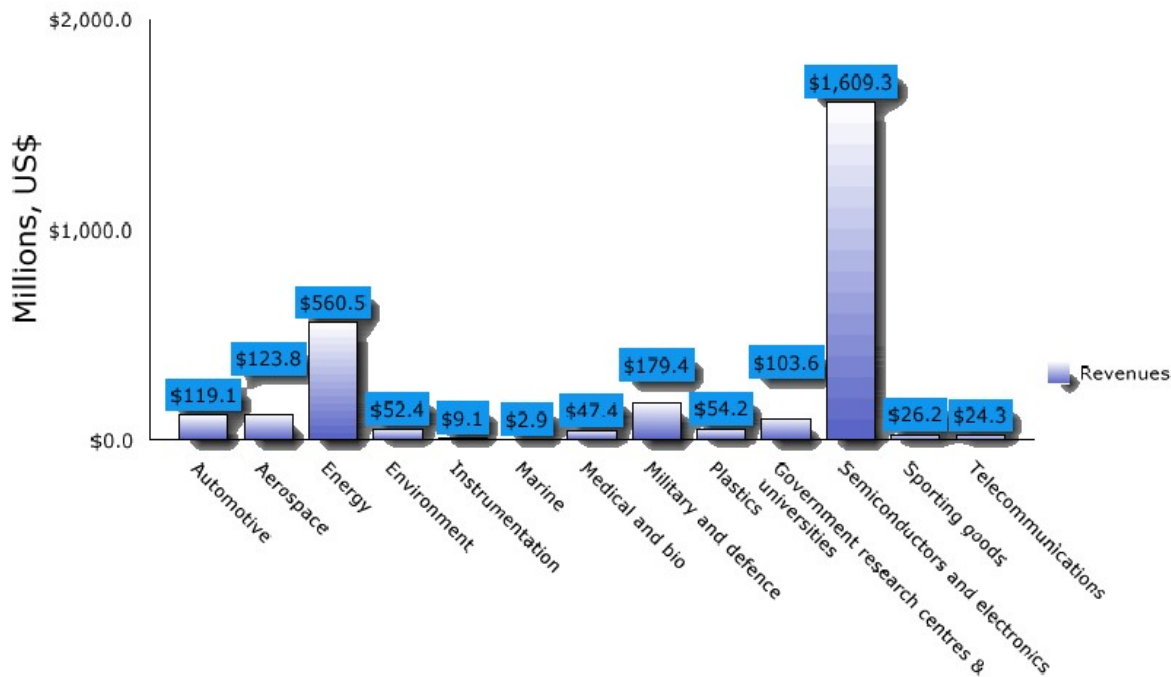


Figure 2: Main markets for carbon nanotubes, carbon nanofibers, fullerenes, POSS and graphene, by revenues, 2015. Presented by Future Markets Inc.

Main market drivers for carbon nanotubes (MCNT, SCNT) carbon nanofibers, fullerenes and POSS and graphene include the need to improve the performance and speed of semiconductors and electronics, reduce costs and increase safety in aerospace and military applications, and increase the efficiency of renewable energy devices.

Nanoparticulate matter has new characteristics but at the same time they underlie new kinds of biological effects in different levels.

1.1.3 Nanomaterials and environment

The ecotoxicity data on the effects of nanoparticles are in much need for the appropriate environmental risk assessment. Different documents already exist which deal with emerging and newly identified health risks (TGD Document, 2003; NANO Risk Framework, 2007; EPA, 2007; Scenih, 2007). Development of a hazard profile is the critical step in characterizing the potential safety of nanoparticles, and the associated health and environmental hazards. A base set of hazard data has been suggested as a reference for characterization and prioritization of nanoparticles (Warheit et al., 2007a).

To characterize nanoparticles and its potential hazards sufficiently, empirical data are necessary. Since the early days of the REACH proposals (REACH, 2006), it has been agreed by all partners that the number of animals used to gain toxicity information on chemicals should be kept to an absolute minimum. Even the nature has beginning first with producing the nanomaterial millions year ago they had played the role of protection and was not harmful for environment the nanomaterials which are produced by anthropogenic way intentional or unintentional can arrived in every natural environment and can be a serious harmful potential for different organism in different levels. The nanomaterial produced by industry, through different way can be speared in air, soil and water as is presented on the figure three (Boxall et al. 2007; Mueller et al, 2008). Nannomaterials released in to the environment submissive different external factors and processes in nature can reach to living organisms in the different ways.

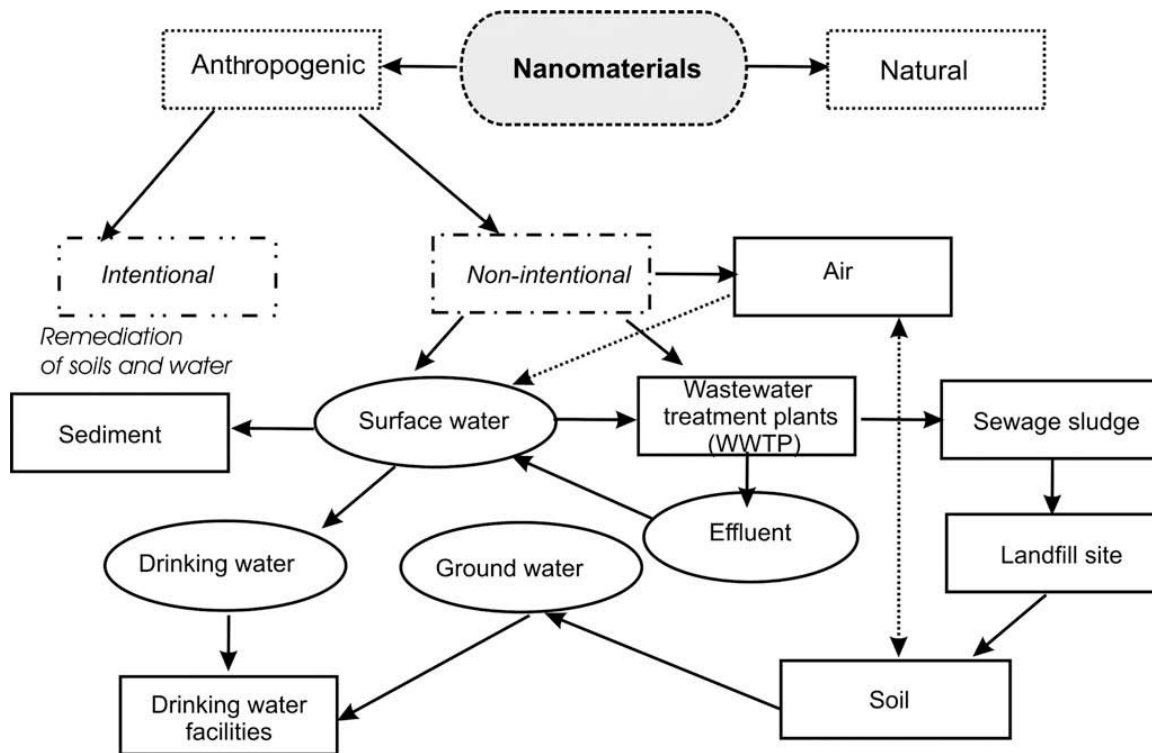


Figure 3: The fate of nanomaterials in the environment. Spreading in the environment of NMs produced in intentional or non intentional ways.

The different assessment risk studies of NMs have been done in the cellular, tissues and organism levels. Inflammation and fibrosis are effects observed on an organism level, whereas oxidative stress, antioxidant activity and cytotoxicity are observed effects on a cellular level (Oberdörster et al, 2005).

There are many studies which present the behavior and ecotoxicity NMs in the aquatic environment, including analytical methods and ecotoxicity assessment. A special attention is given to the surface properties of CNMs, which are vitally important for their aggregation behavior, their mobility in aquatic systems, their interactions with aquatic organisms, and their possible entry into the food chain (Pérze et al. 2009). Ecotoxicological studies show that NP are also toxic to aquatic organisms, both unicellular (e.g. bacteria or protozoa) and animals (e.g. Daphnia or fish). CNT induced a dose-dependent were found to be a respiratory toxicant in rainbow trout (Smith et al, 2007).

At present, research on NMs is focused on development of new NMs or their applications in different areas such are: Energy, Environment and water, Medical, Automobile, Semiconductors and electronics, Telecommunications est. However, concern has arise about the presence of NMs in the environment. For example, the US Environmental Protection Agency (EPA) and the European Community (EC) are paying attention to the study of the fate, transport, and health effects of the NMs in the environment. However, their environmental study is still in its infancy because there is a lack of analytical methods able to detect and to quantify the wide range of NMs and their unique properties. Also, NMs can be modified in the environment by the action of light, oxidants or microorganisms or can be coated with organic matter (Hyung et al.2007).

Moreover, NMs will inevitably aggregate or agglomerate into larger masses, thereby losing their nanoscale-related properties and increasing the difficulty of monitoring them in the environment. (Hyung et al.2007).

Quite a lot of information is available for nano-sized silver particles due to their use as bactericides. The cells of bacteria are damaged in the presence of nano-Ag, finally resulting in death of the organisms (Sondi and Salopek-Sondi, 2004). Nano-Ag appears to be significantly more toxic than Ag^+ -ions towards *E. coli* (Lok et al., 2006).

1.1.3.1 Test of effect of nanomaterials

Despite bright outlooks for the future of nanotechnology, there is an increasing concern that human exposure to some types of engineered nanoparticles, intentionally or unintentionally, may lead to significant adverse health effects. In addition, there is a concern of environmental contamination and associated effects on the ecosystem, which could have significant societal implications.

Engineered nanoparticles are recognized as capable of inducing cellular perturbations according to the oxidative stress paradigm or by interacting directly with biological membranes. A number of authors in their investigation reports that nanofibres and nanoparticles can cause the different damage on the structure and function of the cells and tissues. The cell membrane, mitochondria and cell nucleus are considered as major cell compartments relevant for possible nanoparticle-induced toxicity (Unfried et al. 2007). When nanoparticles interact with cell membranes, they cause defects such as physical disruptions, formation of holes and thinned regions. It was reported that cationic nano-objects pass through cell membranes by generating transient holes, a process undoubtedly associated with cytotoxicity (Verma et al. 2008). It is known that a range of nanofibres and nanotubes affects in in vitro exposure systems the phagocytic ability of the cells (Brown et al. 2007). It was reported that titanium dioxide nanoparticle can decrease the production and activity of some enzymes such as catalase and glutathione-S-transferase (Jemec et al. 2008).

Nano-sized also has been shown to cause adverse effects on a variety of cell types. Examples include the cytotoxicity to rat lung alveolar macrophages [8], human dermal fibroblast and human lung carcinoma cells, apoptosis of Syrian hamster embryo fibroblasts, hepatic injury in mice, and pathologic changes of gills in fish.

Nanoparticles of various types have been used in inhalation studies and have demonstrated various conditions such as pulmonary fibrosis, lung tumours, epithelial cell hyperplasia, inflammation and increased cytokine expression. It is widely recognized that the mechanisms of fibre-induced lung injury with mineral fibres such as asbestos depend on several factors, for example, length (Donaldson et al, 1989), diameter, chemical nature (Hart et al, 1994) and biopersistence (Donaldson et al, 1994). Particles which enter the lung become coated with lung lining material, which is likely to modify the surface reactivity and hence the oxidant generating ability and phagocytosis of the particles.

As for fullerenes, the potential and the growing use of CNTs and their mass production have raised questions about their safety and environmental impact. Research on the toxicity of CNTs has just begun and the data are still fragmentary and subject to criticism. Preliminary results highlight the difficulties in evaluating the toxicity of CNMs. Different characteristics (e.g., structure, size distribution and surface area, surface chemistry, surface charge, agglomeration state and purity) have considerable impact on the reactivity of CNTs. However, available data show that, under some conditions, CNTs can cross membrane barriers and suggest that, if NMs reach organs, they can induce harmful effects (e.g., inflammatory and fibrotic reactions). Further studies on well characterized materials are therefore necessary to determine the safety of CNTs as well as their environmental impact.

The surface properties of CNMs are among the most important factors governing their stability and mobility as colloidal suspensions or their aggregation into larger particles and deposition in aquatic systems. Stable colloidal suspensions of CNMs are a prerequisite for efficient interactions with some aquatic organisms, such as algae, which may lead to uptake or toxic effects.

The processes of deposition and aggregation are also influenced by NM surface properties, which mainly depend on, e.g., temperature, ionic strength, pH, particle concentration and size, steric repulsion or attraction, hydration effects, hydrophobic interactions, magnetic attraction, thus increasing their complexity.

There has been little information to date based on the potential health effects and hazards associated with the inhalation of carbon nanofibrous materials by workers despite their growing use in industry. A number of reports have suggested that risks associated with nanoparticles exposure require investigation due to evidence that these particles can be more inflammogenic and toxic than larger particles comprising of the same material. Also assessed were the toxic effect of the nanomaterials on the cells and the phagocytic ability of the cells after exposure. The studies showed that the cellular response varied with fibre morphology and state of aggregation; long, straight, well-dispersed in monocytic cells. The studies showed that monocytic cell phagocytic ability was reduced after exposure to nanotubes and microscopic examination of the cells after treatment with the nanotubes showed 'frustrated phagocytosis'. The frustrated phagocytosis suggests that clearance of nanotubes from the lungs by macrophages may be impaired. (Brown et al. 2007).

Phagocytic cells play a key role in the removal of deposited material in the lung. However, cells may become overloaded, phagocytic ability impaired and consequently clearance from the lung is reduced.

Impaired macrophage function has been described after instillation of nanoparticles into rat lungs (Renwick et al, 2004).

1.1.3.2 Research of potential effects

Today a lot of different nanomaterials which are produced nowadays are subject of testing in different animals and environments.

Most toxicology studies have been carried out with mammalian cells and the NP were exposed to a cell culture medium containing a mixture of proteins and other biological compounds. Results from such in vitro studies can therefore not be directly transferred to environmental conditions where uptake of NP into the aquatic biota is a major concern. Potential uptake routes include direct ingestion or entry across epithelial boundaries such as gills or body wall. At the cellular level prokaryotes like bacteria may be largely protected against the uptake of many types of NP since they do not have mechanisms for transport of colloidal particles across the cell wall (Moore, 2006). However, for eukaryotes, e.g. protists and metazoans, the situation is different since they have processes for the cellular internalization of nanoscale or microscale particles, namely endocytosis and phagocytosis (Moore, 2006).

For testing the effects of nanofibers and nanoparticles on the digestive tube as a test organism we used invertebrate terrestrial isopod *Porcellio scaber* Latreille, 1809 (Crustacea: Isopoda). This organism is very common and is used as a test model in many toxicology investigations. Terrestrial isopods are widely spread organisms, participating in decomposition of organic material in the leaf-litter layer, which is an indispensable process for ecosystem function (Hassall et al., 1987)

The hepatopancreas is the central metabolic organ of these animals and also has an important role in handling both essential metals involved in normal physiological processes (Wagele, 1992), as well as nonessential metals (Hopkin, 1990, 1989). The structure of hepatopancreatic cells of isopods, including *P. scaber*, is known to reflect influences of internal and external factors, namely moulting (Strus et al, 2001), the daily cycle of secretion (Hames and Hopkin, 1991), starvation (Storch, 1984; Strus, 1987), food quality (Storch, 1984; Strus, 1987) and the presence of metals in food (Kohler et al. 1996).

Hepatopancreatic cells are directly exposed to substances in partly digested food, filtered from the proventriculus into the lumen of the hepatopancreas. Knowledge acquired in our laboratory on the responses of *P. scaber*, such as food consumption and moulting, to elevated concentrations of zinc or cadmium in their food in almost equal experimental conditions (Drobne and Hopkin, 1995; Drobne and Strus, 1996a; Zidar, 1998).

Alterations of cellular ultrastructure were used by several authors for assessing the effects of organic chemicals on cell (Vogt, 1987; Segner and Braunbeck, 1998) and metals (Pawert et al., 1996; Kohler et al, 1996) and effects of nanoparticles (Drobne et al. 1999, Jemec et al. 2008, Drobne et al. 2009,).

In addition, hepatopancreatic cells of metal-exposed animals displayed non-specific, stress-indicating alterations such as cellular disintegration, the reduction of energetic reserves (lipid droplets, glycogen), electron dense cytoplasm, ultrastructural alterations of granular endoplasmic reticulum, the Golgi complex and mitochondria (Znidarsic et al, 2003)

In this study we tested the potential effects of different tungsten nanofibers and silver nanoparticle in the digestive gland epithelium of *Porcelio scaber.L*. The result of this study and discussion of possible effects will be presented in the chapter 4.

We suppose that both cells can be affected by the nanofibers and nanoparticles and such changes can be seen through investigation of the digestive gland epithelium in exposed samples. Such interaction between nanofibers and nanoparticles can be expected because of the properties and morphology of them. The behaviors and interactions of the nanofibers and nanoparticles with the cells surfaces are not very clear and we don't know how fast the organism will answer in the stress and how fast will envelope these nanomaterials to decrease the ability of them in order to be not harmful when they are ingested with treated food.

2. Aims and Hypothesis

During the last decade the production of nanofibers and nanoparticles in industry has increased extremely and the use of them in different fields of life is more common. Even though numerous studies have been done in the past, still there is a lack of data about the toxicity and health risks of nanofibers and nanoparticles on the environment and living organisms.

The objective of this work was to systematically study the epithelial surface of control animals and exposed group of animals to nanofibers and nanoparticles by conventional scanning electron microscopy combined with FIB/SEM in order to find the characteristic changes on the morphology of the digestive tube, shape and size of epithelium cells, shape and size of microvilli, presence of bacteria or any changes that resulted as a consequence of the treatment with nanofibers and nanoparticles.

The aim of this work was to prove if the different ingested nanofibers and nanoparticles can cause morphological defects on the digestive gland epithelium of test animal *Porcelio scaber* L.(Isopoda, Crustaceae) or damage the surface structure of the epithelium cells after exposure of animals to stress. The research work aims to answer the following questions: When ingested with food, do nanofibers and nanoparticles cause morphological defects of gland epithelium cells like shape changes of cells, size changes, loss of microvilli etc.? How long after the ingestion of contaminated food these changes are detected? Are nanoparticles and nanofibers cleared from the body after the transfer of animals on clean food? Is there any interaction between the surface of gland epithelium and nanofibers and nanoparticles on the other hand?

We will combine the SEM results with histological investigations of the very same tissue to see if any change in the digestive gland epithelium occurs.

Another aim of this research work was to use the potential of SEM for morphological investigation of the digestive gland epithelium surface after exposure of animals under stress, and to prove that SEM is the best method for investigation of surface morphological characteristics.

We hypothesize that ingested nanofibers and nanoparticles will interact with the digestive gland epithelial and cause morphological alterations of cells such as: shape changes of cells, changes on the size, loss of the microvilli, create holes in cells, penetrate into the cells, or even remain in the cells.

These alterations are expected because of the properties of nanofibers and nanoparticles. We think that all of this alternation changes can be detected by scanning electron microscopy, because nanofibres and nanoparticles are large enough to be detected by scanning electron microscopy, and with additional EDS analysis we will conform the presence of them in surface epithelium. Data will be compared with similar data obtained in studies with nanofibers and nanoparticles.

3. Materials and Methods

3.1. Materials

3.1.1 Test organism

To test effects of nanaofibers and nanoparticles on the digestive tube a test organism is used terrestrial isopoda *Porcellio scaber* Latreille, 1809 (Crustacea: Isopoda). Terrestrial isopods, including *Porcellio scaber*, have become organisms of choice in (eco) toxicology and (eco) physiology (Drobne 1997; Paoletti and Hassall 1999; Hassall et al. 2005). The animals were collected under concrete blocks and pieces of decaying wood in three different locations near the Ljubljana. In the laboratory, the animals were kept in a terrarium (20/35/20 cm) for acclimatization in period of three months.

The terrarium is filled with a 2-5-cm layer of moistened sand and soil and a thick layer of partly decomposed hazelnut tree leaves (*Corylus avellana*). The substratum in the terrarium was heated to 80 °C for several hours to destroy predators (spiders) before the introduction of the isopods. The culture was kept at controlled room temperature (21 ±1 °C), a 16:8-h light, dark photoperiod, and high humidity.

The hepatopancreas is the endodermal part of the digestive system, consisting of four blind-ending tubules, which open into the stomach and are composed of one layered epithelium comprising B and S cells, surrounded by the neuromuscular network (Wagele, 1992; Hames and Hopkin, 1989).

Cellular ultrastructure varies in accordance with physiological processes, also reflecting responses to environmental stress factors (Žnidaršič et al, 2003; Pawert et al, 2006)

It is well known that hepatopancreatic cells of isopod crustaceans are involved in the metabolism of essential and non-essential metals. In numerous studies isopods from uncontaminated and metal-contaminated environments were analyzed and the role of hepatopancreatic cells in the accumulation and/or detoxification of metals were discussed (Hopkin and Martin, 1982; Hopkin, 1989, 1990).

Accumulation of copper, calcium, zinc, cadmium, lead and iron in the granules in B and/or S cells is a well known feature of isopodian hepatopancreatic cells (Prosi and Dallinger, 1988; Hopkin, 1989).

The digestive system of *Porcellio scaber* is compound by : stomach, gut , hepatopancreas and rectum(Figure 6,b) . The hepatopancreas has a big role in the metabolism and secretion (enzymes). Other role of hepatopancreas is to store the carbohydrates and lipids and to release them when the body needs them. Hepatopancreas is combined from two different cells “B”(big cells) and “S” cells (small cells) which alternate in the tube.

The normal shape of the B cells called dome shape, the dimension of the cells is around from 30-80 µm. In normal digestive tube the S cells are between big cells and are not seen because they are covered from the big B cells.

The surface of the cells are covered with homogenous microvilli which are free directed in the lumen, or grouped in the different size covered with digestive juice, digestive food and small numbers of bacteria. Some time the microvilli are decayed in apical part or completely decayed, or in some regions they are loosed. In the hepatopancreas, some time cells are extruding the different size of the lipid droplets in to the lumen. In the unstressed animals the thickness of epithelium and abundance of lipid droplets is bigger than in stressed animals (Leser et al, 2008). These criteria can be taken in consideration to estimate the stress status of the animals. In case when the lipid droplets are much bigger, this is a consequence of the infection with the bacteria from the genus *Rickettsiella-Rickettsiella grylli* (Drobne et al, 1999).

Hepatopancreas contain a number of different bacteria which has a different role in the digestive process. Most common bacteria in the hepatopancreas are: streptococci, enterococci, soil bacteria e.g. bacillus and pseudomonas (Kostanjšek et al,2004). Another bacteria which is present and play a role in hepatopancreas digestive tube is *Candidatus Rhabdochlamydia porcellionis* (Vang et al, 2004 a, 2004 b).

3.1.2 Food preparation

Hazelnut tree leaves were collected in uncontaminated woodland and dried at room temperature. Dry leaves were cut into pieces of similar surface area and then weighed. Pieces of approximately 100 mg were selected for the experiments. Before the application of the Tungsten oxides (WO_3) and silver particles (Ag) dispersion, the leaves were kept in humid Petri dishes to facilitate the absorption of nanofibers and nanoparticles dispersion. Afterward, the leaves were dried for 24 hours at room temperature. The leaves were indirectly exposed to light with an intensity of 350 lux for 16 h and 10 lux for 8 h. The periods of maintenance of leaves in humid environment and conditions for drying of the leaves were the same in all experiments.

The tungsten oxides nanofibers and silver nanoparticles were suspended in bidistilled water using a vortex (20 s, 18 g the real dose for all of them) and prepared fresh before each experiment.

We applied 150 μ l of the dispersion per 100 mg of leaf onto the lower leaf surfaces. Before pipetting, the dispersion was rotated each time on a vortex for 5 s. The sonicated dispersion was prepared using a sonicator (30 min, 10-s pulses; Sonics Vibra-Cell, Ultrasonic processor VCX 750 Watt; Sonics & Materials). Animals in the control group were fed up with leaves prepared in the same way but treated with the bidistilled water only.

3.1.3 Experimental design

Porcellio scaber adults (Figure 6, a) with body weights ranging from 30 to 80 mg and of both sexes and all molt stages were exposed to tungsten and silver (within 2 week) after collection in the field.

Each animal was placed individually in a Petri dish, to which individual pieces of dry leaves dosed with tungsten and silver were added. Humidity in the Petri dishes was maintained by regular spraying with tap water on the internal side of the lids. All Petri dishes were placed in a large, plastic-covered glass container maintained at relative humidity close to 100% and a 16:8-h light:dark photoperiod without direct proximity of the lamp (illumination for 16 h with 15 lux and 8 h with 5 lux).

To investigate the effects of nanofibers and nanoparticles in digestive gland epithelium of test animals we have prepared a lot of control and treated samples which are shown in the table 1. Experiment number 26 had contained the samples from control and samples exposed to WO_x nanofibers. Experiment number 29 had contained the samples from control and samples exposed to WO_x (WO_4) nanofibers and experiment number 31 had contained the samples from control and samples exposed to Ag nano particles.

Both samples from the control group and exposed were investigated by the SEM in order to find the changes and effect in the morphology of digestive gland epithelium. The large regions from 100 – 500 μ m systematically were observed in order to find out the different appearance of digestive tube, shape of cell, presence and shape of microvilli, extrusion of lipids droplets, presence of bacteria and presence of protrusions.

First were observed a control group of samples from experiment nr. 26, and all characteristics of the digestive gland epithelium are recorded in the table 3, then a group of the exposed samples from the experiment 26 and all so all characteristic of the digestive gland epithelium are recorded in the table 4.

The same procedure was applied for the experiment 29 and 31. All characteristics of the digestive gland epithelium from experiment 29 are presented in the table 5 for control group and table 6 for exposed group. Also data from experiment nr.31 are presented in the table 6 for control group and in the table 7 for exposed group.

Animal mortality was recorded, the surviving animals were weighed at the end of the experiments, and the leaves were dried at room temperature for 24 h prior to weighing. Faecal pellets were counted and weighed after drying in the exsiccator for 48 h. Faecal palettes from control and exposed animals were analyzed by the ICP-EAS method(figure 8,a) to se the difference (table nr 10) .

For the chemical analyze 20 animals were exposed on nanoparticle and nanofibers for 4 week. The method of feeding was the same, but the hepatopancreas was separated in order to measure the presence of elements. Analyze is done on fecal palettes of animals which were exposed with naanofibers and nanaoparticle. All date from chemical analyze of fecal palettes are presented in the table 11 which showed the presence of the tungsten in the fecal of animals which are treated with tungsten oxides. The data of the presence of tungsten oxides in the hepatopancreas and gut are presented in the table 11 and table 12.

3.1.4 Nonofibers and nanoparticles tested

We had tested different tungsten oxide nanofibers and silver nanoparticle, (WO_x 39, WO_x 48, WO_x 65) which were produced at Josef Stefan Institute (figure 4). The nanoparticle and nanofibers are produced with method of grow up.

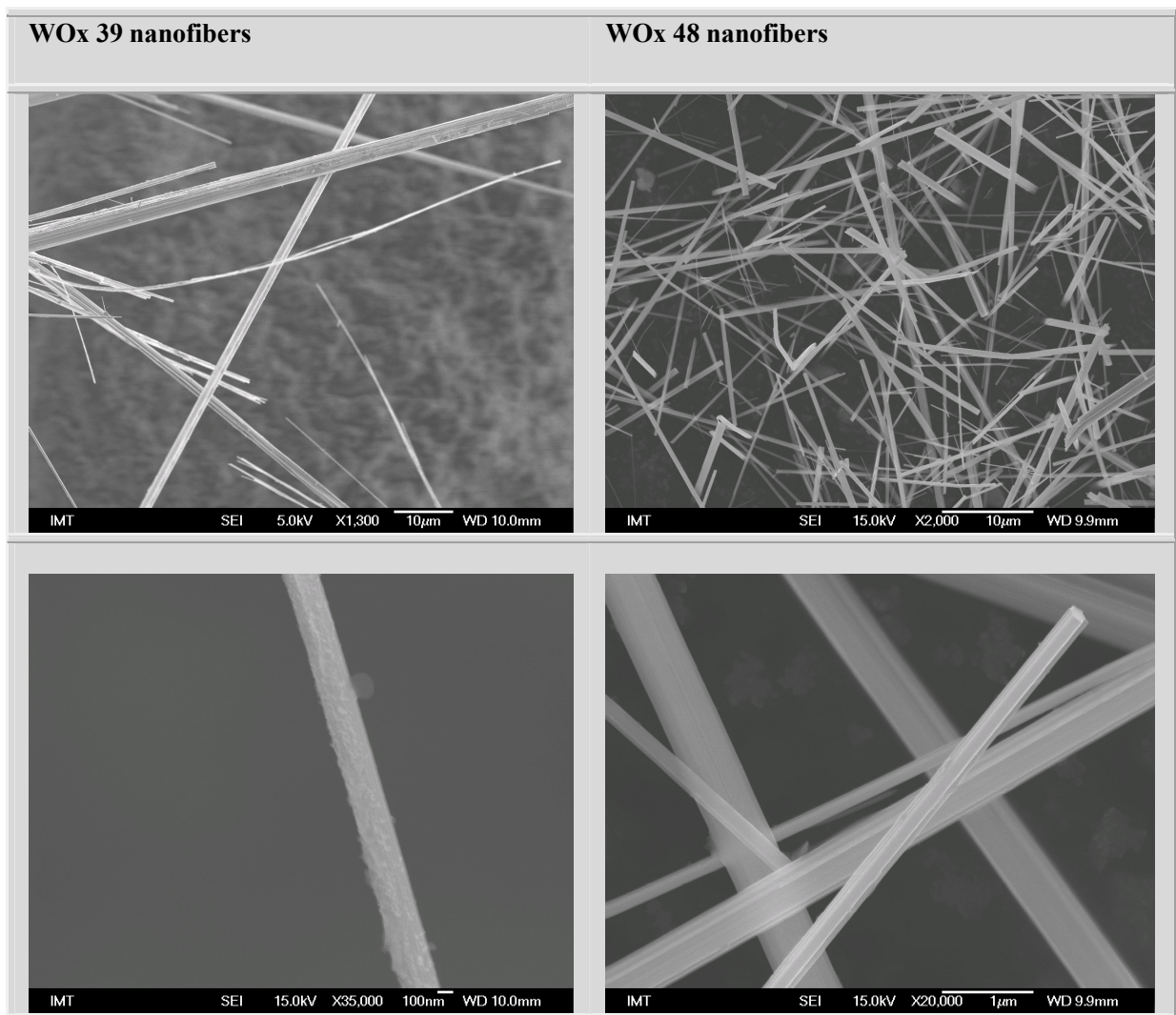


Figure 4.a Nanofibers tested in the experiment number 26 and 29: tungsten oxides nanofibers. Numbers 39, 48, are code from producer Josef Stefan Institute (JSI).

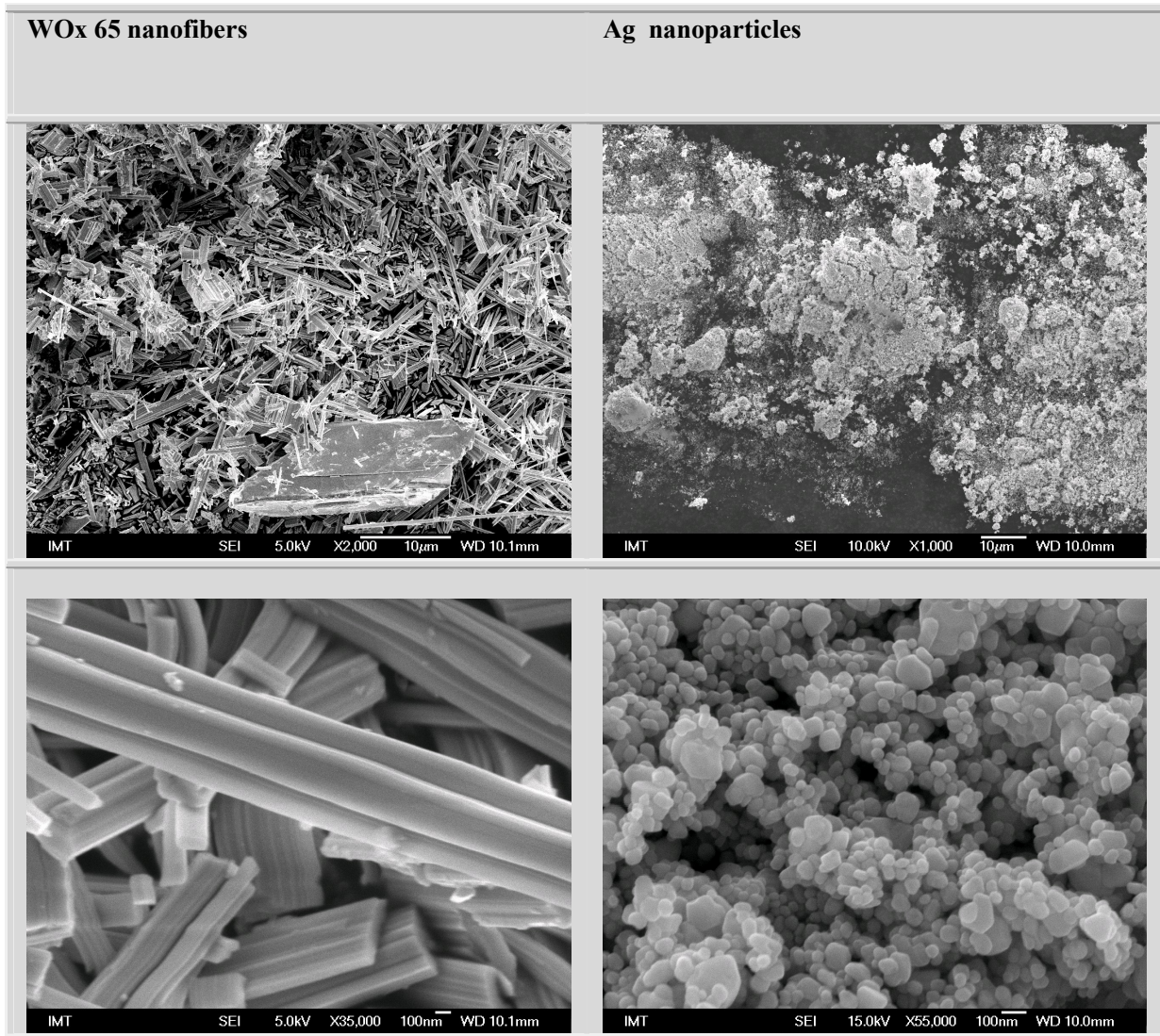


Figure 4.b: Nanofibers and nanoparticle tested in the experiment number 26, 29 and 31. Tungsten oxides nanofibers and silver nanoparticles. Number 39, 48, 65 are code from producer Josef Stefan Institute (JSI).

3.2 Methods

Chemical fixation continues to dominate the field of biological electron microscopy despite the advantages in cryopreservation methods. In SEM, the most frequently used fixative is glutaraldehyde or a combination of glutaraldehyde and formaldehyde. Glutaraldehyde is efficient in cross-linking proteins and maintaining cell ultrastructure, but it penetrates the tissue rather slowly. Formaldehyde is the smallest and the simplest aldehyde and penetrates tissues rapidly, apparently due to its low molecular weight. For postfixation, osmium tetroxide appeared most popular. It acts not only as a fixative but also as an electron stain. It preserves many lipids and it is able to stabilize some proteins by transforming them into clear gels, without destroying many of the structural features. The biphasic effect of osmium tetroxide on tissue constituents is well known; first it gels and then extracts certain cellular components. The prefixation with glutaraldehyde does not prevent leaching of some proteins when specimens are postfixated with osmium tetroxide (Hayat, 2000). In the standard protocols for SEM, specimens are dried, mounted onto the specimen stub and coated with a conductive layer of a few to 20 nm.

3.2.1 Biological samples prepared for SEM

For scanning electron microscopy a specimen is normally required to be completely dry, since the specimen chamber is at high vacuum. Hard, dry materials such as wood, bone, feathers, dried insects or shells can be examined with little further treatment, but living cells and tissues and whole, soft-bodied organisms usually require chemical fixation to preserve and stabilize their structure. Fixation is usually performed by incubation in a solution of a buffered chemical fixative, such as glutaraldehyde, sometimes in combination with formaldehyde and other fixatives, and optionally followed by postfixation with osmium tetroxide. The fixed tissue is then dehydrated. Because air-drying causes collapse and shrinkage, this is commonly achieved by critical point drying which involves replacement of water in the cells with organic solvents such as ethanol or acetone and replacement of these solvents in turn with a transitional fluid such as liquid carbon dioxide at high pressure. The carbon dioxide is finally removed while in a supercritical state, so that no gas-liquid interface is present within the sample during drying. The dry specimen is usually mounted on a specimen stub using an adhesive such as epoxy resin or electrically-conductive double-sided adhesive tape, and sputter coated with gold or gold/palladium alloy before examination in the microscope. Gold has a high atomic number and sputter coating with gold produces high topographic contrast and resolution. However, the coating has a thickness of a few nanometers, and can obscure the underlying fine detail of the specimen at very high magnification.

There are different samples preparation methods of biological samples for SEM imaging, (figure nr.6) in which is presented the scheme of digestive glands preparation methods for observation with focused ion beam / scanning electron.

3.2.1.1 Fixation

Fixation is usually the first stage in a multistep process to prepare a sample of biological material for microscopy. Therefore, the choice of fixative and fixation protocol may depend on the additional processing steps and final analyses that are planned. Fixation is a chemical process by which biological tissues are preserved from decay, either through autolysis or putrefaction. Fixation terminates any ongoing biochemical reactions, and may also increase the mechanical strength or stability of the treated tissues.

Fixation preserves a sample of biological material (tissue or cells) as close to its natural state as possible in the process of preparing tissue for examination. To achieve this, several conditions usually must be met. First, a fixative usually acts to disable intrinsic biomolecules – particularly proteolytic enzymes which otherwise digest or damage the sample. Second, a fixative typically protects a sample from extrinsic damage. Fixatives are toxic to most common microorganisms (bacteria in particular) that might exist in a tissue sample or which might otherwise colonize the fixed tissue. In addition, many fixatives chemically alter the fixed material to make it less palatable (either indigestible or toxic) to opportunistic microorganisms. Finally, fixatives often alter the cells or tissues on a molecular level to increase their mechanical strength or stability. This increased strength and rigidity can help preserve the morphology (shape and structure) of the sample as it is processed for further analysis.

Even the most careful fixation does alter the sample and introduce artifacts that can interfere with interpretation of cellular ultrastructure. Standardization of fixation and other tissue processing procedures takes this introduction of artifacts into account, by establishing what procedures introduce which kinds of

artifacts. Researchers who know what types of artifacts to expect with each tissue type and processing technique can accurately interpret sections with artifacts, or choose techniques that minimize artifacts in areas of interest.

3.2.1.2 Glutaraldehyde

Glutaraldehyde is an organic compound with the formula $\text{CH}_2(\text{CH}_2\text{CHO})_2$. Glutaraldehyde is used in biological electron microscopy as a fixative. It kills cells quickly by crosslinking their proteins and is usually employed alone or mixed with formaldehyde as the first of two fixative processes to stabilize specimens such as bacteria, plant material, and human cells. A second fixative procedure uses osmium peroxide to crosslink and stabilizes cell and organelle membrane lipids. Fixation is usually followed by dehydration of the tissue in ethanol or acetone followed by embedding in an epoxy resin or acrylic resin.

3.2.1.3 Formaldehyde

Formaldehyde (systematic name: methanal) is an organic compound with the formula CH_2O . Formaldehyde solutions are used as a fixative for microscopy and histology. Formaldehyde-based solutions are also used in embalming to disinfect and temporarily preserve human and animal remains. It is the ability of formaldehyde to fix the tissue that produces the tell-tale firmness of flesh in an embalmed body. Several European countries restrict the use of formaldehyde, including the import of formaldehyde-treated products and embalming. Starting September 2007, the European Union banned the use of formaldehyde due to its carcinogenic properties as a biocide (including embalming) under the Biocide Products Directive(98/8/EC).

3.2.1.4 Osmium tetroxide

Osmium tetroxide is the chemical compound with the formula OsO_4 . The compound is noteworthy for its many uses, despite the rarity of osmium. OsO_4 is a widely used staining agent used in transmission electron microscopy (TEM) to provide contrast to the image. As a lipid stain, it is also useful in scanning electron microscopy (SEM) as an alternative to sputter coating. It embeds a heavy metal directly into cell membranes, creating a high secondary electron emission without the need for coating the membrane with a layer of metal, which can obscure details of the cell membrane. Additionally, osmium tetroxide is also used for fixing biological samples in conjunction with HgCl_2 . Its rapid killing abilities are used to quickly kill specimen like protozoa. OsO_4 stabilizes many proteins by transforming them into gels without destroying structural features. Tissue proteins that are stabilized by OsO_4 are not coagulated by alcohols during dehydration. Osmium tetroxide is also used as a stain for lipids in optical microscopy.

3.2.1.5 Acetone

Acetone is the organic compound with the formula $(\text{CH}_3)_2\text{CO}$. Owing to the fact that acetone is miscible with water it serves as an important solvent in its own right, typically as the solvent of choice for cleaning purposes in the laboratory.

3.2.1.6 Critical point dry

Supercritical drying is a process to remove liquid in a precisely controlled way, similar to freeze drying. It is useful in the production of microelektromechanical systems(MEMS), in the drying of spices and in the preparation of biological specimens for scanning electron microscopy. Fluids suitable for supercritical drying include carbon dioxide (critical point 304.25 K at 7.39 Mpa or 31.1 degrees Co at 1072 psi) and freon (~300 K at 3.5-4 MPa or 25 to 30 °C at 500-600 psi).

In most such processes, acetone is first used to wash away all water, exploiting the complete miscibility of these two fluids. The acetone is then washed away with high pressure liquid carbon dioxide. The liquid carbon dioxide is then heated until its pressure goes beyond the critical point, at which time the pressure can be gradually released, allowing the gas to escape and leaving a dried product.

3.2.1.7 Sputter coating

Sputter coating in microscopy is a process of covering a specimen with a very thin layer of heavy metal, generally a gold/palladium (Au/Pd) mixture. This coating increases the ability of a specimen to conduct electricity and emit secondary electrons when in a scanning electron microscope, acting as a "stain" for electron microscopy. Biological specimens, composed largely of carbon compounds, are usually poor emitters of secondary electrons due to the low atomic number of carbon. Rather than absorbing electrons from the electron source of the microscope and then emitting electrons for detection, carbon compounds tend to collect a charge. The coating of samples was done with Precesion etching coating system Gatan Model 682 (figure 7, e).

3.2.2 SEM investigation

After the preparation, each sample was investigated by the SEM (Field Emission Scanning Electron Microscope JEOL JMS- 6500 F) in the Institute of Metals and Technology, Ljubljana (figure 5). During the investigation is used EDX analyze to be sure if the presence of some elements are present in the area which was analyzed.

The imaging of the sample was done on that way: the sample was fixed in the specimen holder and than transferred in to the specimen exchange chamber. With the help of specimen exchange rod the sample is putted into the specimen chamber on height vacuum specimen. The image was viably after the electron gun was opened. The work distance (WD) was 10 mm and the acceleration voltage (kV) was 5 kV because the height acceleration voltage can damage the biological samples. First was taken the images of samples from low magnification (x 25) and step bay step the images in to higher magnification (x 40.000). Fore each sample we took between 20- 30 images, but in some case we got more. All images are saved on separated folders which are renamed by the number of samples. Process of saving of images is programmed automatically by the machine). To avoid the miss and confusion of the images we renamed all of them with the trademark Ps_ number of the sample_ method of preparation_ number of the image because the number of images in the end is very huge.

3.2.2.1 SEM (Field Emission Scanning Electron Microscope JEOL JMS- 6500 F)

The JSM- 6500 basic unit is compound of an electron optical system, an operational and disply system and an oil rotary pump. The electron optical system is comprised by: column, vacuum, system and main console. The operational and display system is comprised by: personal computer, PC control interface, optimal three axis motor stage controller, image processing system, operational panel, keyboard, mouse, main power supply and sip/ bake out power supply and observation display (figure 5).

Currently there are numerous microscopy methods available to provide subcellular structural information at resolutions as low as 1–2 nm [1–3] but simultaneous imaging of intracellular structures and tissue gross morphology continues to be a challenge in the structural investigation of biological samples. Recently, focused ion beam/scanning electron microscopes (FIB/SEM) have been used in the field of life sciences and offer an attractive possibility with which to expand sample surface investigations by subsurface structural research at any location of interest (Drobne et al,2008). In this study, we tested the applicability of a FIB/SEM system for morphological research into gland epithelium and other morphological characteristics of the cells.



Figure 5: Field Emission Scanning Electron Microscope JEOL JMS- 6500 F (manufactured JEOL Ltd. Japan) Institute of Metals and Technology, Ljubljana.

3.2.3 Samples preparation

The animals were dissected, and the digestive glands (hepatopancreas) were isolated with tweezers and immediately transferred to the primary fixative 1 % glutalaldehyde and 0.4% paraformaldehyd for 2.5 hours. After that the digestive tube was transferred in 0.1 M sodium cacodylate buffer for 10 minutes, the procedure was repeated three times. After that the digestive tube was transferred in the 1% osmium tetroxide in distilled water (one hour). The digestive tube is washed three times for 10 minutes. Then the tube was transferred in saturated thiocarbohydrazide in distilled water for 30 minutes and again was washed with the distillate water three times for 10 minutes. The tube is transferred again in the 1% osmium tetroxide in distilled water for 1 hour and washed with distillate water three time for 10 minutes and then transferred in the saturated thiocarbohydrazide in distilled water for 30 minutes. For the third time the tube is transferred in the 1% osmium tetroxide in distilled water for 1 hour and washed again with distillate water three times for 10 minutes.

After these steps were done the digestive tube is dehydrated in the serial of ethanol with different percentage. First the tube is transferred in the 30% ethanol for 10 minutes, then is transferred in the 50% ethanol for 10 minutes, 70-% ethanol for 10 minutes, 80 % ethanol for 10 minutes, 96% ethanol for 10 minutes and in the end in absolute ethanol twice for 10 minutes.

The dehydration is followed with the absolute ethanol: acetone which was mixed 1:1 for 10 minutes, after that the tube was transferred in the acetone for 10 minutes three times. The next step was transference of the tube in solution of acetone: HMDS (hexamethyldisilazane) mixed in report 1:1 twice for 10 minutes. After the dehydration the tubes need to be dried. For that we use critical point dryer or hexamethyldisilazane (HMDS) the time takes 2-16 hour.

For SEM investigation the tubes were mounted on specimen stub with silver paste for better electrical contact and standing. In the specimen stub is written the number of samples twice up and down of the stub

in order not to mix them. All samples were coated with gold/palladium alloy and the thickness of the layer was between 5- 10 nm, we used the Precision etching coating system Gatan Model 682 (figure 6 e) for that.

The specimen stubs with samples are stored in the boxes (figure 6 c) and all of them are stored in the desiccator figure 6 d). The samples were investigated with the SEM to be able to provide as much as possible the information of the morphological structure of digestive glad epithelium.

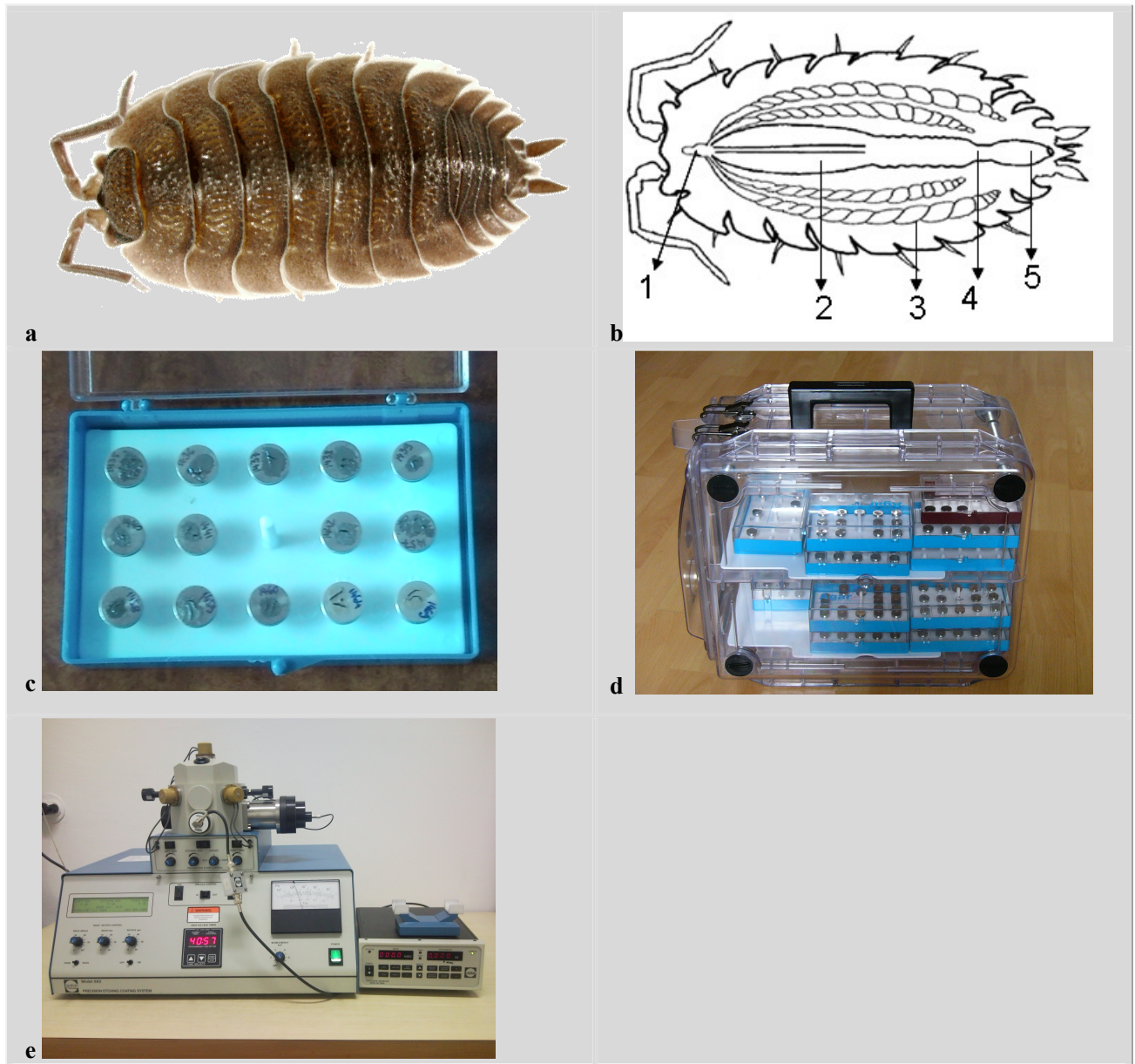


Figure 6: a) Porcellio scaber, adult ,b) Scheme of digestive system of porcellio scaber 1. Stomach 2.Gut 3. Hepatopancreas 4. Sphincter 5. Rectum. c) Boxes with the samples in holders, d) Desiccators with box of samples, e) Precision etching coating system Gatan Model 682.

All this procedure for samples preparation for SEM, chemicals, duration, temperature and repetitions and steps are showed in sample preparation for scanning electron microscopy (table 2).

This method (OTOTO) is taken mostly for the sample preparation and those samples are recorded as a B samples , but some tubes are prepared in the different way and are recorded as A samples or ones Osmium treated (table 1). The number of samples, other codes, number of experiment, samples preparation and date of investigated is present in the table1.

All these steps are done in laboratory, during the sample preparation with the chemicals or material which is carcinogen and harmful for the health is used the digester, gloves and glasses.

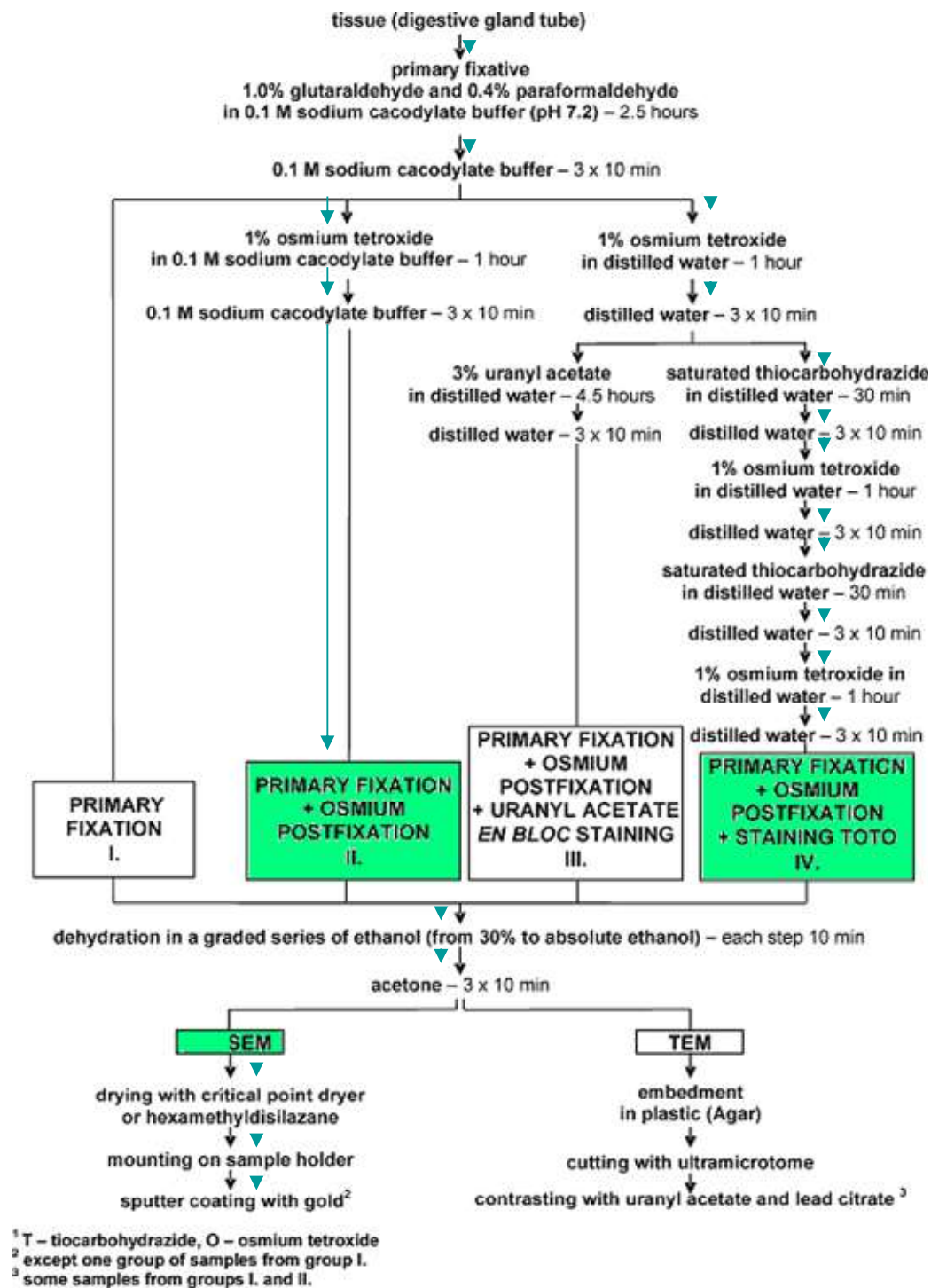


Figure 7: Scheme of digestive glands preparation methods for observation with focused ion beam/scanning electron microscopy and transmission electron microscopy TEM.

Samples marked as OS are prepared for SEM investigation with primary fixation and osmium postfixation (protocol II). Samples marked as OTOTO are prepared with primary fixation plus osmium postfixation plus staining OTOTO.

Table 1 Framework of experiment: Total number of control and treated animals, experiment number and test, sample preparation, date of SEM investigation.

Nr	number of samples	Other code	Experiment number and test	Samples preparation	Date of SEM investigation
1	1430 B	K1	Control (experiment nr. 29)	OTOTO	09.03.2010
2	1431 B	K2	Control (experiment nr. 29)	OTOTO	23.03.2010
3	1432 B	K3	Control (experiment nr. 29)	OTOTO	23.03.2010
4	1433 B	K4	Control (experiment nr. 29)	OTOTO	24.03.2010
5	1434 B	K5	Control (experiment nr. 29)	OTOTO	29.03.2010
6	1435 B	WOx	Exposed tow week (experiment nr.29)	OTOTO	13.04.2010
7	1436 B	WOx	Exposed tow week (experiment nr.29)	OTOTO	14.04.2010
8	1437 B	WOx	Exposed tow week (experiment nr.29)	OTOTO	21.04.2010
9	1438 B	WOx	Exposed tow week (experiment nr.29)	OTOTO	22.04.2010
10	1439 B	WOx	Exposed tow week (experiment nr.29)	OTOTO	23.04.2010
11	1440 B	WOx	Exposed tow week (experiment nr.29)	OTOTO	28.04.2010
12	1441 B	WOx	Exposed tow week (experiment nr.29)	OTOTO	29.04.2010
13	1442 B	WOx	Exposed tow week (experiment nr.29)	OTOTO	29.04.2010
14	1362 B/A	K 1	Control for tow week (experiment nr.26)	OTOTO / OS	07.01.2010
15	1363 B/A	K 2	Control for tow week (experiment nr.26)	OTOTO / OS	13.01.2010
16	1364 B/A	K 3	Control for tow week (experiment nr.26)	OTOTO / OS	15.01.2010
17	1365 B/A	K 4	Control for tow week (experiment nr.26)	OTOTO / OS	22.01.2010
18	1366 B/A	nSiO ₂ 11	Exposed tow week (experiment nr.26)	OTOTO / OS	22.01.2010
19	1367 B/A	nSiO ₂ 12	Exposed tow week (experiment nr.26)	OTOTO / OS	22.01.2010
20	1370 B/A	WOx 21	Exposed tow week (experiment nr.26)	OTOTO / OS	17.12.2009
21	1371 B/A	WOx 22	Exposed tow week (experiment nr.26)	OTOTO / OS	22.12.2009
22	1372 B/A	WOx 23	Exposed tow week (experiment nr.26)	OTOTO / OS	18.12.2009
23	1373 B/A	WOx 24	Exposed tow week (experiment nr.26)	OTOTO / OS	18.01.2010
24	1457	K	Control (experiment nr. 31)	OTOTO	30.04.2010
25	1458	K	Control (experiment nr. 31)	OTOTO	11.05.2010
26	1459	K	Control (experiment nr. 31)	OTOTO	12.05.2010
27	1460	K	Control (experiment nr. 31)	OTOTO	17.05.2010

28	1461	K	Control (experiment nr. 31)	OTOTO	17.05.2010
30	1462	K	Control (experiment nr. 31)	OTOTO	17.05.2010
31	1463	K	Control (experiment nr. 31)	OTOTO	20.05.2010
32	1464	1000	Exposed too week (experiment nr. 31)	OTOTO	20.05.2010
33	1465	1000	Exposed too week (experiment nr. 31)	OTOTO	20.05.2010
34	1466	1000	Exposed too week (experiment nr. 31)	OTOTO	20.05.2010
35	1467	1000	Exposed too week (experiment nr. 31)	OTOTO	05.05.2010
36	1468	5000	Exposed too week (experiment nr. 31)	OTOTO	05.05.2010
37	1469	5000	Exposed too week (experiment nr. 31)	OTOTO	05.05.2010
38	1470	5000	Exposed too week (experiment nr. 31)	OTOTO	01.06.2010
39	1471	5000	Exposed too week (experiment nr. 31)	OTOTO	01.06.2010

Table 2: **Method for sample preparation for scanning electron microscopy-SEM**

Protocol	Chemical	Temperature	Time	Repetitions
Primary fixation	1.0 % glutalaldehyde and 0.4% paraformaldehyd in 0.1 M sodium cacodylate buffer (pH = 7.2)	room	2.5 hours	1
Wash	0.1 molar sodium cacodylate buffer	room	10 minutes	3
Secondary fixation or post fixation	1% osmium tetroxide in distilled water	room	1 hours	1
Wash	distilled water	room	10 minutes	3
	Saturated thiocarbohydrazide in distilled water	room	30 minutes	1
Wash	distilled water	room	10 minutes	3
Secondary fixation or post fixation	1% osmium tetroxide in distilled water	room	1 hours	1
Wash	distilled water	room	10 minutes	3
	Saturated thiocarbohydrazide in distilled water	room	30 minutes	1
Wash	distilled water	room	10 minutes	3
Secondary fixation or post fixation	1% osmium tetroxide in distilled water	room	1 hours	1
Wash	distilled water	room	10 minutes	3
Dehydration	30% ethanol	room	10 minutes	1
	50% ethanol		10 minutes	1
	70-% ethanol		10 minutes	1
	80 % ethanol		10 minutes	1
	96% ethanol		10 minutes	1
	absolute ethanol		10 minutes	2
	Absolute ethanol: acetone (1:1)		10 min	1

Dehydration	Acetone	room	10 minutes	3
	Acetone :HMDS (1:1)		10 min	1
	HMDS (hexamethyldisilazane)		10 min	1
Critical point dryer or HMDS			2- 16 hour	1
Mount on specimen stub with silver paste				
Coat with gold/palladium alloy			layer 5-10 nm	1-2
Store stubs in desiccators				

3.2.4 Chemical analyze

In order to know if the nanofibers and nanoparticle are going through digestive system or the animals can avoid them as a food material, we have measure the presence of the elements in the fecal palettes. The Inductively coupled plasma optical emission spectrometry (figure 8) was used to analyze the fecal palettes from control animals and animals which were treated with nanaofibers and nanoparticle.

At the end of experiment fecal pellets were removed completely from the leaves using a brush, they were counted and weighted. Also, the leaves were weighted. The feeding rate and defecation rate of isopods were calculated as the mass of consumed leaf and mass of fecal pellets per animal wet weight per day, respectively.



Figure 8: Inductively coupled plasma optical emission spectrometry (ICP-OES), model: PERKINELMER Optima 3100 RL (IMT, Laboratory for chemistry)

Inductively coupled plasma optical emission spectrometry (ICP-OES), is an analytical technique used for the detection of trace metals. It is a type of emission spectroscopy that uses the inductively coupled plasma to produce excited atoms and ions that emit electromagnetic radiation at wavelengths characteristic of a particular element. The intensity of this emission is indicative of the concentration of the element within the sample.

The ICP-OES is composed of two parts: the ICP and the optical spectrometer. The ICP torch consists of 3 concentric quartz glass tubes. The output or "work" coil of the radio frequency generator surrounds part of this quartz torch. Argon gas is typically used to create the plasma.

4. Results

The results of the investigation show that significant morphological changes were observed in the surface of the B-cells on the hepatopancreas of the *Porcelio scaber.L.* on different areas of exposed animals. Those changes were found only in small areas of the digestive gland epithelium and only in B-cells of the hepatopancreas. In the experiment of exposed animals to WOx nanofibers it is shown that tungsten nanofibers are present in the digestive gland epithelium and they began to interact with the cells in some places. The interactions between tungsten nanofibers and surface of the cells are presented in figures 26.a, 26.b and 26.c. After two weeks such interactions can be visible in the digestive gland epithelium with scanning electron microscopy. Tungsten nanofibers ingested with the food can cause different changes into the digestive B-cells. The nanofibers can penetrate through the membranes of cells and destroy the cells, in some cases they will pass the cell membranes and enter the cell environment, as is shown in figures 26.a, 26.b and 26.c. This phenomenon is more common in the bottom part of the digestive gland and not in the top part. The interaction begins when the nanoparticles enter the digestive gland epithelium through food and during the contractions (peristaltic of gut) of digestive gland the nanofibers are pushed in the direction of cells by some neighbor cells as is shown in fig 26. b. The presence of parts of the same nanofiber in both cells which were involved in the phenomena, as observed in the electron microscope, serves as an argument of this interaction. This phenomenon is presented in figures 26.a, 26.b and 26.c.

We have noticed a small difference in the morphology of hepatopancreas epithelium in the experiment with the nanofibers and nanoparticles. The short exposure time of the animals to nanofibers and nanoparticles might have been a reason for this, since they were fed with this kind of food only for two weeks. Given a longer feeding period maybe more noticeable differences in the morphology would have been observed.

We found a small differences in morphological characteristics of digestive gland epithelium between control animals of *Porcelio scaber.L.* which were used in the experiment number 26, 29 (WOx nanofibers) and experiment 31 (Ag nanoparticles) and exposed animals. The animals which were infected with high amounts of bacteria in the digestive gland epithelium were not taken in consideration.

A large amount of nanofibers and nanoparticles which were taken from animals with treated food passes through digestive gland tube in the environment with faeces and only very small amount of them will have opportunity to stop and interact with the epithelium of digestive gland. For this reason only small numbers of these phenomena were recorded in samples which were treated with nanofibers and nanoparticles.

During the research on the effect of nanofibers and nanoparticles in the digestive gland epithelium of test organism we have encountered some advantage and disadvantage of the work methodology.

An advantage of the SEM method for analyzing biological samples is the ability to investigate large areas of the specimen and look for the morphological characteristics or changes in the surface. Also it has the ability to focus in very small areas, as well as use very high magnifications and enables images with high resolution.

But in the other hand the disadvantage of this method is that if we want to analyze the quantity of certain elements in the specimen with EDS or EDX you will not get enough signals because the biological material envelops the material to be analyzed.

Another problem that arises when analyzing tungsten in the specimen through EDS is the overlapping of the tungsten spectra with the osmium spectra which was used as a fixative for the biological samples. The same problem was also by analyzing the elements in Auger electron spectroscopy (AES).

5. Discussion

Experiment number 26- control animals and animals exposed to WOx nanofibers.

a) Control animals

The control animals were fed for two weeks with untreated food. We have investigated four samples of control animals. After the preparation of the digestive gland epithelium of these animals we have investigated these characteristics: shape of epithelium cells, morphological characteristics of the digestive gland epithelium, presence and shape of bacteria, presence and shape of microvilli, presence of lipid droplets and other characteristics.

Morphology of hepatopancreatic epithelia of all animals in the control group were 50% partly flat as is shown in figures 15.a and 15. b and 50% predominant flat epithelium as presented in figure 16.a and 16.b . Low or completely flat hepatopancreatic appearance is described by many authors as normal stages in the daily cycle (Hames and Hopkin, 1991).

The digestive gland epithelium is composed of B-cells with flat and predominantly flat appearance on most of the gland as is shown in figures 11.a and 11.b and figures 12.a and 12.b. In both types of cells (B and S) the presence of normal shape of microvilli is seen on the surface as is shown in figures 20.a and 20.b. Microvilli in the surface of the cells are covered with different food material as it is presented in figures 23.a and 23.b.

Other characteristic which is investigated was the presence of bacteria, their shape and sizes. We found different bacteria in the surface of the cells that are presented in figures 17.a and 17.b. The amount of bacteria in the digestive gland of control animals alternate from densely colonized in some areas as is shown in figures 18.a, 18.b and small amounts in some locations (figures 19.a and 19.b). We didn't observe the presence of lipid droplets extrusion from the cells and the presence of protrusions between cells in the control samples. All data of morphological characteristics of the digestive gland epithelium, shape of epithelium cells, presence and shape of bacteria, presence of microvilli, extrusion of lipid droplets from the cells and other characteristics which are investigated in the control samples are presented in table nr. 3.

b) Exposed animals to WOx nanofibers

The exposed animals for experiment number 26 were fed for two weeks with treated WOx nanofibers, food which was prepared in the way explained in the methodology. We have investigated six samples of exposed animals. The same characteristics as: morphological characteristic of digestive gland epithelium, shape of epithelium cells, presence and shape of bacteria, presence and shape of microvilli and presence of lipid droplets were investigated as in control animals in order to see changes after two weeks.

From the result of exposed samples in experiment 26 we find out that: morphology of hepatopancreatic epithelia of animals exposed to WOx nanofibers was predominantly dome shaped as presented in figures 13.a, 13b and partly flat epithelium as is shown in figures 115.a and 15.b. Half of the digestive gland epitheliums are composed of B-cells with the normal appearance as presented in figures 9.a, 9.b, and half with the B-cells with partly flat appearance as is shown in figures 15.a and 15.b. In both, B-cells and S-cells the presence of normal shape of mikrovilli is seen on the surface as is shown in figures 20.a and 20.b. Microvilli in the surface of cells are covered with the material of food which was present on the digestive gland as is presented in figures 23.a and 23.b. Half of the microvilli were grouped in apical part as is presented in the figure 22.a. In the digestive gland epitheliums different bacteria are present as presented in figures 17.a and 17.b. The bacteria were in dense as well as small amounts as is shown in figures 18.a, 18.b, 19.a, 19.b. Some of the cells in the digestive gland epithelium were extruded lipid droplets in different size and shape as is presented in figures 24.a and 24.b. The presence of protrusions is not observed in this group of exposed

animals. All data which we have investigated on exposed animals, such as: morphological characteristic of the digestive gland epithelium, shape of epithelium cells, presence and shape of bacteria, presence of microvilli, extrusion of lipid droplets and other characteristics are presented in the table 4.

Experiment number 29: control and exposed animals to WOx nanofibers.

a) Control animals

We have investigated five samples of control animals for this experiment. The control animals were fed for two weeks with untreated food. After preparation of the digestive gland epithelium of these animals we have investigated these characteristics: morphological characteristic of digestive gland epithelium, shape of epithelium cells, presence and shape of bacteria, presence and shape of microvilli, presence of lipid droplets and other characteristics.

The results from control experiment number 29 showed that: hepatopancreatic epithelia of control animals were predominantly dome shaped half as is presented in figures 13.a and 13.b and half of them had partly flat epithelium appearance as is shown in figures 15.a and 15.b. The digestive gland epithelium is composed of normal B-cells and S-cells with normal shape and size as is shown in figures 9.a and 9.b. In the same digestive gland some regions with partly flat appearance of B-cells are seen, as shown in figures 11.a and 11.b. In both cells the presence of normal mikroovilli in the surface is seen as is presented in figures 20.a and 20.b, but in some areas cells are without mikroovilli as is shown in figures 21.b and 22.a. In the surface of the cells mostly the mikroovilli were covered with the material from food as is shown in figures 23.a and 23.b. Different bacteria are present in the digestive gland tube, half of cells of the digestive gland epithelium were colonized from the bacteria with high amount, half of them were colonized with a small amount as is shown in the figure 17.a, 17.b, 18.a, 18.b, 19.a and 19.b. Only in one sample the extrusion of lipid droplets was found, as shown in figures 24.a and 24.b. The presence of protrusions was found only in one sample as is shown in figures 25.a and 25.b. All the data which was found in the control animals from the experiment number 29 as: morphological characteristic of digestive gland epithelium, shape of epithelium cells, presence and shape of bacteria, mikroovilli, extrusion of lipid droplets and other characteristics are presented in table 5.

b) Animals exposed to WOx nanofibers

The exposed animals for experiment number 29 were fed for two weeks with treated WOx nanofibers as are presented in figures 4.a and 4.b, food which was prepared in the way explained in the methodology. We have investigated six samples of animals exposed to WOx nanofibers. The same characteristics as: morphological characteristic of digestive gland epithelium, shape of epithelium cells, presence and shape of bacteria, presence and shape of mikroovilli, presence of lipid droplets and other different changes on the cells were investigated as in control animals in order to see changes after two weeks.

The results from experiment 29 of animals exposed to WOx nanofibers showed that: hepatopancreatic epithelia of animals were in 75% with predominantly dome shaped appearance as is presented in figures 13.a and 13.b and 25 % partly flat epithelium as is shown in figures 15.a and 15.b. The hepatopancreas gland epithelium is composed from normal B-cells with normal shape and size as is presented in figures 9.a and 9.b in some areas and in others area B-cells were with partly flat appearance as is shown in figures 11.a and 11.b. In both cells the presence of normal mikroovilli on the surface were 75 % as is shown in figures 20.a and 20.b, but a few regions of the cells are without mikroovilli as is shown in the figure 21.b. In the apical part of mikroovilli is present material of food which has covered them as is shown in figures 23.a and 23.b. In all of the samples the mikroovilli are grouped in the apical part as is presented in figure 22.a. Different bacteria were present in digestive glands as is presented in figures 17.a and 17.b but the amount of them is not very high as is shown in figure 19.a and 19.b. In some areas, B-cells have extruded lipid droplets as is presented in figures 24.a and 24.b. The presence of the protrusions is very high in most of the samples as is presented in the figure 25.a and 25.b. A very significant finding in this experiment was the presence of the nanofibers on the surface of the cells in some small regions. In these regions the cells were attacked from different nanofibers approximately 1µm with the size as are presented figure number 26.a, 26.b and 26.c. Presence of the nanofibers was detected in half of the samples. All the data which were found in the exposed animals from the experiment number 29 as: morphological characteristic of digestive gland epithelium, shape of epithelium cells, presence and shape of bacteria, presence and shape of mikroovilli, extrusion of lipid droplets and other characteristics are presented in the table 6.

Experiment number 31: control animals and animals exposed to Ag nanoparticles

a) Control animals

We have investigated seven samples of control animals for this experiment. The control animals were fed for two weeks with untreated food. After preparation of digestive gland epithelium of these animals we have investigated these characteristics: morphological characteristics of digestive gland epithelium, shape of epithelium cells, presence and shape of bacteria, presence and shape of microvilli, presence of lipid droplets and other characteristics.

The results from control animals of experiment 31 showed that: hepatopancreatic epithelia of animals in the control group were half predominantly dome shaped as is presented in figures 13.a and 13.b. and partly flat epithelium as is presented in the figures 15.a and 15.b. The digestive gland epithelium is composed of normal B-cells and S-cells with normal shape and size as is shown in figures 9.a and 9.b. and partly flat and flat appearance as is presented in figures 11.a, 11.b, 12.a. and 12.b. In both cells the presence of normal mikrovilli on the surface with normal structure is seen more than 75 % as is presented in figures 20.a and 20.b. Mikrosvilli were covered with the material in most of cells as is shown in figures 23.a and 23.b, in some regions they are grouped and decaying in the apical part as are shown in figures 22.a and 22.b. Different bacteria are present in digestive gland tube figures 17.a and 17.b, in some cells they are very dense as is shown in figures 18.a and 18.b, in others cells small amount of bacteria is present as is shown in figures 19.a and 19.b. Only in one sample the presence of extrusion of lipid droplets was found, as is shown in figures 24.a and 24.b. Also the presence of protrusions is not common and is found only in one sample, figure 25.a and 25.b. All data from control animals of experiment 31: morphological characteristics of the digestive gland epithelium, shape of epithelium cells, presence and shape of bacteria, mikrosvilli, extrusion of lipid droplets and other characteristics are presented in the table number 7.

b) Exposed animals to Ag nanoparticles

The exposed animals to Ag nanoparticles were fed for two weeks with treated WOx nanofibers as can be seen in figures 4.a and 4.b, food which was prepared in the way explained in the methodology. We have investigated six samples of exposed animals. The same characteristics as: morphological characteristic of digestive gland epithelium, shape of epithelium cells, presence and shape of bacteria, presence and shape of mikrosvilli, presence of lipid droplets and other different changes on the cells were investigated as in control animals in order to see changes after two weeks.

The results from experiment with exposed animals on Ag nanoparticles showed that: hepatopancreatic epithelia of animals were mostly predominantly dome shaped as in figures 13.a and 13.b, and partly flat epithelium is shown in figures 15.a and 15.b. The digestive gland epithelium is composed of normal B-cells with normal shape and size as is presented in figures 9.a and 9.b and in some areas they were with different shape partly flat or complete flat as is shown in figures 11.a and 11.b. or in the figures 12.a and 12.b. In both cells: B-cells and S-cells the presence of normal mikrosvilli on the surface is seen as is presented in figures 20.a and 20.b, but in some small regions cells were without mikrosvilli as is shown on figures 21.a and 22.b. On the surface mikrosvilli were covered with the material in all of the samples as is shown in figures 23.a and 23.b, and they are grouped in the apical part like in figure 22.a. The shape and size of mikrosvilli was different form the mikrosvilli of control animals. Different bacteria are present in the hepatopancreatic gland in small amounts, as is shown in figures 17.a and 17.b. B-cells have extruded lipid droplets in to the lumen in some regions as is presented in figures 24.a and 24.b. The presence of protrusions in the hepatopancreatic gland tubes is very high as is presented in figures 25.a and 25.b. All data from exposed animals to Ag nanoparticles as: morphological characteristics of digestive gland epithelium, shape of epithelium cells, presence and shape of bacteria, mikrosvilli, extrusion of lipid droplets and other characteristics are presented in the table number 8.

Table 3: Experiment 26. – Control samples

Control samples		1.Shape of epithelial cells						2.Morphological characteristic of the epithelium				3. Presence of bacteria on the cell surface			4. Presence and shape of microvilli			5. Extrusion of lipid droplets	6. Others			
Nr. of samples	Investigated region	1.1.Normal appearance		1.2 Abnormal appearance		1.2.1 Not smooth surface	1.2.2 Enlarge cells	1.2.3 Partly flat	1.2.4 Flat	2.1 Predominantly (dome shaped)	2.2 Enlarge cells , not smooth surface	2.3 Partly flat epithelium (less than 50 %)	2.4 Predominant flat epithelium (more than 50%)	3.1 Presence of bacteria	3.2 Densely (big amount)	3.3 Low amount	4.1 Normal (equal shape 0.5 µm, individual	4.2 Abnormal (shorter, grouped, absent, decayed)	4.3 Partly covered with material	5.1 Extrusion of lipid droplets	6.1 Presence of cellular protrusions	6.2 Interaction with NP
		+	-	+	-																	
1362	2 mm	-	+	-	-	+	+	-	-	+	+	50 %	50 %	+	-	+	+	+	+	-	-	
1363	500 µm	-	+	-	-	-	+	-	-	-	-	+	100 %	-	-	-	+	+	+	-	-	
1364	2 mm	-	+	-	-	-	+	-	-	-	-	+	100 %	+	+	-	+	+	+	-	-	
1365	2 mm	-	+	-	-	-	+	-	-	-	-	+	100 %	+	+	-	*	*	+	-	-	

* N/A –data not available

** - can not be assessment

Table 4: Experiment 26. – Exposed samples to WOx

Exposed samples to WOx		1. Shape of epithelial cells						2. Morphological characteristic of the epithelium				3. Presence of bacteria on the cell surface			4. Presence and shape of microvilli			5. Extrusion of lipid droplets	6. Others									
Nr. of samples	Investigated region	1.1. Normal appearance		1.2. Abnormal appearance		1.2.1 Not smooth surface		1.2.2 Enlarge cells		1.2.3 Partly flat		1.2.4 Flat		2.1 Predominantly (dome shaped)	2.2 Enlarge cells, not smooth surface	2.3 Partly flat epithelium (less than 50%)	2.4 Predominant flat epithelium (more than 50%)	3.1 Presence of bacteria	3.2 Densely (big amount)	3.3 Low amount	4.1 Normal (equal shape 0.5 µm, individual grouped)	4.2 Abnormal (shorter, grouped, absent, decayed)	4.3 Partly covered with material	5.1 Extrusion of lipid droplets	6.1 Presence of cellular protrusions	6.2 Interaction with NP		
		1366	2 mm	+	+	-	-	+	-	+	25%	-	+	75%	-	+	-	+	+	-	*	N/A	*	N/A	-	-	-	*
1367	1 mm	-	+	-	-	+	+	-	-	-	+	25%	+	75%	-	+	-	-	-	+	100%	-	+	-	-	-	*	N/A
1370	2 mm	-	+	-	-	+	-	-	-	-	+	100%	-	-	+	+	+	-	*	N/A	*	N/A	-	-	-	-	*	N/A
1371	4 mm	+	-	-	-	-	-	+	100%	-	-	-	-	-	+	-	+	+	+	100%	-	+	+	-	-	-	*	N/A
1372	2.5 mm	+	+	-	-	+	-	+	75%	-	+	25%	-	+	-	+	+	+	+	100%	-	+	+	-	-	-	*	N/A
1373	2mm	-	+	-	-	+	-	-	-	+	50%	+	50%	-	+	+	+	+	-	+	100%	-	+	-	-	-	*	N/A

* N/A – data not available

Table 5: Experiment 29. – Control samples

Control samples		1.Shape of epithelial cells						2.Morphological characteristic of the epithelium				3. Presence of bacteria on the cell surface			4. Presence and shape of microvilli			5. Extrusion of lipid droplets	6. Others						
Nr. of samples	Investigated region	1.1.Normal appearance		1.2 Abnormal appearance		1.2.1 Not smooth surface	1.2.2 Enlarge cells	1.2.3 Partly flat	1.2.4 Flat	2.1 Predominantly (dome shaped)	2.2 Enlarge cells , not smooth surface	2.3 Partly flat epithelium (less than 50 %)	2.4 Predominant flat epithelium(more than 50%)	3.1 Presence of bacteria	3.2 Densely (big amount)	3.3 Low amount	4.1 Normal (equal shape 0.5 µm, individual grouped)	4.2 Abnormal (shorter, grouped, absent, decayed)	4.3 Partly covered with material	5.1Extrusion of lipid droplets	6.1 Presence of cellular protrusions	6.2 Interaction with NP			
		+	-	+	-																		+	-	+
1430	2 mm	+	-	-	-	-	-	-	+	100%	-	+	-	+	-	+	+	75 %	+	25 %	+	-	-	-	
1431	2 mm	+	-	-	-	-	-	-	+	100%	-	-	-	+	+	-	*	N/A	*	N/A	+	-	-	-	
1432	3 mm	-	+	-	-	+	+	-	-	-	+	50 %	+	50 %	-	-	-	+	75 %	+	25 %	+	-	-	-
1433	3 mm	+	+	-	-	+	-	-	+	75 %	-	+	25 %	+	-	+	+	50 %	+	50 %	+	+	-	-	-
1434	2 mm	+	+	-	-	+	-	-	+	75 %	-	+	25 %	-	-	-	+	+	75 %	+	25 %	+	-	+	-

* N/A – data not available

Table 6: Experiment 29. – Exposed samples to WO_x

Exposed samples to WO _x		1. Shape of epithelial cells						2. Morphological characteristic of the epithelium				3. Presence of bacteria on the cell surface			4. Presence and shape of microvilli			5. Extrusion of lipid droplets	6. Others							
Nr. of samples	Investigated region	1.1. Normal appearance	1.2. Abnormal appearance			1.2.1 Not smooth surface	1.2.2 Enlarge cells	1.2.3 Partly flat	1.2.4 Flat	2.1 Predominantly (dome shaped)	2.2 Enlarge cells, not smooth surface	2.3 Partly flat epithelium (less than 50%)	2.4 Predominant flat epithelium (more than 50%)	3.1 Presence of bacteria	3.2 Densely (big amount)	3.3 Low amount	4.1 Normal (equal shape 0.5 µm, individual grouped)	4.2 Abnormal (shorter, grouped, absent, decayed)	4.3 Partly covered with material	5.1 Extrusion of lipid droplets	6.1 Presence of cellular protrusions	6.2 Interaction with NP				
1435	3 mm	+	+	-	-	+	-	+	75%	-	+	25%	-	+	-	+	+	75%	+	25%	+	-	+	*	N/A	
1436	3.5 mm	+	+	-	-	+	-	+	50%	-	+	50%	-	+	-	+	+	75%	+	25%	+	-	+	*	N/A	
1437	4 mm	+	+	-	-	+	-	+	75%	-	+	25%	-	-	-	+	+	75%	+	25%	+	-	+	*	N/A	
1438	2 mm	+	+	-	-	+	-	+	75%	-	+	25%	-	+	-	+	+	75%	+	25%	+	-	+	+	+	
1439	2 mm	+	-	-	-	-	-	+	100%	-	-	-	-	+	-	+	+	75%	+	25%	+	+	+	+	+	
1440	4 mm	-	+	-	-	+	+	-	-	-	+	50%	+	50%	+	+	+	75%	+	25%	+	+	+	+	*	N/A
1441	2 mm	+	+	-	-	+	-	+	75%	-	+	25%	-	+	-	+	+	75%	+	25%	+	-	+	+	+	
1442	2 mm	-	+	-	-	+	-	-	-	-	+	100%	-	N/A	-	-	+	+	75%	+	25%	+	-	-	+	

* N/A – data not available

Table 7: Experiment 31. - Control samples

Control samples		1.Shape of epithelial cells						2.Morphological characteristic of the epithelium				3. Presence of bacteria on the cell surface			4. Presence and shape of microvilli			5. Extrusion of lipid droplets	6. Others								
Nr. of samples	Investigated region	1.1.Normal appearance		1.2 Abnormal appearance		1.2.1 Not smooth surface		1.2.2 Enlarge cells		1.2.3 Partly flat		1.2.4 Flat		2.1 Predominantly (dome shaped)	2.2 Enlarge cells , not smooth surface	2.3 Partly flat epithelium (less than 50 %)	2.4 Predominant flat epithelium(more than 50%)	3.1 Presence of bacteria	3.2 Densely (big amount)	3.3 Low amount	4.1 Normal (equal shape 0.5 µm, individual grouped)	4.2 Abnormal (shorter, grouped, absent, decayed)	4.3 Partly covered with material	5.1Extrusion of lipid droplets	6.1 Presence of cellular protrusions	6.2 Interaction with NP	
		1457	1 mm	+	-	-	-	-	-	-	-	-	-	-	+	100%	-	-	-	+	-	+	***	***	+	+	+
1458	2.5 mm	+	-	-	-	-	-	-	-	-	-	-	+	100%	-	-	-	+	-	+	+	+	+	-	-	-	-
1459	3.5 mm	+	-	-	-	-	-	-	-	-	-	-	+	100%	-	-	-	-	-	+	+	+	+	-	-	-	-
1460	4 mm	-	+	-	-	+	+	-	-	-	-	-	-	-	+	50 %	+	50 %	-	+	+	+	+	-	+	-	-
1461	4 mm	-	+	-	-	+	-	-	-	-	-	-	-	-	+	100%	-	+	-	+	+	+	-	-	-	-	-
1462	4 mm	+	+	-	-	+	-	+	-	-	-	-	+	25 %	-	+	-	+	-	+	+	+	+	+	-	-	-
1463	3 mm	+	+	-	-	+	-	+	-	-	-	-	+	75 %	-	+	-	+	-	+	+	+	+	-	-	-	-

N/A – data not available

+** - can not be assessment

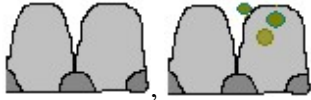





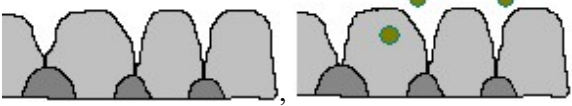
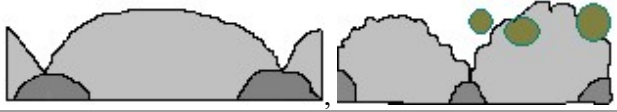


Table 8: Experiment 31. – Exposed samples to Ag (1000 ppm)

Exposed samples to Ag		1.Shape of epithelial cells						2.Morphological characteristic of the epithelium				3. Presence of bacteria on the cell surface			4. Presence and shape of microvilli			5. Extrusion of lipid droplets	6. Others						
Nr. of samples	Investigated region	1.1.Normal appearance		1.2.Abnormal appearance		1.2.1 Not smooth surface	1.2.2 Enlarge cells	1.2.3 Partly flat	1.2.4 Flat	2.1 Predominantly (dome shaped)	2.2 Enlarge cells , not smooth surface	2.3 Partly flat epithelium (less than 50 %)	2.4 Predominant flat epithelium (more than 50%)	3.1 Presence of bacteria	3.2 Densely (big amount)	3.3 Low amount	4.1 Normal (equal shape 0.5 µm, individual grouped)	4.2 Abnormal (shorter, grouped, absent, decayed)	4.3 Partly covered with material	5.1Extrusion of lipid droplets	6.1 Presence of cellular protrusions	6.2 Interaction with NP			
		+	-	+	-																		+	-	+
1464	2 mm	+	+	-	+	+	-	+	50 %	+	25 %	+	25 %	-	+	+	-	+	75 %	+	25 %	+	+	-	-
1465	2 mm	+	+	-	+	-	-	-	75 %	+	25 %	-	-	+	-	+	+	+	75 %	+	25 %	+	+	-	-
1466	5 mm	+	-	-	-	-	-	-	100%	-	-	-	-	+	-	+	+	+	50 %	+	50 %	+	+	-	-
1467	2.5 mm	+	-	-	-	-	-	-	100%	-	-	-	-	+	-	+	+	+	75 %	+	25 %	+	-	-	-

Table 9: Experiment 31. – Exposed samples to Ag (5000 ppm)

Exposed samples to Ag		1.Shape of epithelial cells						2.Morphological characteristic of the epithelium				3. Presence of bacteria on the cell surface			4. Presence and shape of microvilli			5. Extrusion of lipid droplets	6. Others						
Nr. of samples	Investigated region	1.1.Normal appearance		1.2.Abnormal appearance		1.2.1 Not smooth surface	1.2.2 Enlarge cells	1.2.3 Partly flat	1.2.4 Flat	2.1 Predominantly (dome shaped)	2.2 Enlarge cells , not smooth surface	2.3 Partly flat epithelium (less than 50 %)	2.4 Predominant flat epithelium (more than 50%)	3.1 Presence of bacteria	3.2 Densely (big amount)	3.3 Low amount	4.1 Normal (equal shape 0.5 µm, individual grouped)	4.2 Abnormal (shorter, grouped, absent, decayed)	4.3 Partly covered with material	5.1Extrusion of lipid droplets	6.1 Presence of cellular protrusions	6.2 Interaction with NP			
		+	-	+	-																		+	-	+
1468	1 mm	+	+	-	-	+	-	+	50 %	-	+	50%	-	-	-	+	+	50 %	+	50 %	+	-	-	-	
1469	5 mm	+	+	-	-	+	-	+	75 %	-	+	25 %	-	+	-	+	+	25 %	+	75 %	+	+	+	-	-
1470	3 mm	+	+	-	-	-	+	+	50 %	-	-	+	50 %	-	-	-	+	+	25 %	+	75 %	+	-	+	-
1471	4 mm	+	+	-	-	-	+	+	50 %	-	-	+	50 %	+	-	+	+	25 %	+	75 %	+	-	+	-	-

Table 10: Schematic presentation of digestive gland epithelium characteristics

Characteristics		Typical representing figure	Schematic
1. Shape of epithelial cells	1.1 Normal appearance	Figure 9 a. Figure 9 b.	
	1.2 Abnormal appearance	Figure 10 a, 10 b. Figure 11 a, 11 b. Figure 11 a, 11 b.	
	1.2.1 Not smooth surface	Figure 10 a. Figure 10 b.	
	1.2.2 Enlarge cells	Figure 10 a. Figure 10 b.	
	1.2.3 Partly flat	Figure 11 a. Figure 11 b.	
	1.2.4 Flat	Figure 12 a. Figure 12 b.	
2. Morphological characteristic of the epithelium	2.1 Predominantly (dome shaped)	Figure 13 a. Figure 13 b.	
	2.2 Enlarge cells , not smooth surface	Figure 14 a. Figure 14 b.	
	2.3 Partly flat epithelium (less than 50 %)	Figure 15 a. Figure 15 b.	
	2.4 Predominant flat epithelium (more than 50 %)	Figure 16 a. Figure 16 b	










3. Presence of bacteria on the cell surface	3.1	Presence of bacteria	Figure 17 a. Figure 17 b.	
	3.2	Densely (big amount)	Figure 18 a. Figure 18 b.	
	3.3	Low amount	Figure 19 a. Figure 19 b.	
4. Presence and shape of microvilli	4.1	Normal (equal shape 0.5 μm, individual not grouped)	Figure 20 a. Figure 20 b.	
	4.2	Abnormal (shorter, absent or decayed in apical part)	Figure 21 a. Figure 21 b. Figure 22 a. Figure 22 b.	
	4.3	Partly covered with material	Figure 23 a. Figure 23 b.	
5. Extrusion of lipids droplets	5.1	Extrusion of lipid droplets	Figure 24 a. Figure 24 b.	
6. Others	6.1	6.1 Presence of cellular protrusions	Figure 25 a. Figure 25 b.	
	6.2	Interaction with NT	Figure 26 a. Figure 26 b. Figure 26 c.	

Figure 9.a: Shape of cells in digestive gland epithelium (hepatopancreas)- normal appearance.

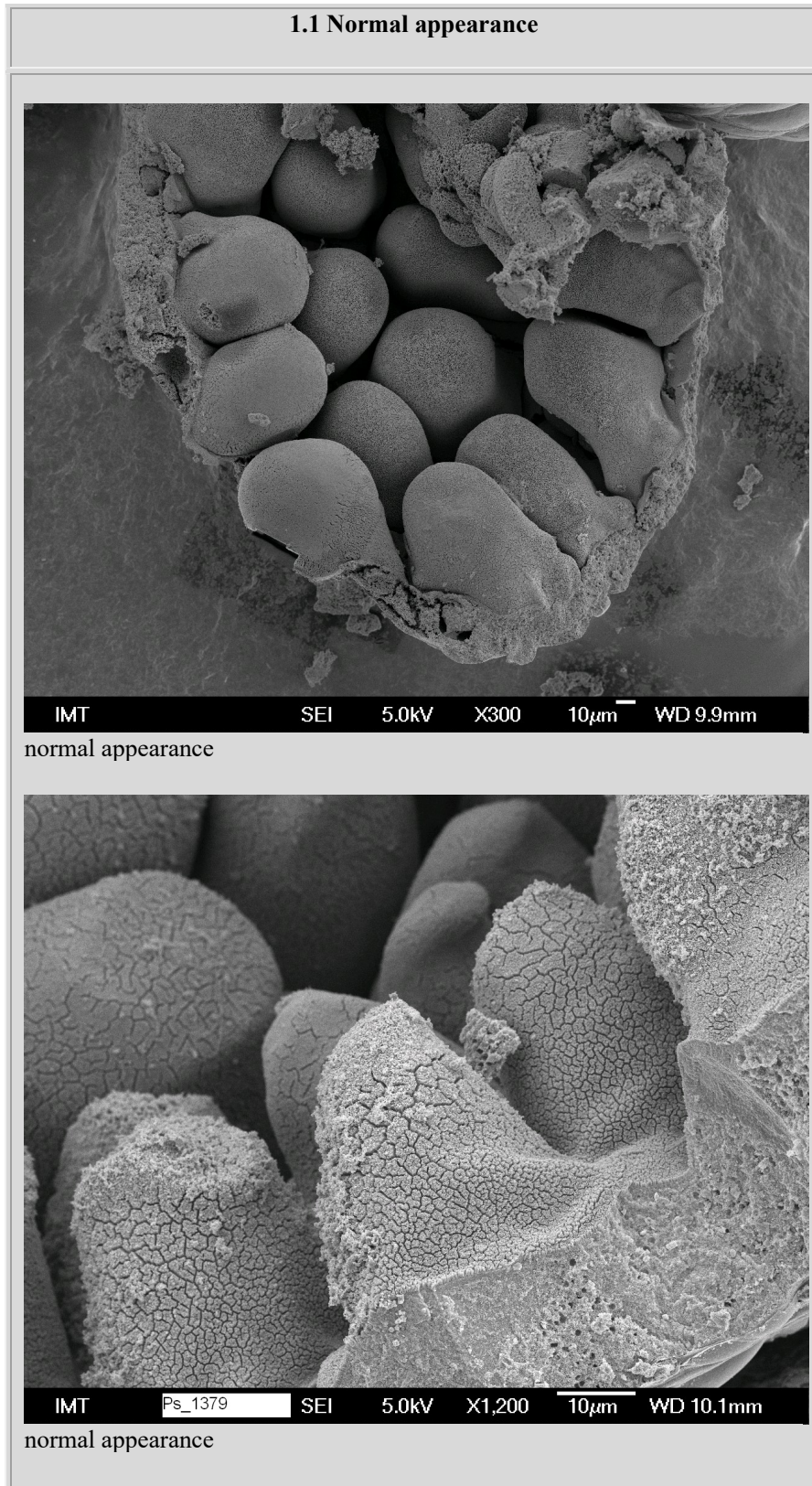
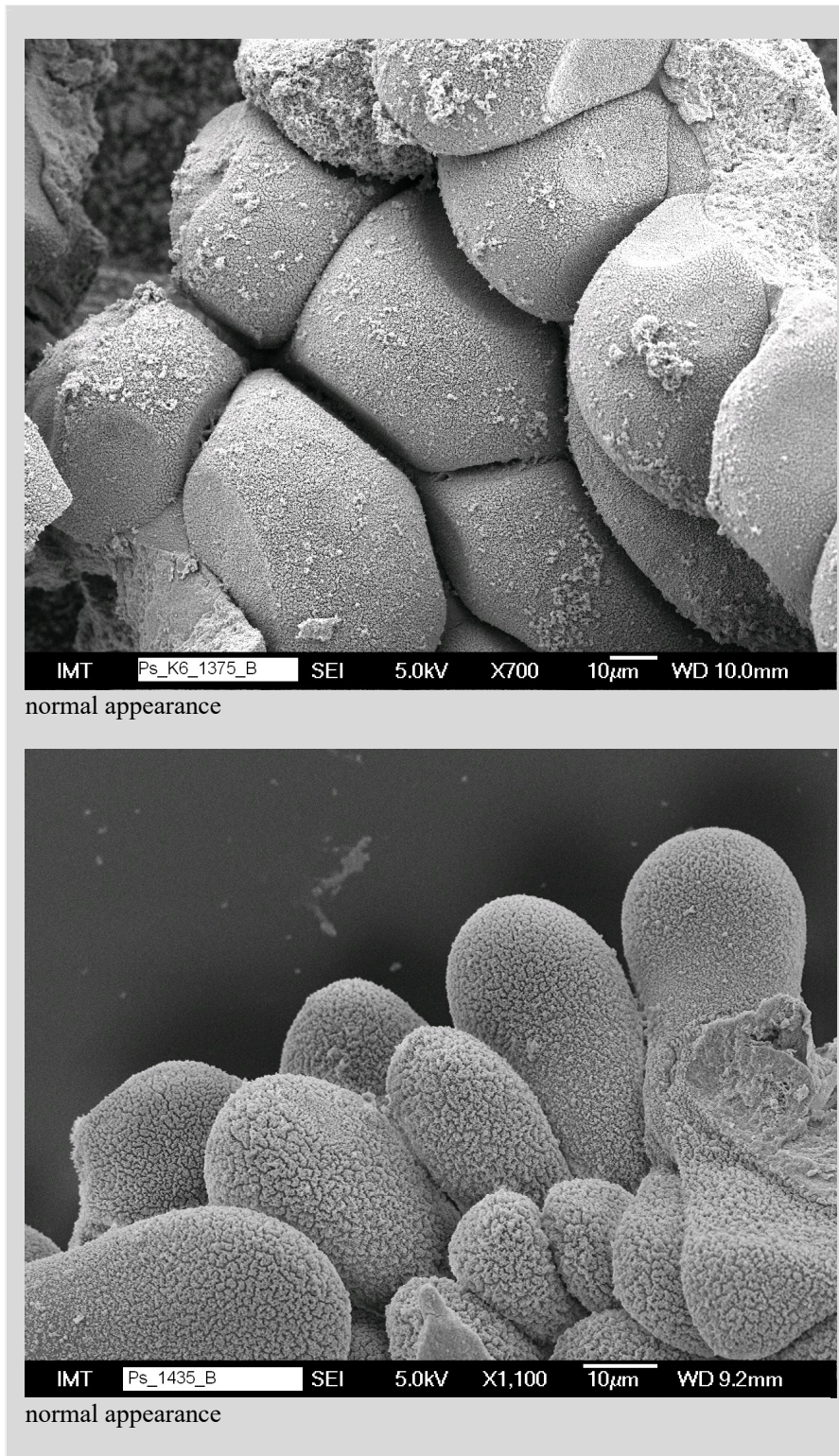


Figure 9.b: Shape of the cells in digestive gland epithelium (hepatopancreas)- normal appearance.



The shape of the cells is dome- shape, with normal size length 50- 80 μm , width 30-50 μm , covered with homogenous microvilli in the surface.

Figure 10.a: Shape of the cells in digestive gland epithelium (hepatopancreas)- abnormal appearance.

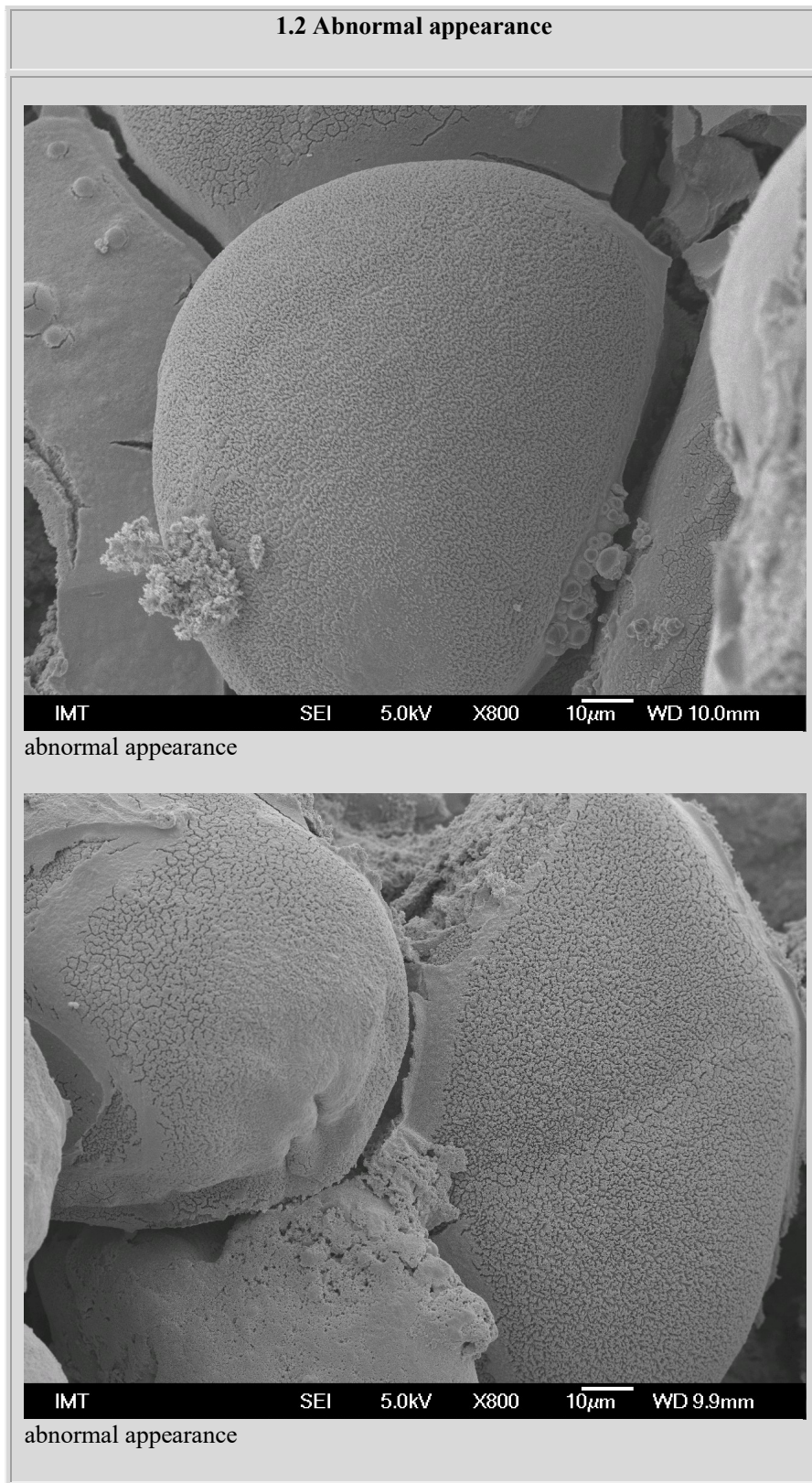
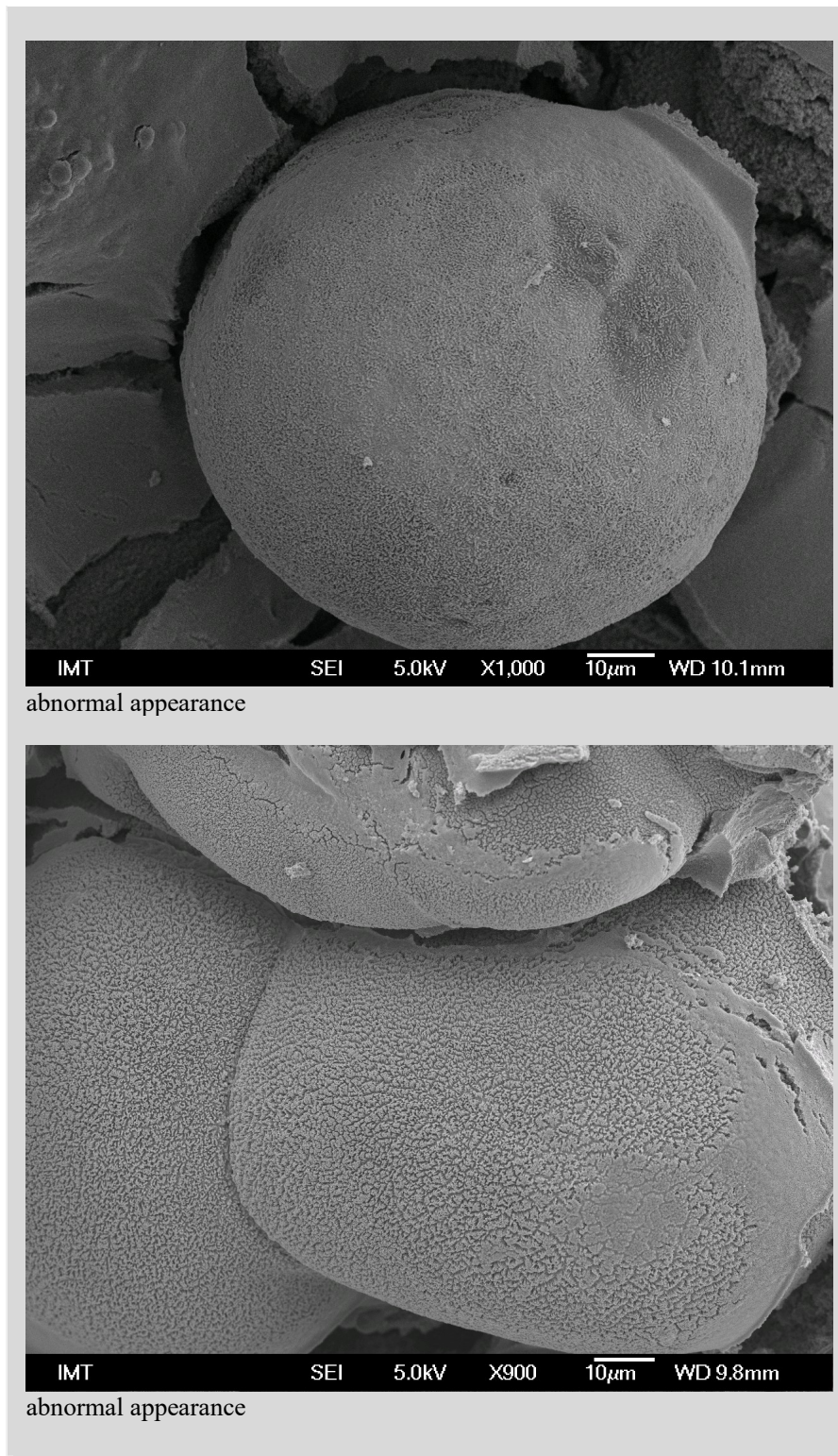


Figure 10.b: **Shape of the cells in digestive gland epithelium (hepatopancreas)- abnormal appearance.**



The abnormal appearance is when the shape of cells is different from the dome-shape. Abnormal appearance is when shape of cells is like pyramidal, not smooth surface and sometimes much bigger (more than 100 µm).

Figure 11.a: Shape of the cells in digestive gland epithelium (hepatopancreas)- partly flat appearance.

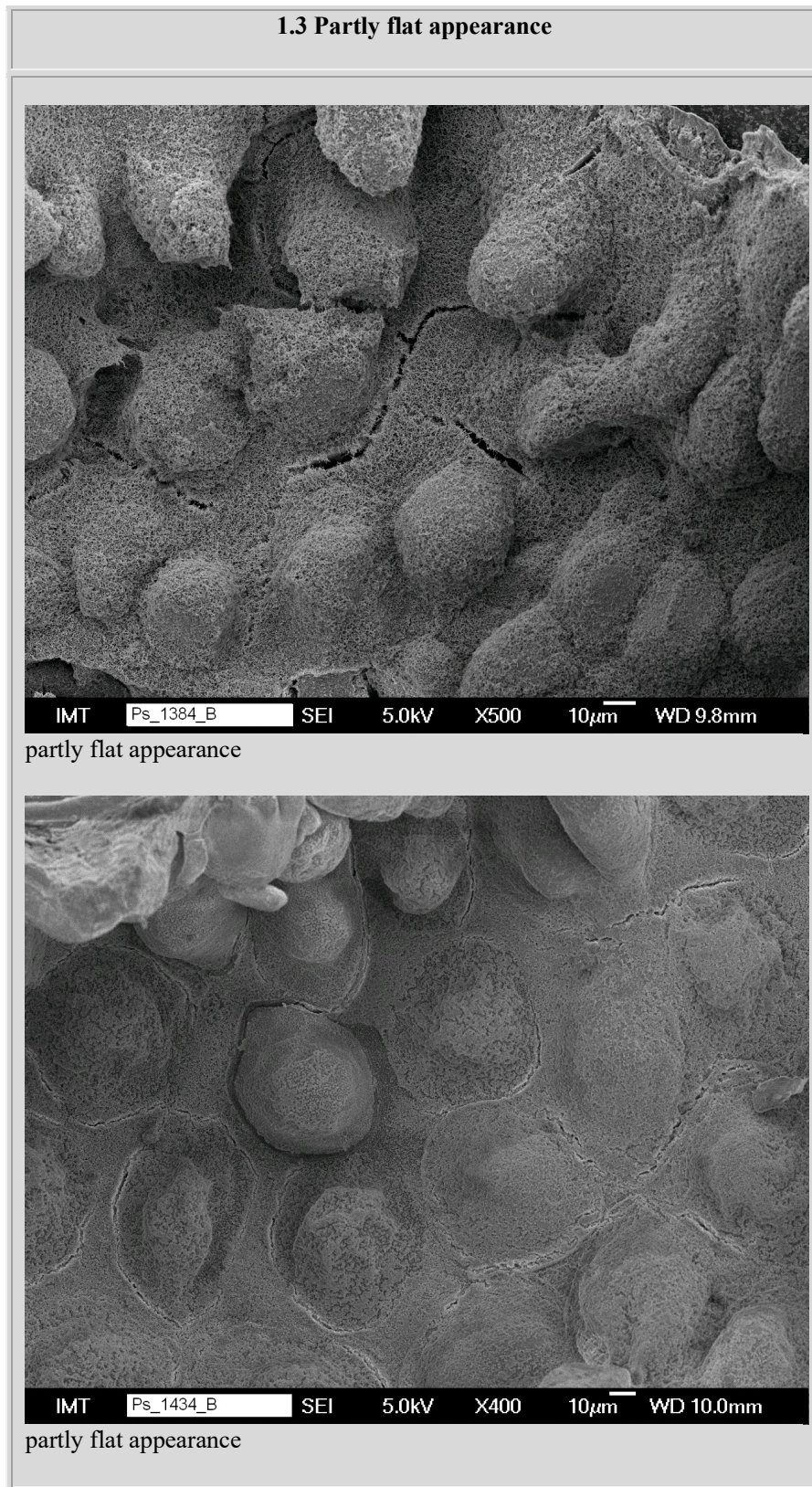
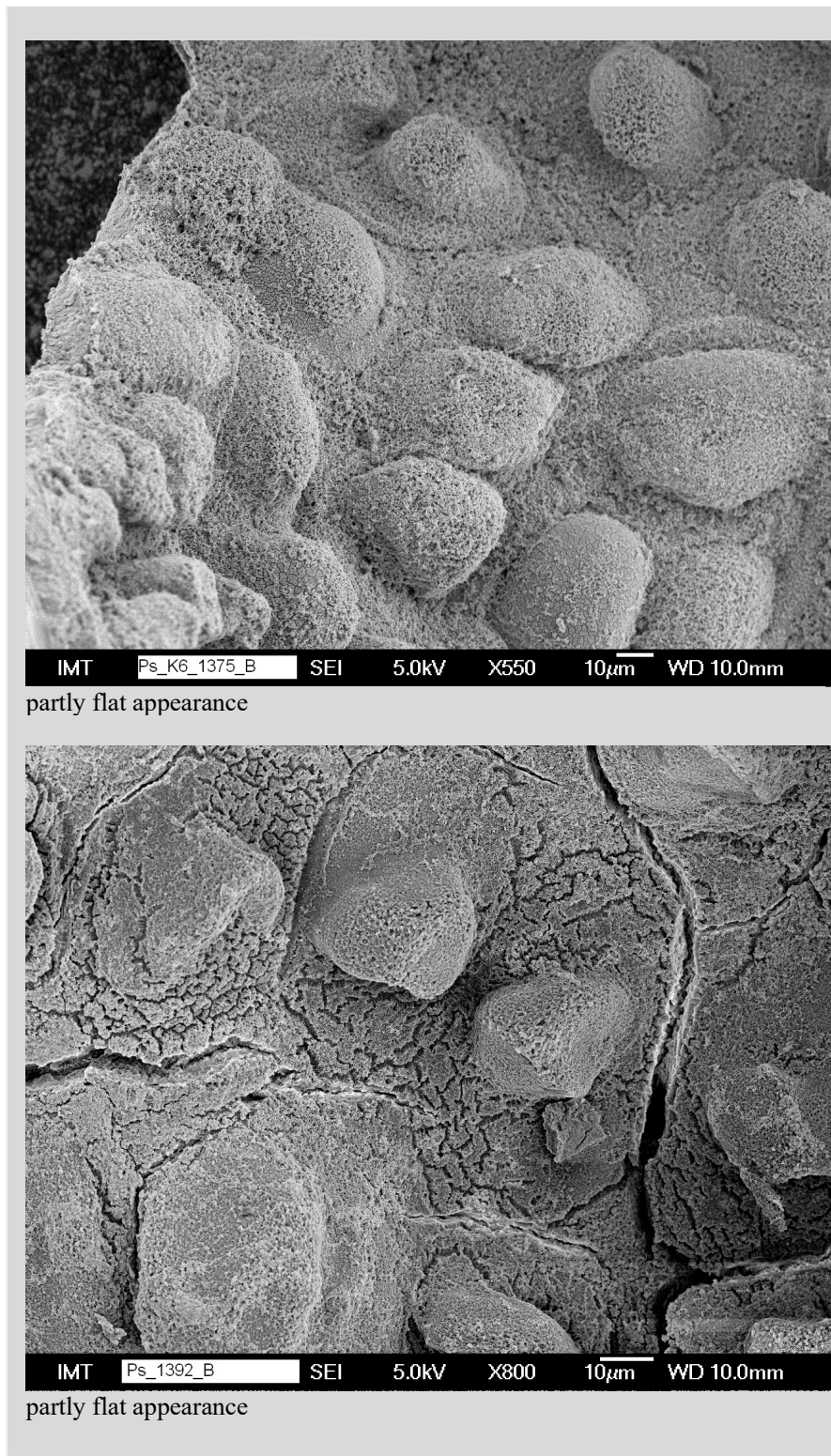


Figure 11.b: Shape of the cells in digestive gland epithelium (hepatopancreas)- partly flat appearance.



The partly flat appearance is encountered in cases when less than 50 % of cells have changed the form from the normal dome shaped.

Figure 12.a: Shape of the cells in digestive gland epithelium (hepatopancreas)- flat appearance.

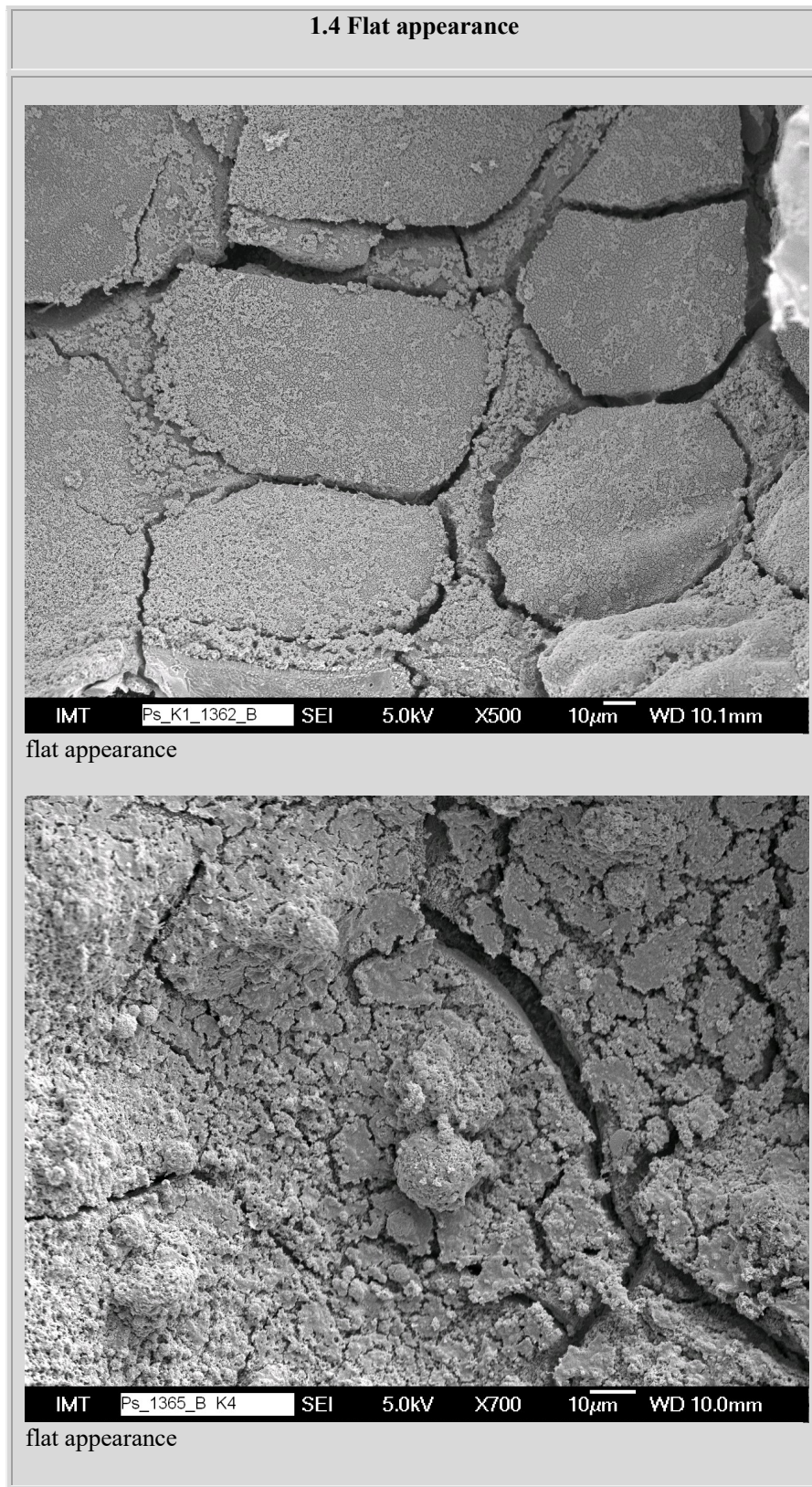
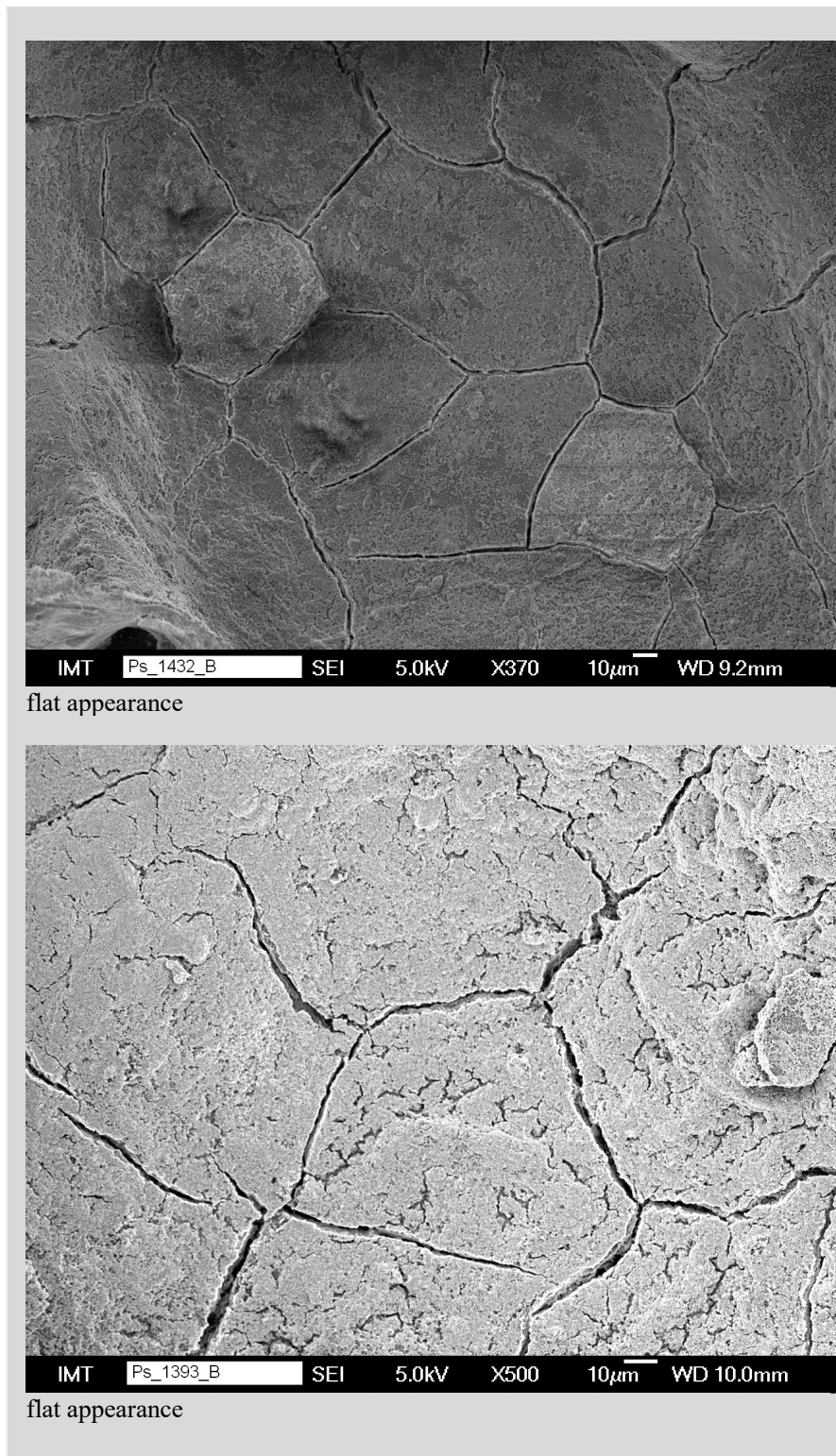


Figure 12.b: Shape of the cells in digestive gland epithelium (hepatopancreas)- flat appearance.



The flat appearance is encountered in cases when more than 50 % of cells have changed the form from the normal dome shaped. Low or completely flat hepatopancreatic B cells are taken as a abnormal appearance (Leser at al, 2008)

Figure 13.a: **Morphological characteristics of digestive gland epithelium (hepatopancrease)- Predominantly (Dome shaped)**

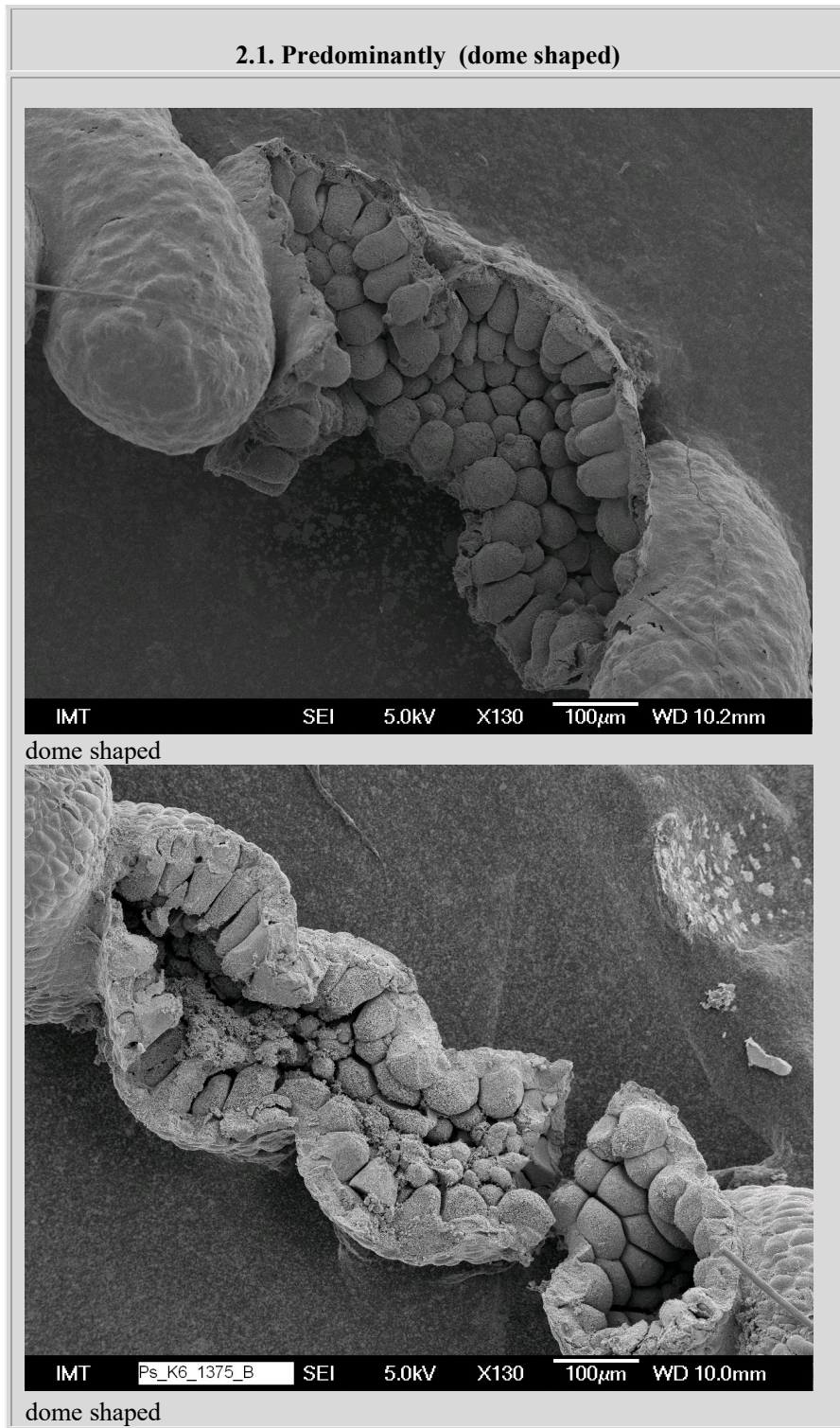
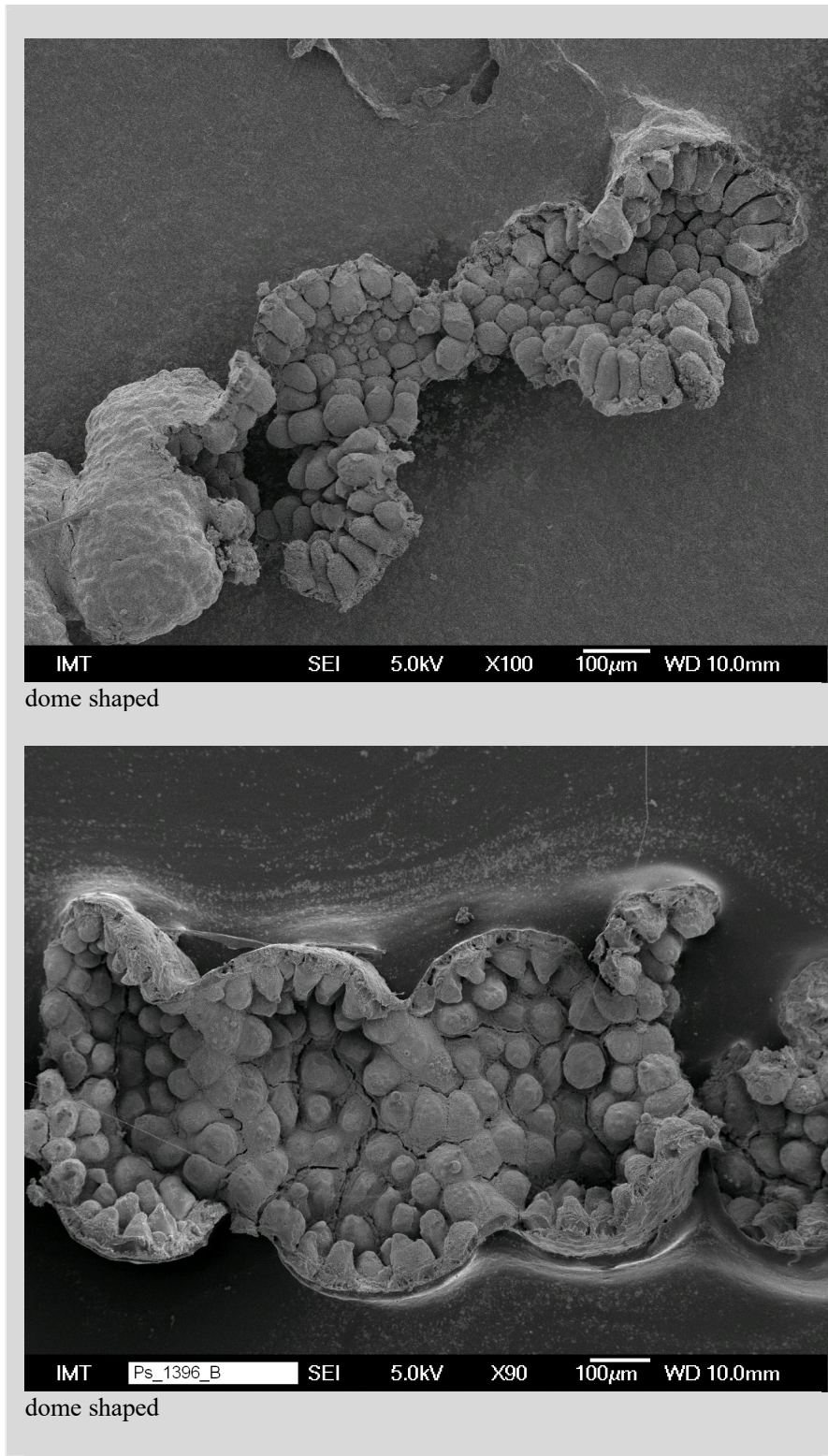


Figure 13.b: 2.Morphological characteristics of digestive gland epithelium (hepatopancrease)-
Predominantly dome shaped



Hepatopancrease digestive tube is combined from two different cells: B-cells and S-cells which alternate in the tube surrounded by the neuromuscular network (Wagele, 1992; Hames and Hopkin, 1989). Cells which are bigger are called B-cells and cells which are smaller are called S-cells.

Dome shape is called the normal shape of B-cells; the dimension of B-cells is around from 30-80 μm . In normal digestive tube the S-cells are much smaller; they are not seen because they are covered from the big B-cells. The cells are covered with microvilli which are homogenously distributed on the surface, but under some conditions they can be lost completely, or only in some regions. Normal micro-flora should be present in the digestive tube (hepatopancrease) but in the case of infection the amount of bacteria will colonize the cells (Drobne et al, 1999; Kostanjšek et al, 2004).

The thickness of digestive gland epithelium and extrusion of lipid droplets is different in organism. The thickness of digestive gland epithelium is bigger on the organisms which are in normal condition and is thinner in the organisms under the stress condition (Lešer et al, 2008).

Figure 14.a: **Morphological characteristics of digestive gland epithelium (hepatopancrease)- abnormal appearance.**

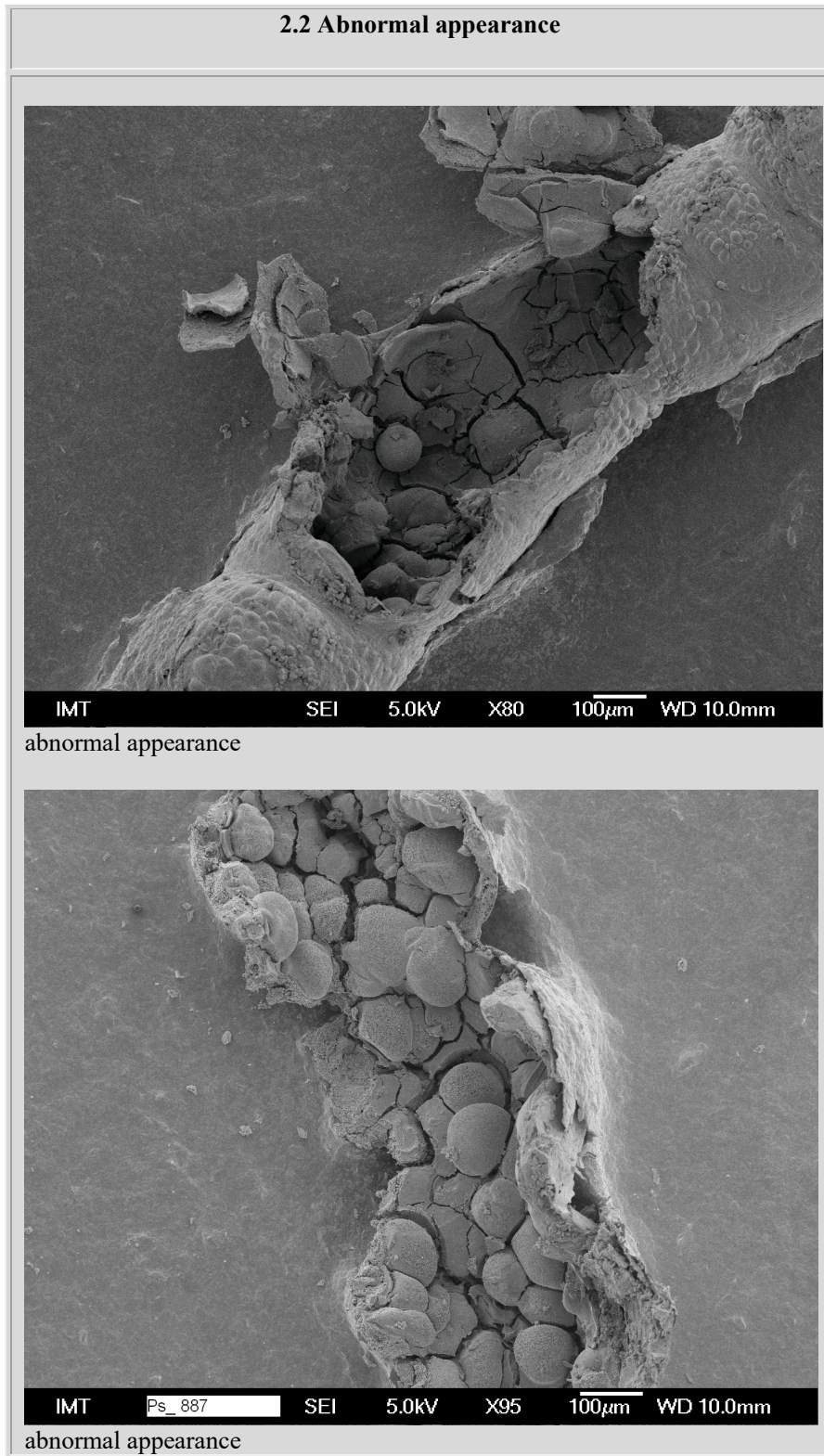


Figure 14.b: **Morphological characteristics of digestive gland epithelium (hepatopancrease)- abnormal appearance.**

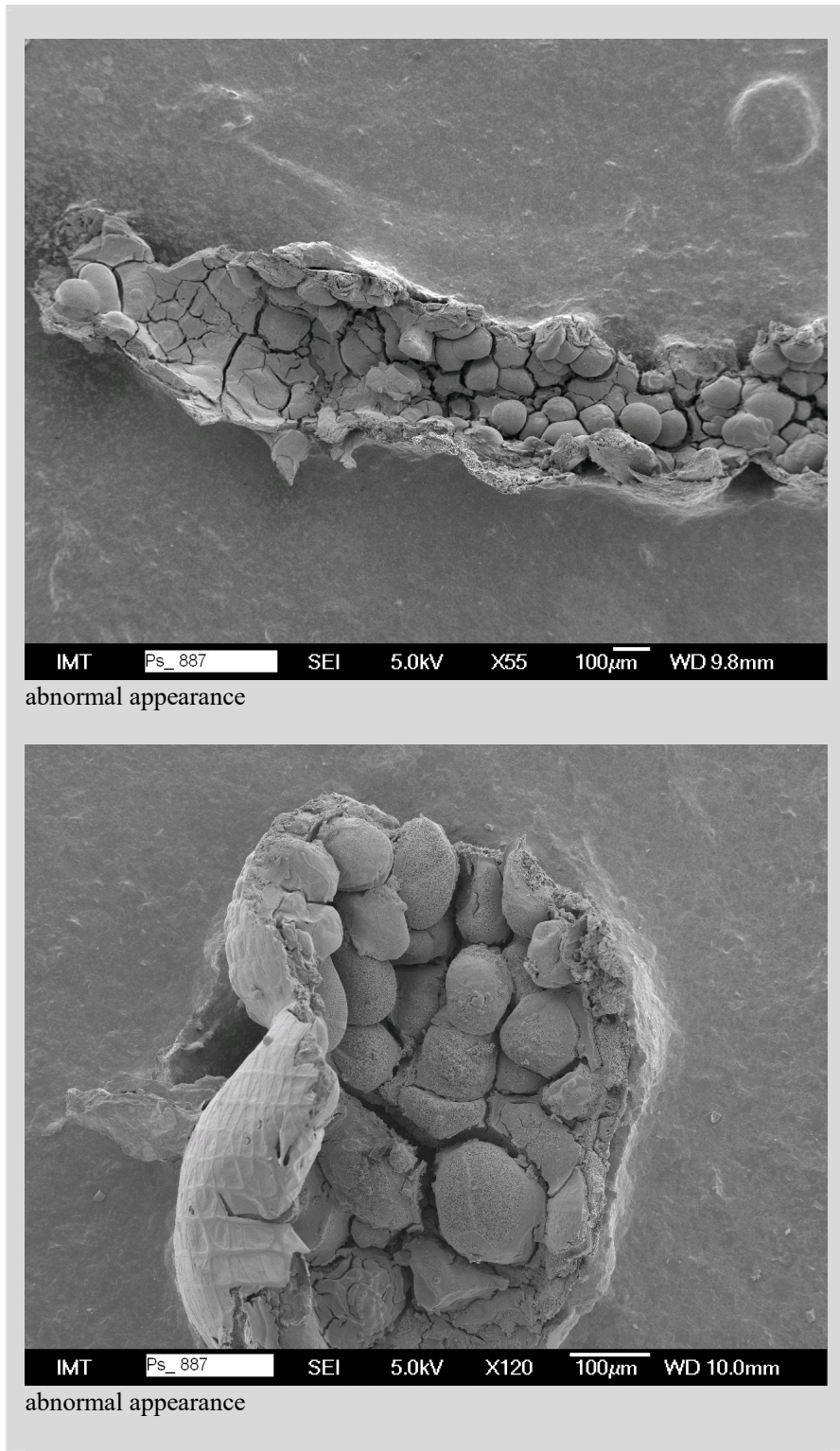


Figure 15.a: Morphological characteristics of digestive gland epithelium (hepatopancrease)- Partly flat epithelium (less than 50 %)

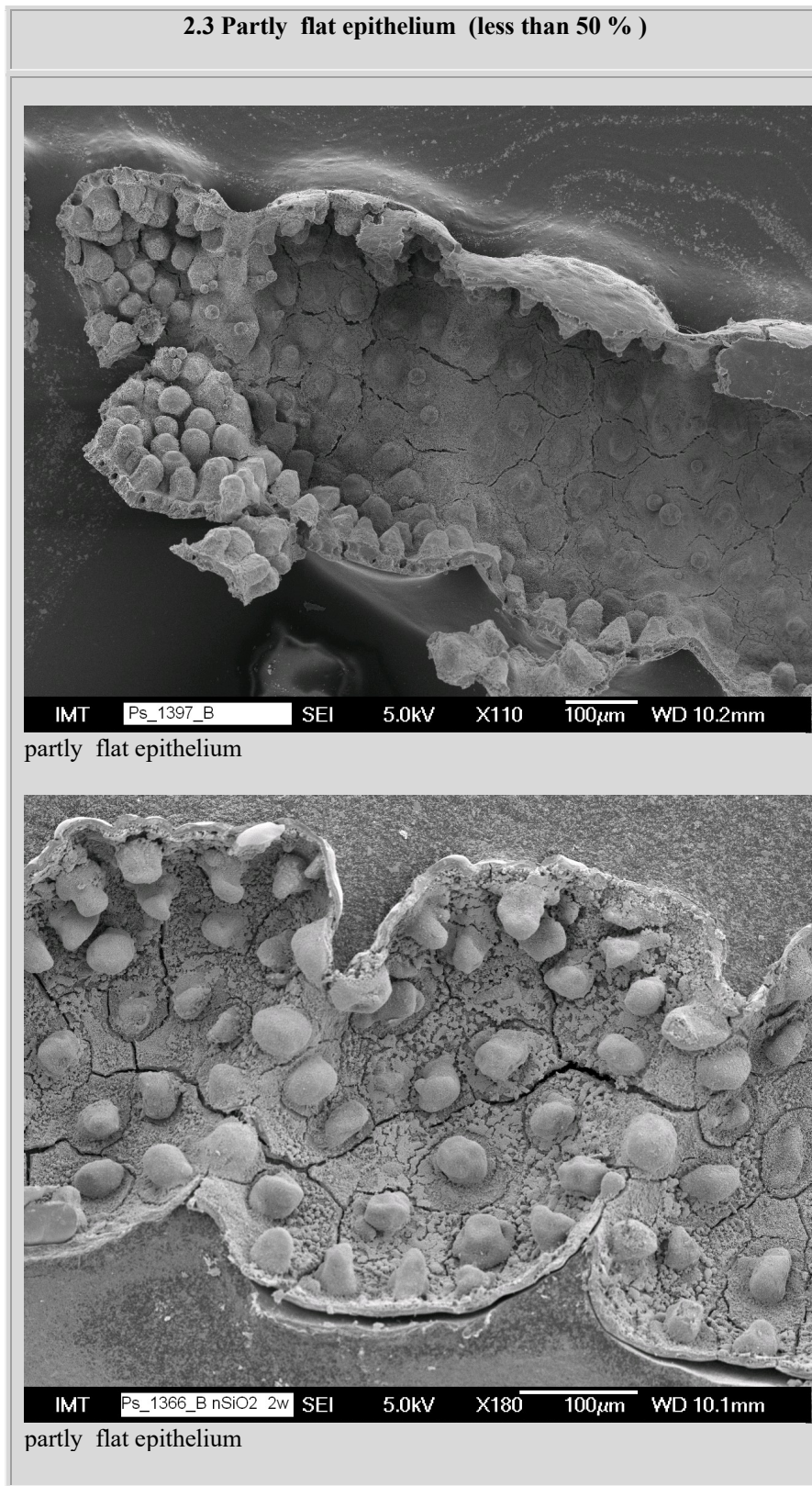
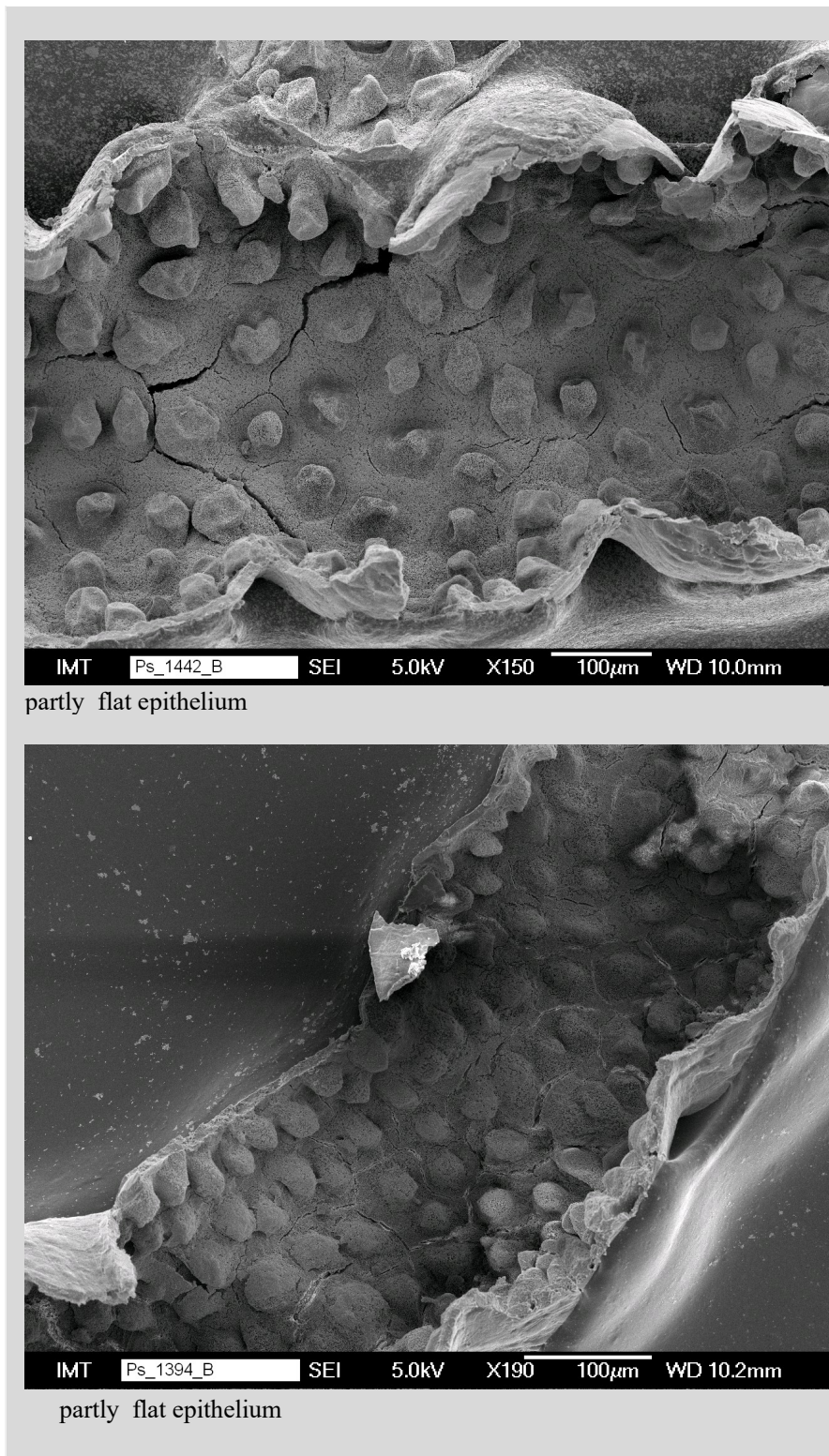


Figure 15.b Morphological characteristics of digestive gland epithelium (hepatopancrease)- Partly flat epithelium (less than 50 %)



A partly flat epithelium (less than 50 %) appearance is present in some digestive tube. Cells (dome shape) with normal shape and size are combined with the cells which are flat in some regions of digestive tube.

Figure 16.a: **Morphological characteristics of digestive gland epithelium (hepatopancrease)- Predominant flat epithelium (more than 50 %)**

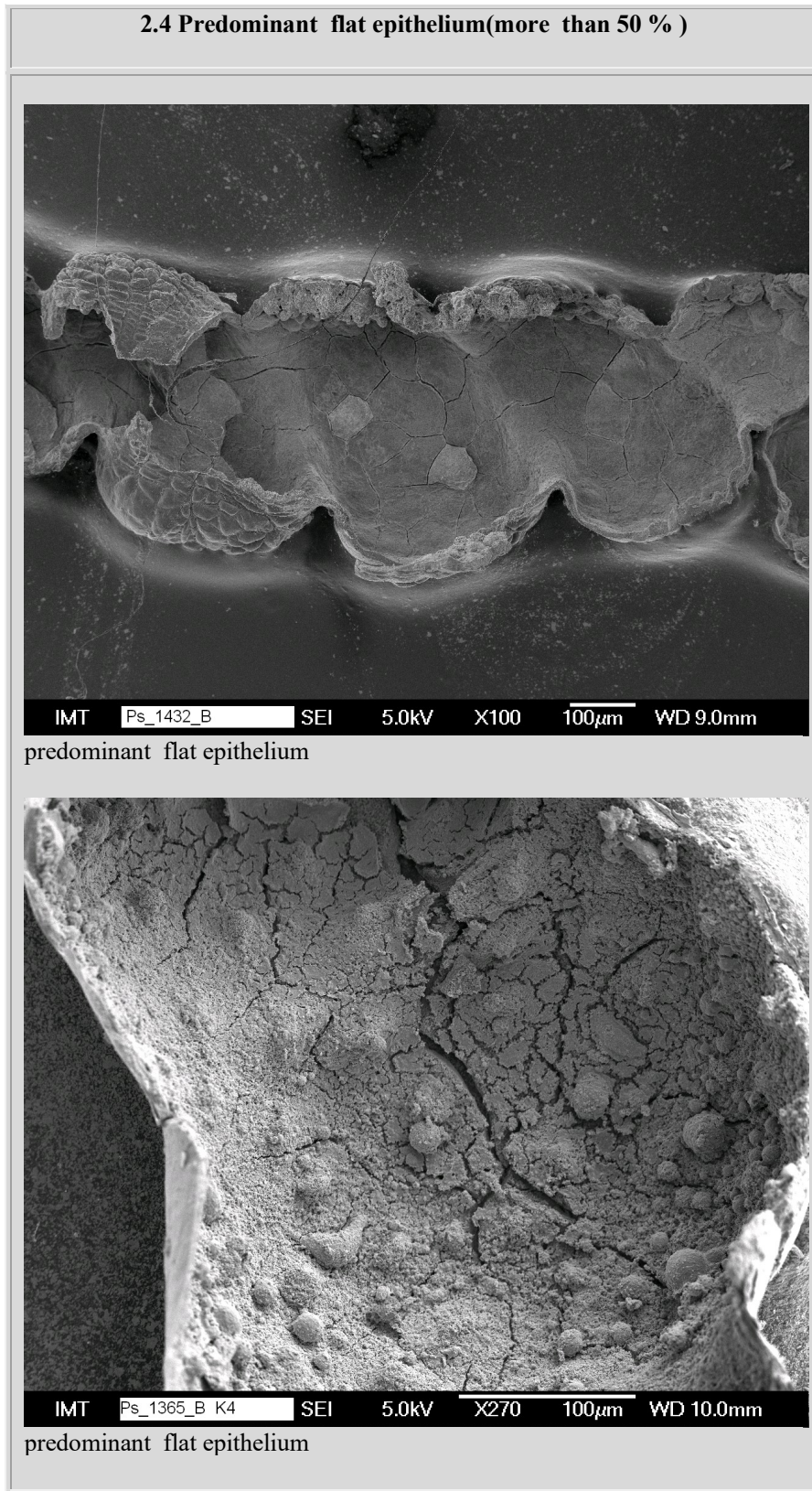


Figure 16.b: **Morphological characteristics of digestive gland epithelium (hepatopancrease)- Predominant flat epithelium (more than 50 %)**

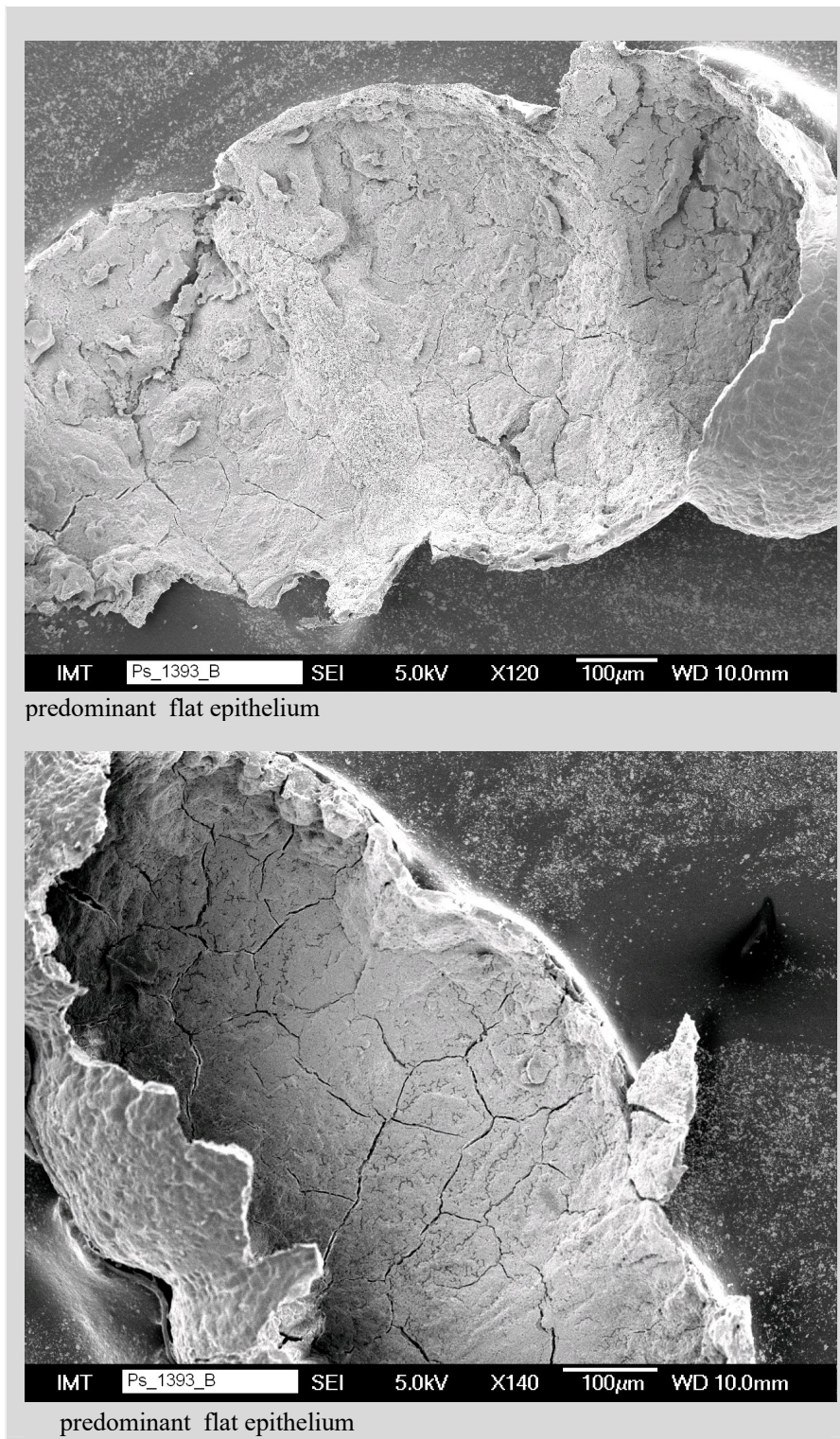


Figure 17.a: Presence of the bacteria in cells surface of digestive tube (hepatopancreas) – same and different bacteria on surface.

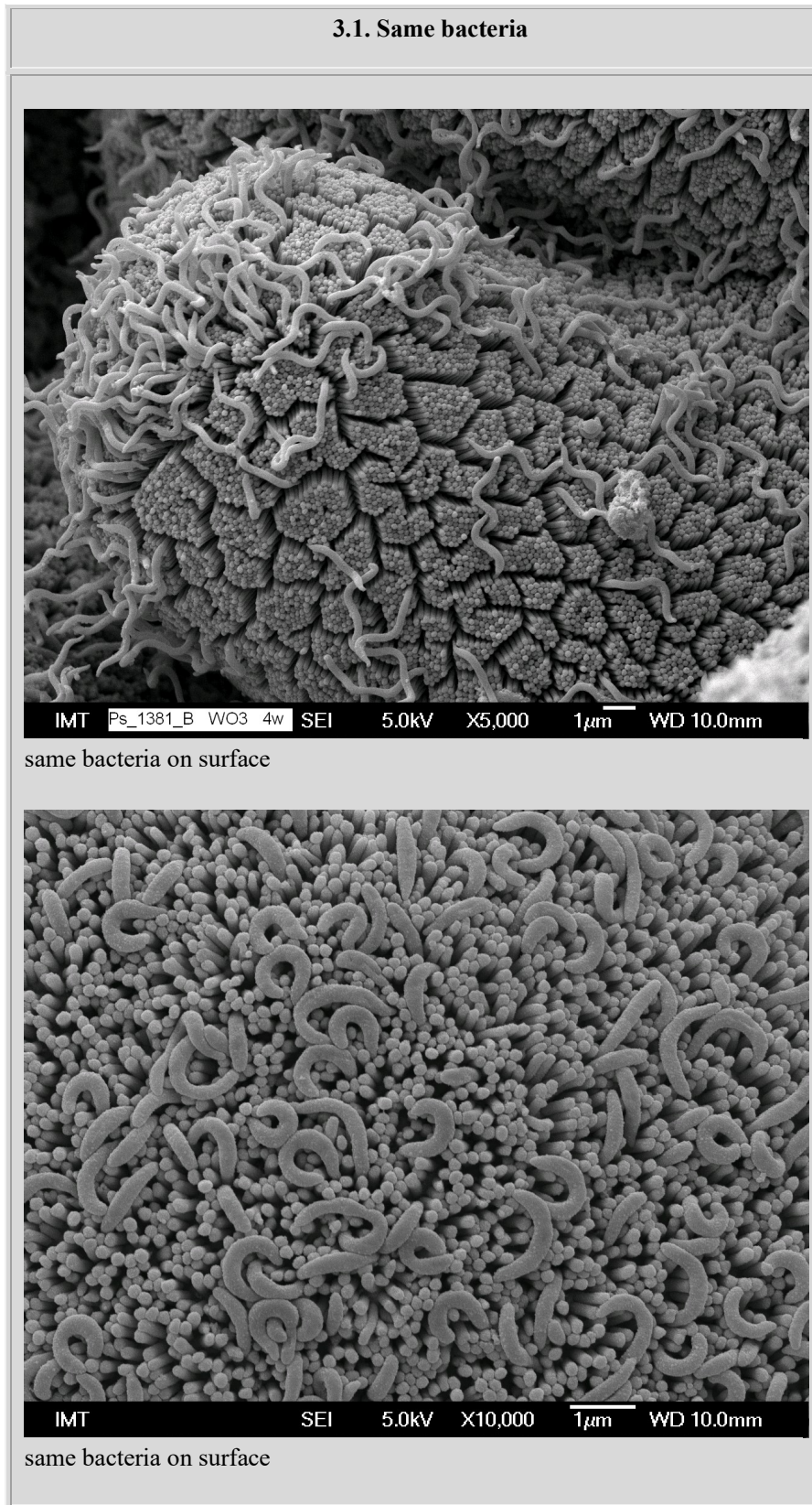
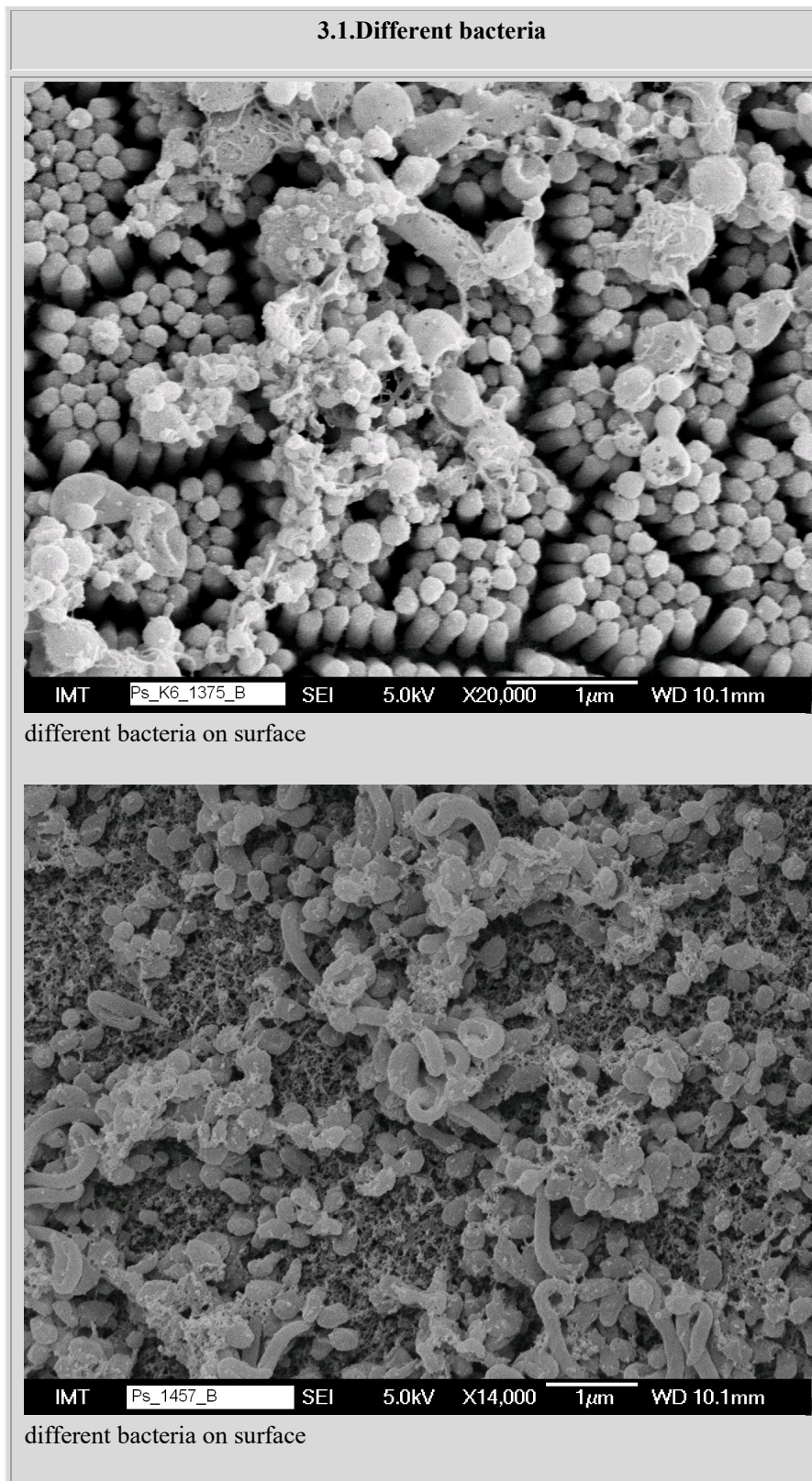


Figure 17.b: Presence of the bacteria in cells surface of digestive tube (hepatopancreas) – same and different bacteria on surface.



Different bacteria are part of digestive tube environment; they play a very significant role in the digestive process.

Some of the bacteria can cause different infections in the hepatopancreas tube. The bacteria which are present belong to these genes: bacillus, staphylococcus, enterococcus, pseudomonas ect.(Kostanjsek et al, 2002)

Figure 18.a: **Presence of the bacteria in cells surface of digestive tube (hepatopancreas) – densely colonized.**

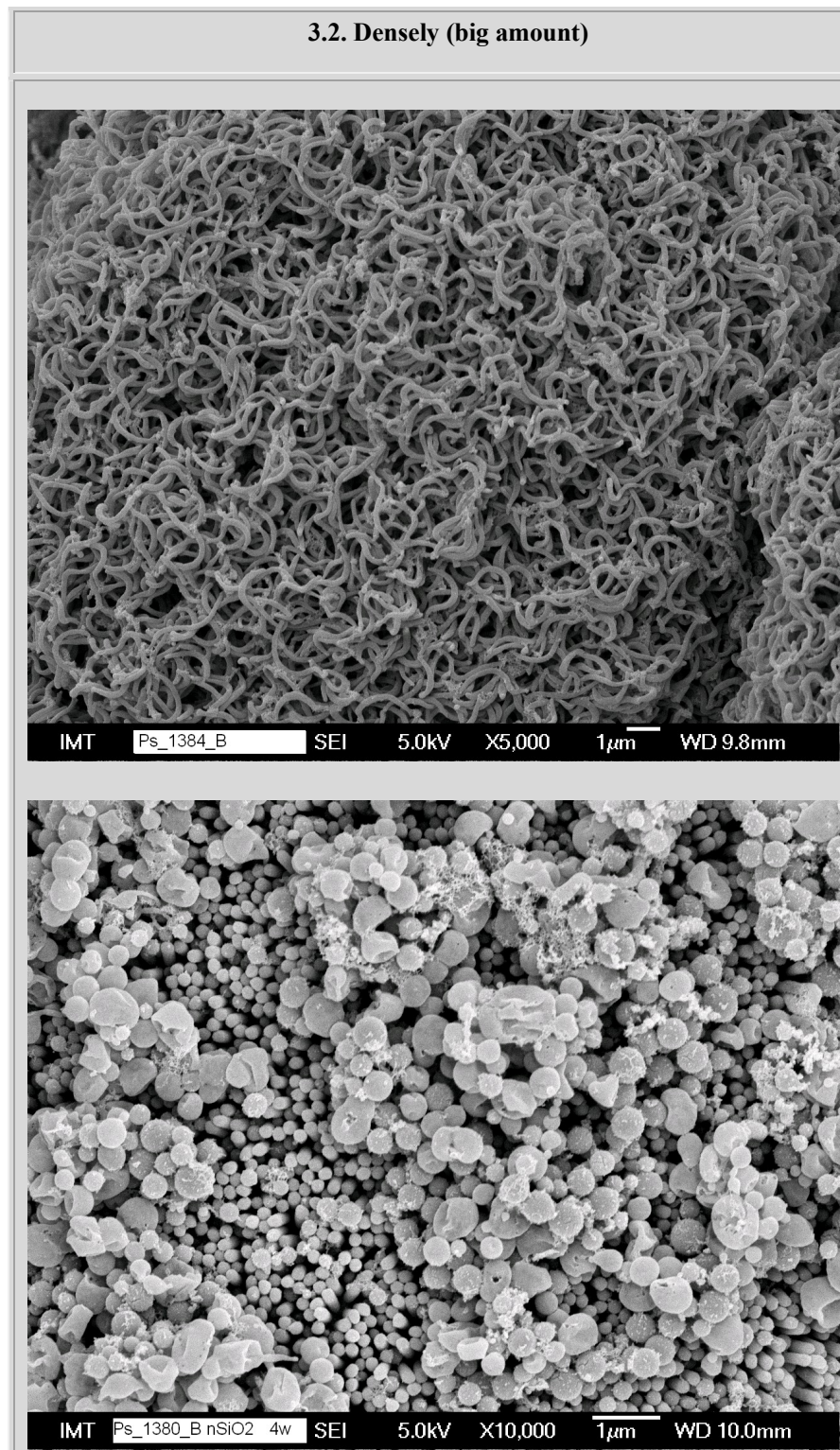
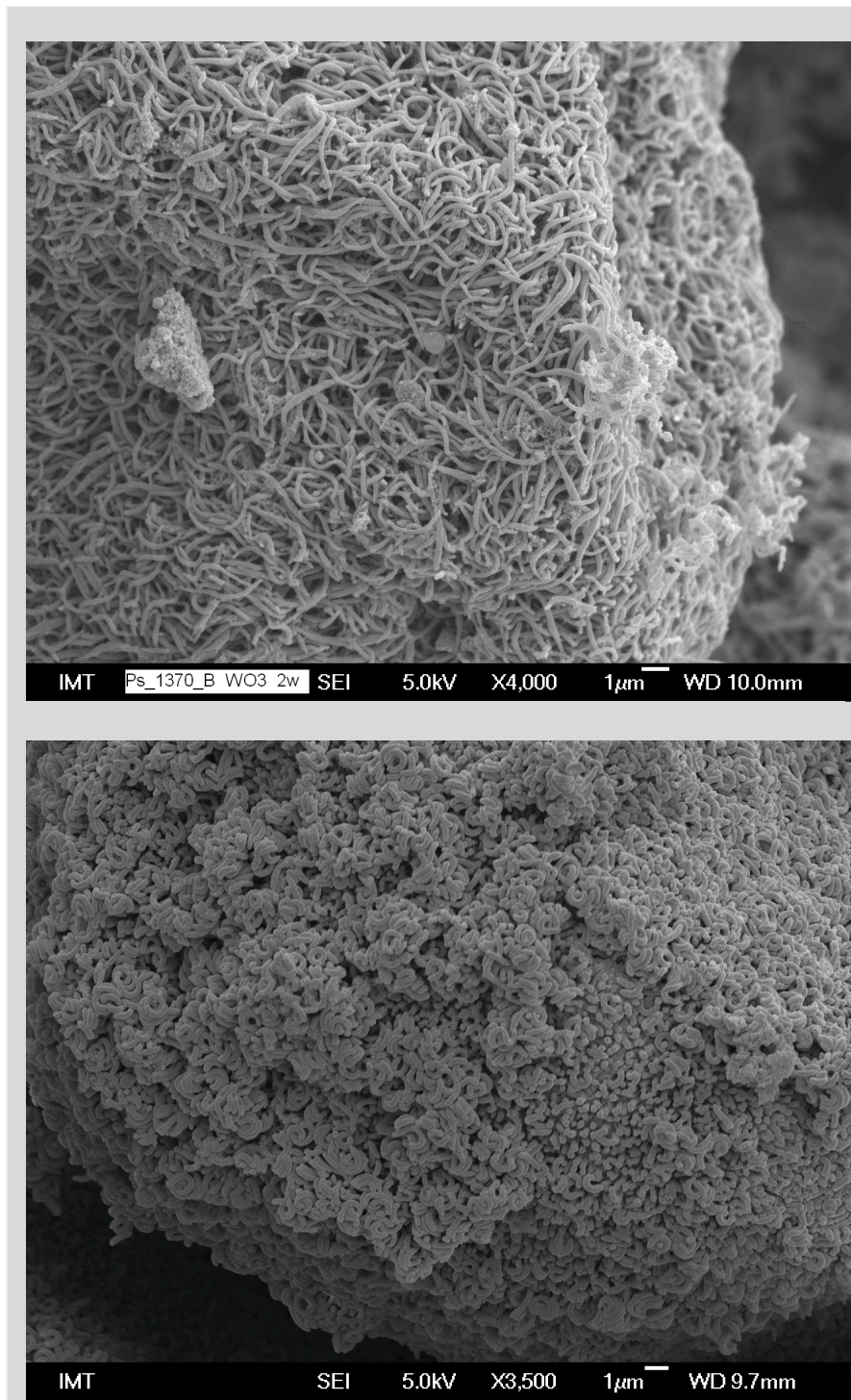


Figure 18.b: Presence of the bacteria in cells surface of digestive tube (hepatopancreas) – densely colonized.



We observed very often hepatopancreas tubs which were infected with bacteria completely or in some parts of tube. When the hepatopancreas is infected with bacteria we can see on the surface of cell a high amount of different bacteria. In this case the microvilli and the surface of the cells are unseen. From the histological investigation is proved that bacteria also are inside of the cell vesicle (Drobne at all, 1999).

Figure 19.a: Presence of the bacteria in cells surface of digestive tube (hepatopancreas) – low amount.

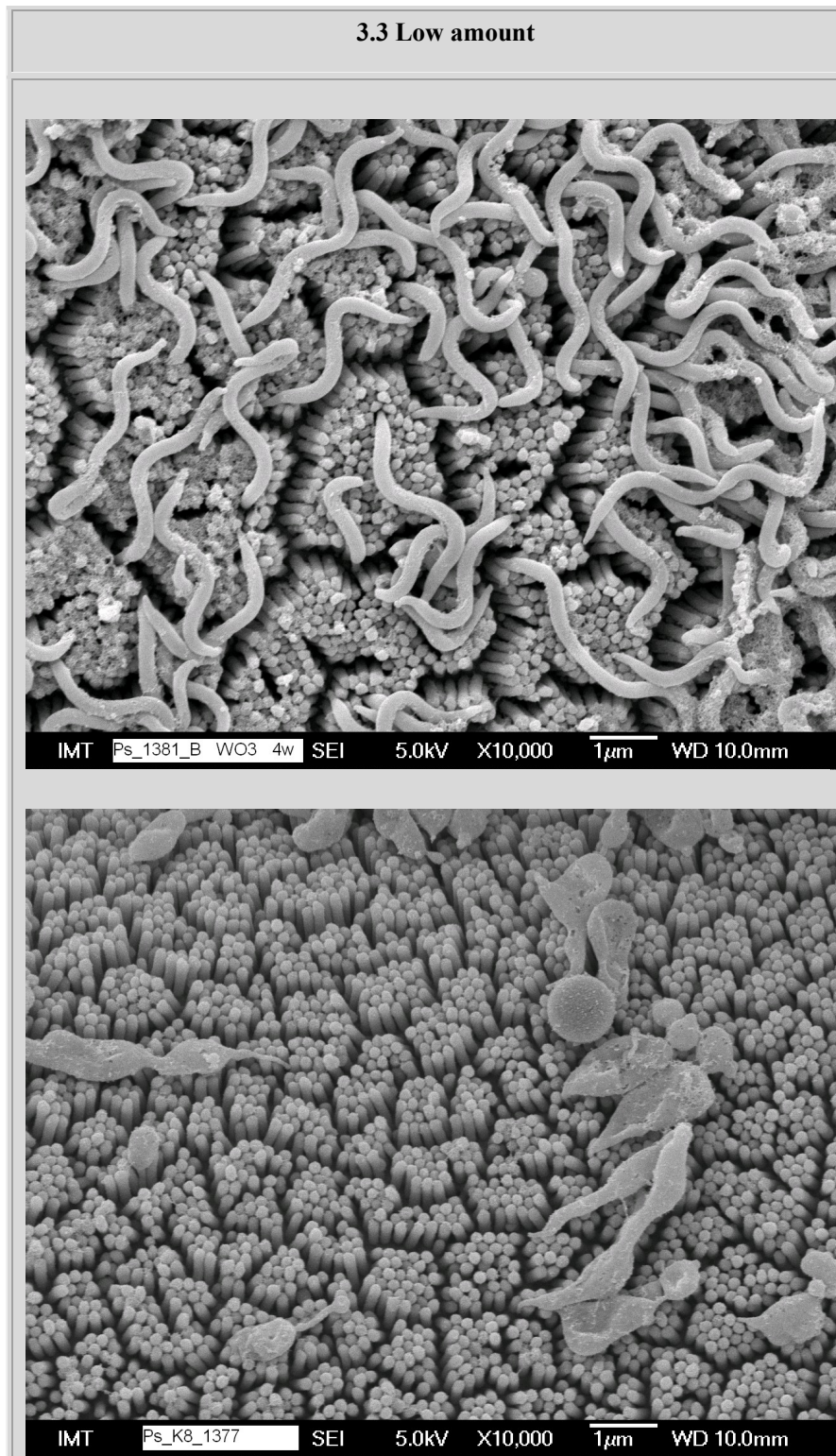


Figure 19.b: Presence of the bacteria in cells surface of digestive tube (hepatopancreas) – low amount.

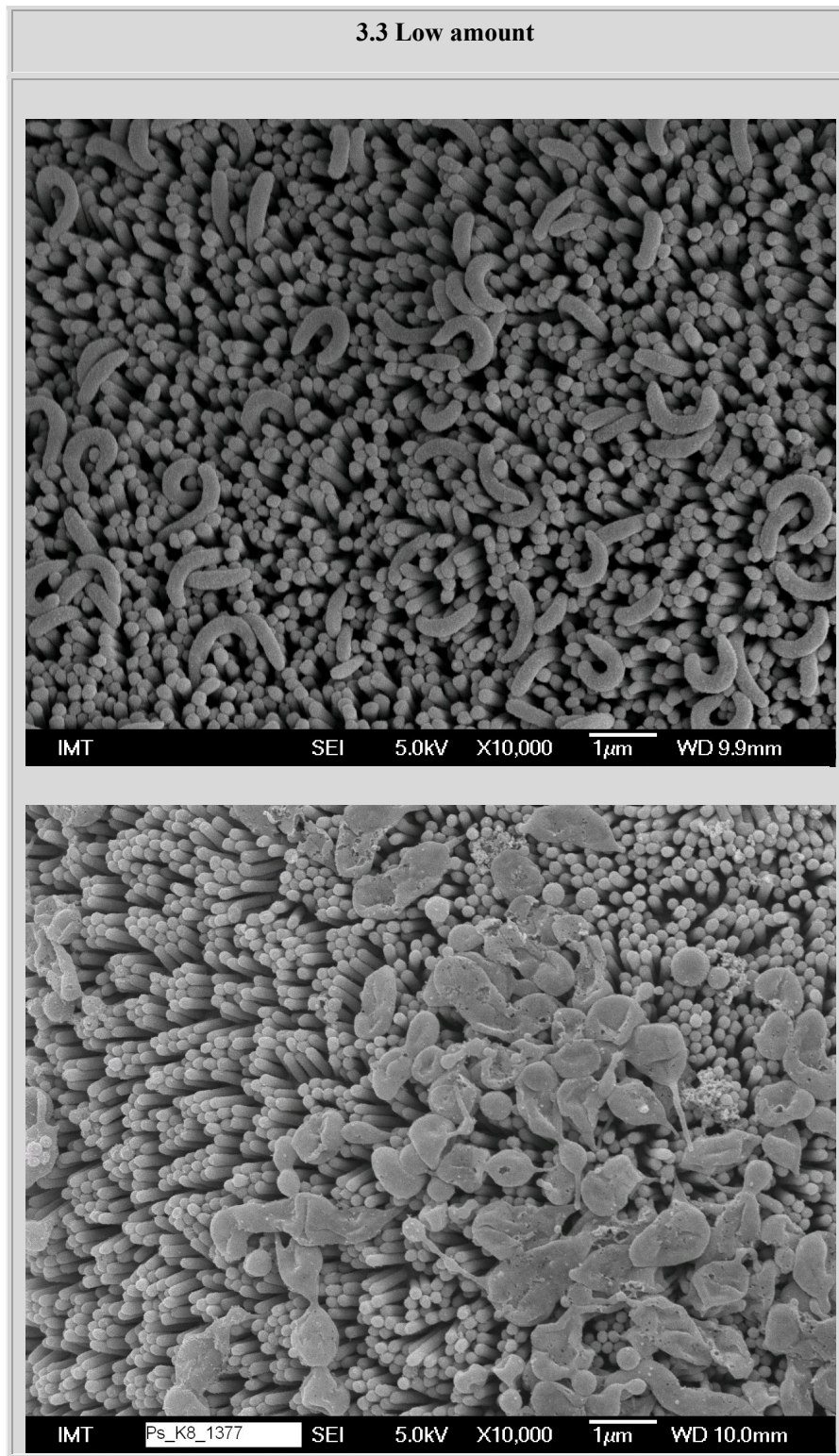


Figure 20.a: Presence and shape of microvilli in cells surface - normal appearance.

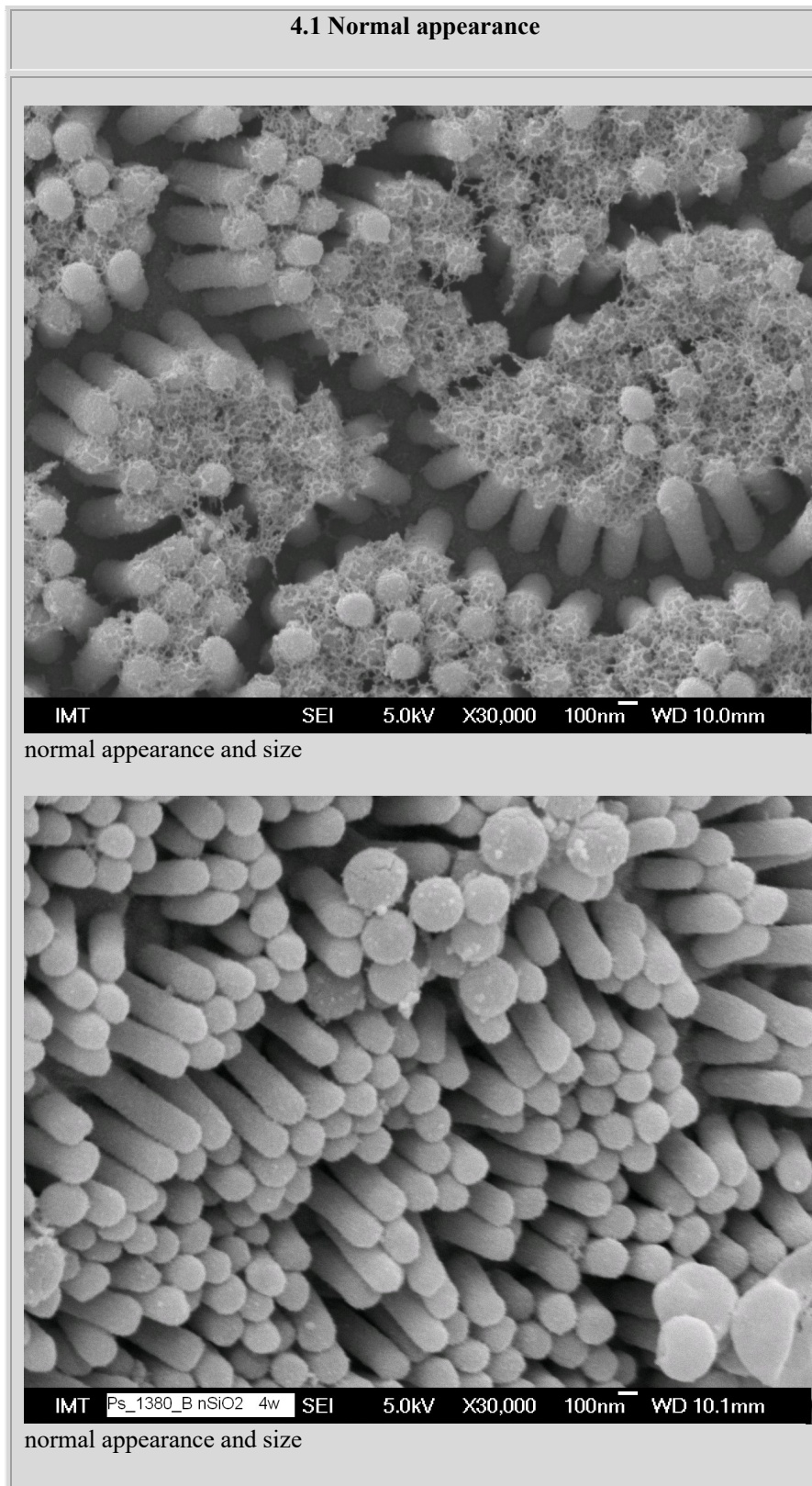
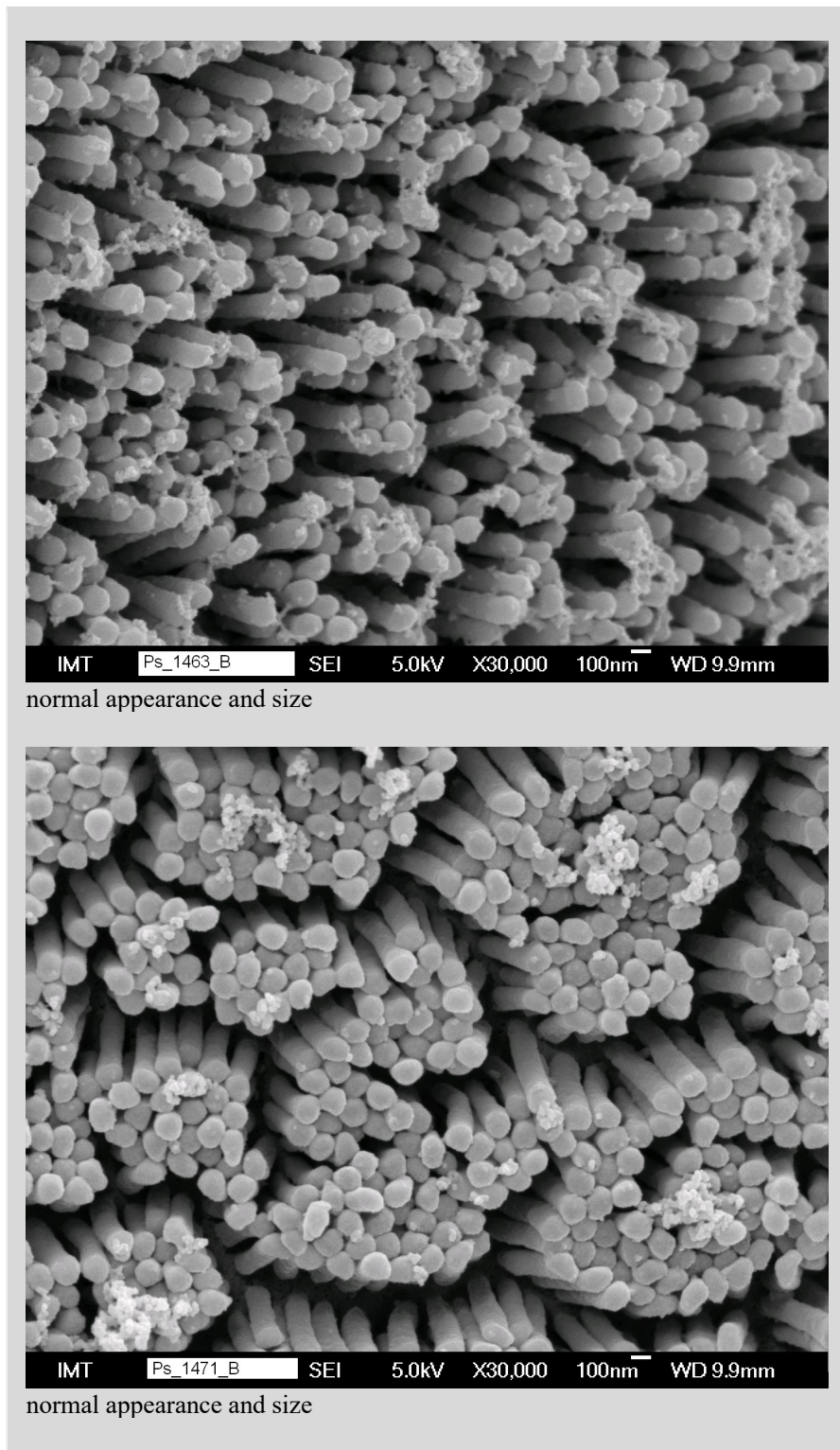


Figure 20.b: **Presence and shape of microvilli in cells surface - normal appearance.**



The normal size of the microvilli in hepatopancreas gland epithelium of *Porcelio scaber L.* is around 400- 550 nm length and 100 nm width. Normal appearance of microvilli is when they are individually free directly to the lumen or somehow grouped in the small groups.

Figure 21.a: Presence and shape of microvilli in cells surface - abnormal appearance.

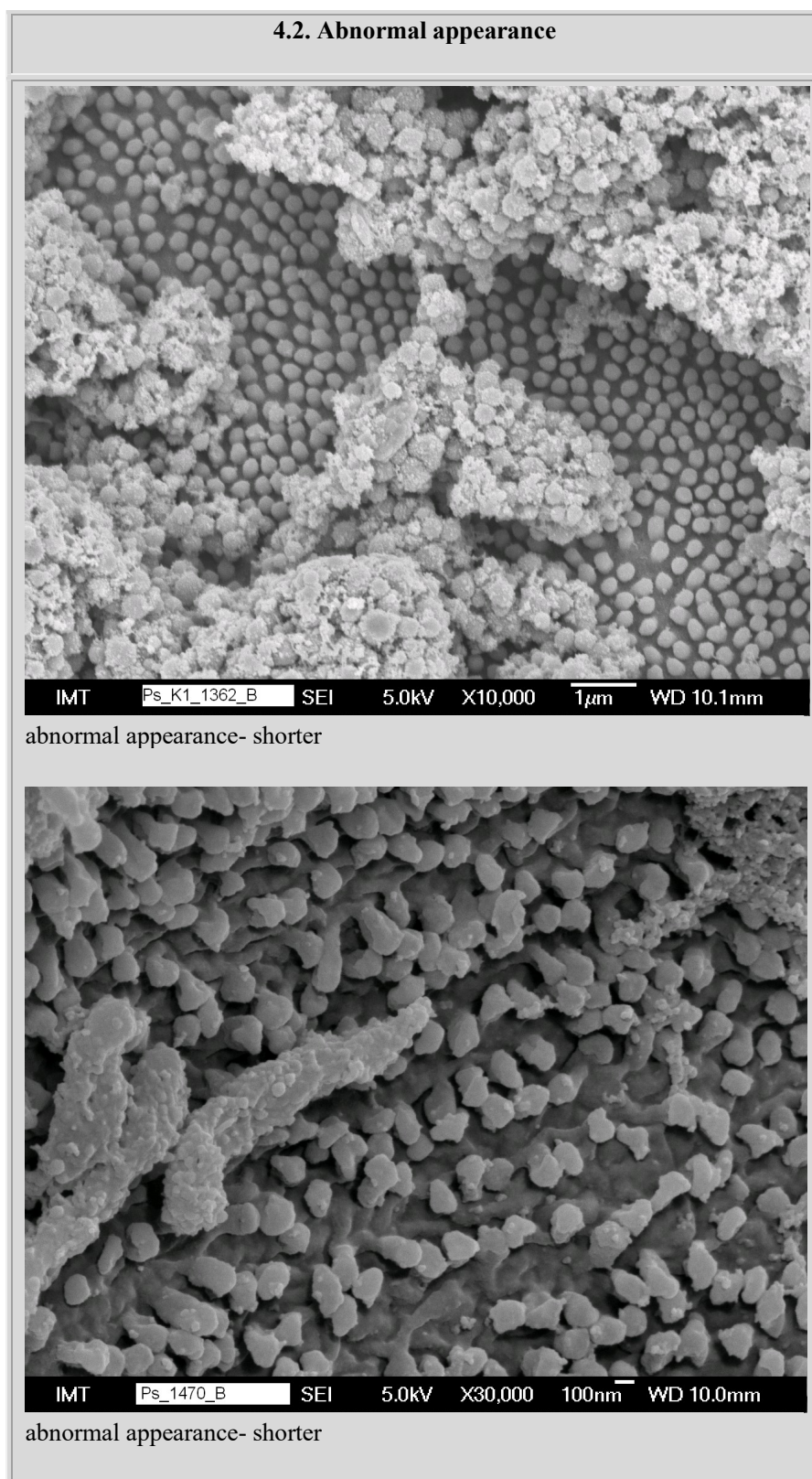


Figure 21.b: Presence and shape of microvilli in cells surface - abnormal appearance.

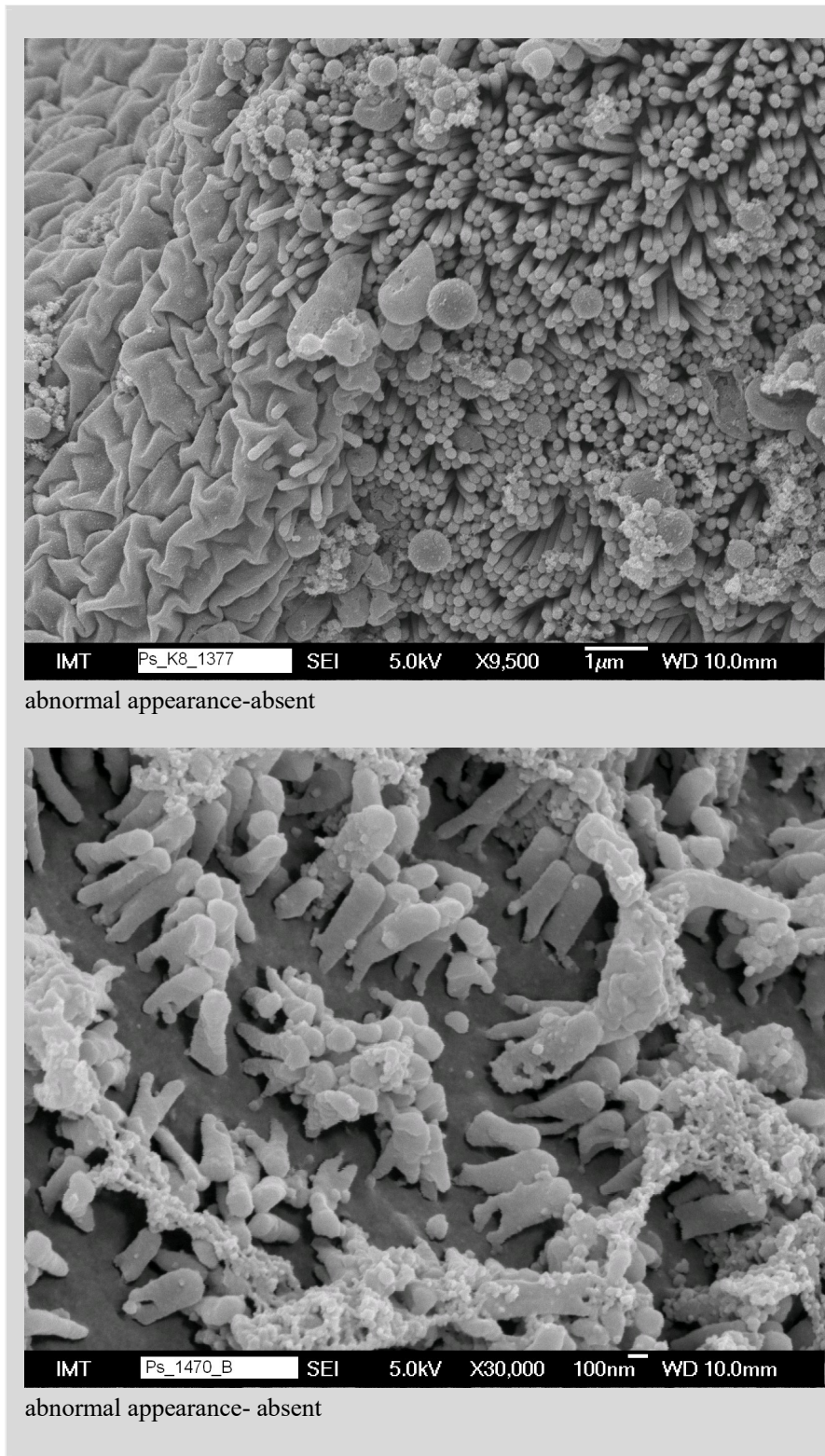


Figure 22.a Presence and shape of microvilli on cells surface - abnormal appearance.

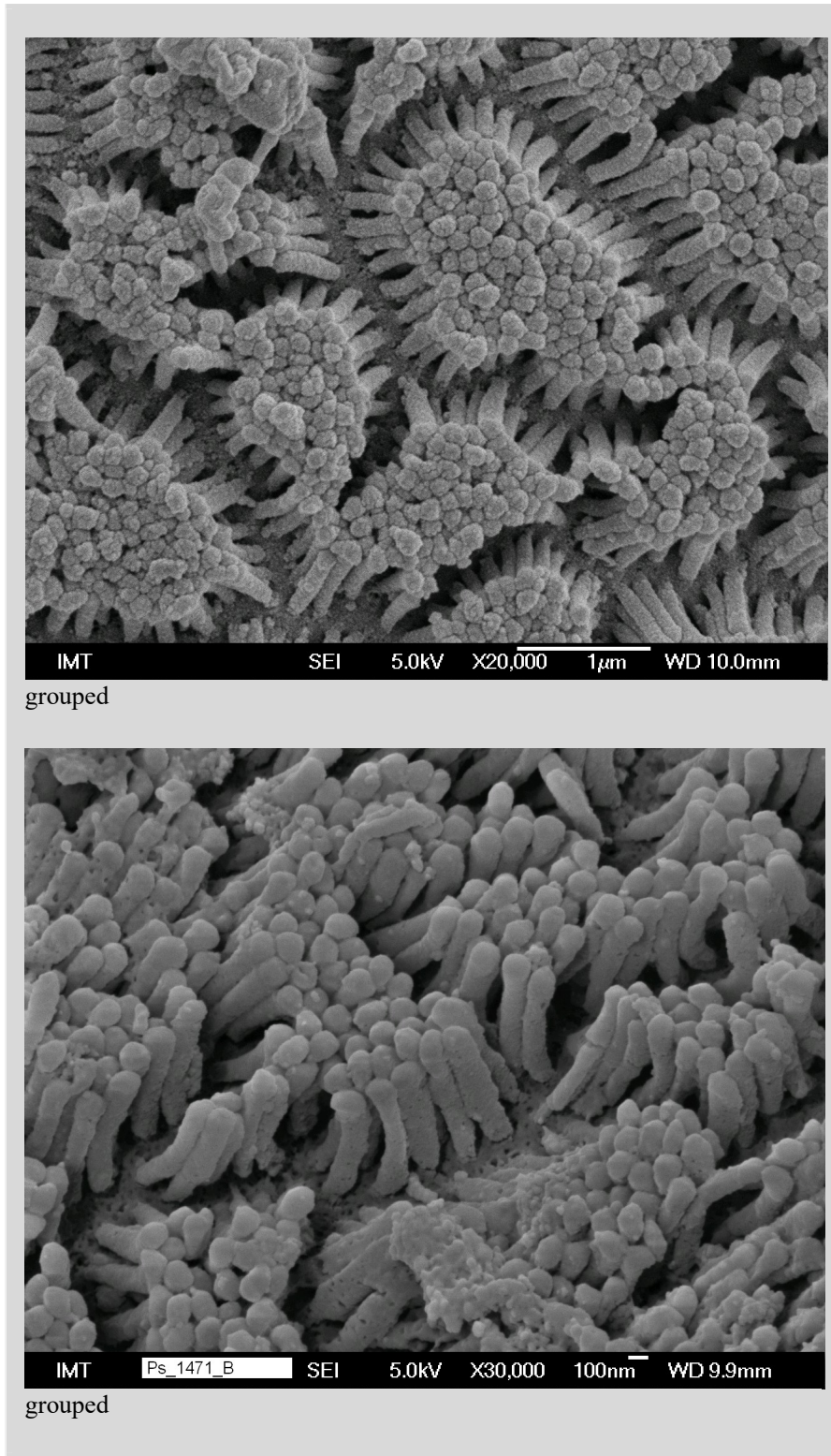
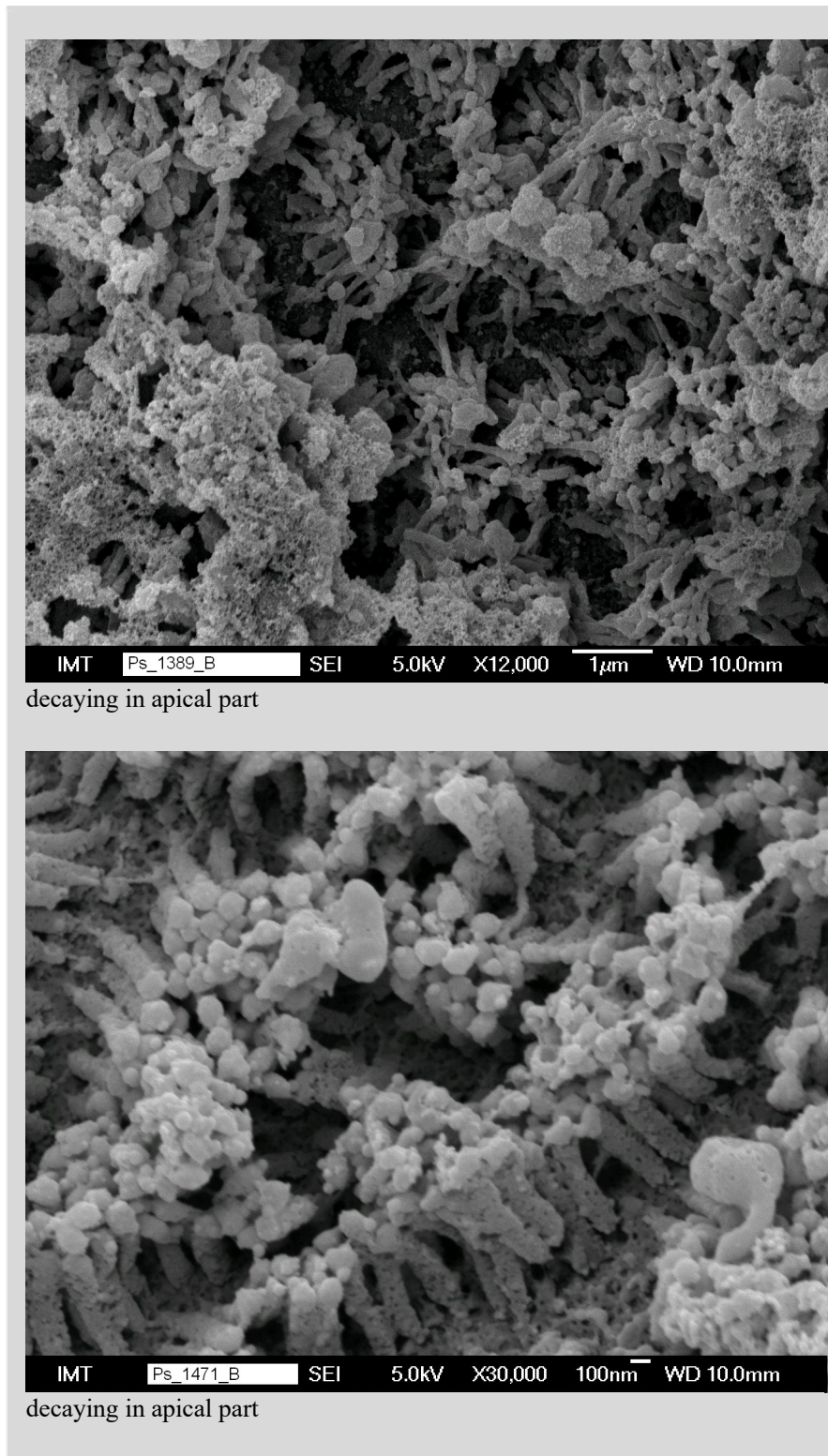


Figure 22.b: Presence and shape of microvilli in cells surface –abnormal appearance



Microvilli grouped in high groups are common in the cell surface of hepatopancrease. This appearance of microvilli is recognized as abnormal. Microvilli sometimes lose their properties and began to decay in the apical part of them or completely. The role of the microvilli is to increase the surface of absorption during the digestive process.

Figure 23.a: Presence and shape of microvilli in cells surface - partly covered with material

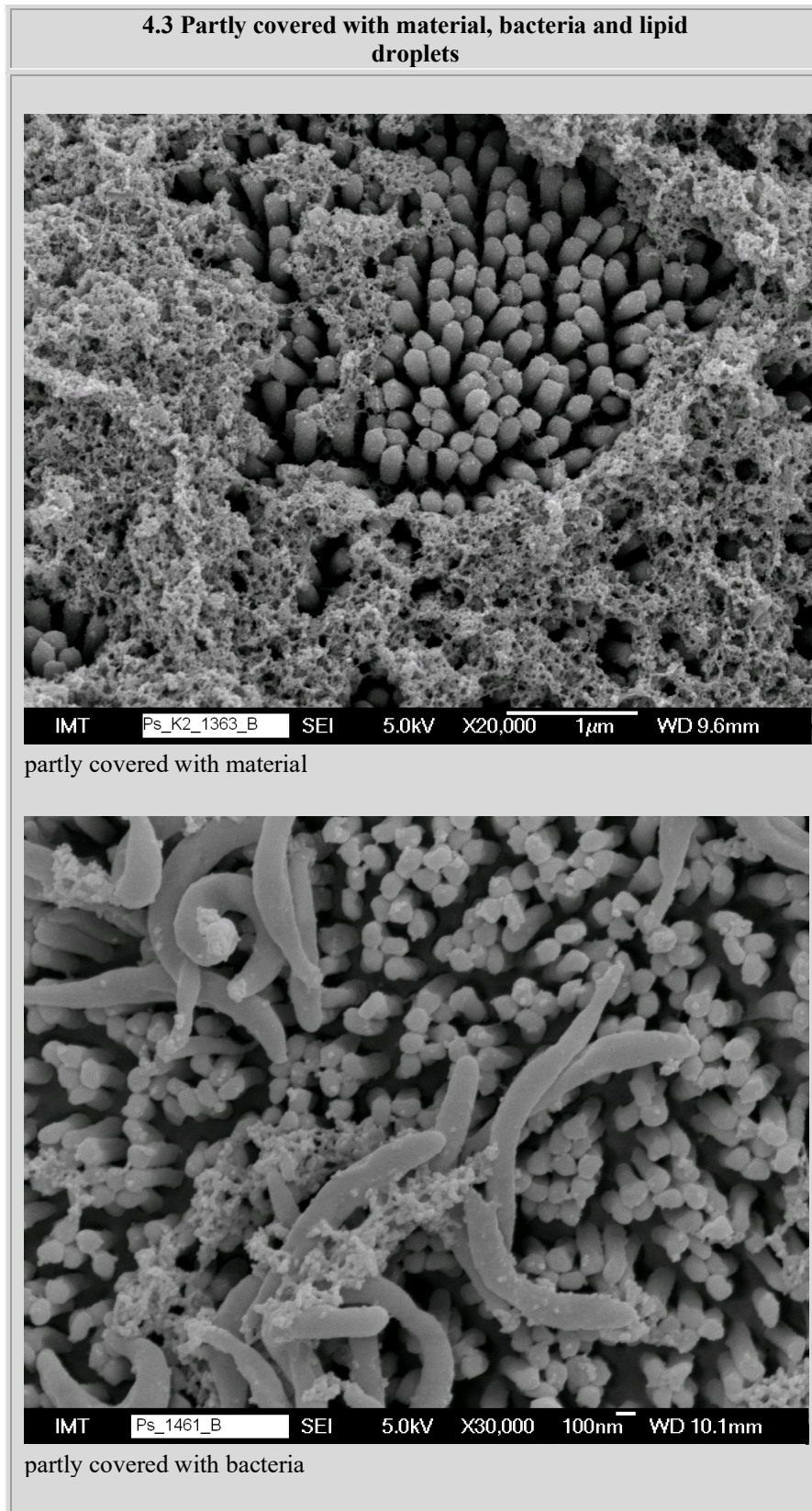


Figure 23.b: Presence and shape of microvilli in cells surface - partly covered with material

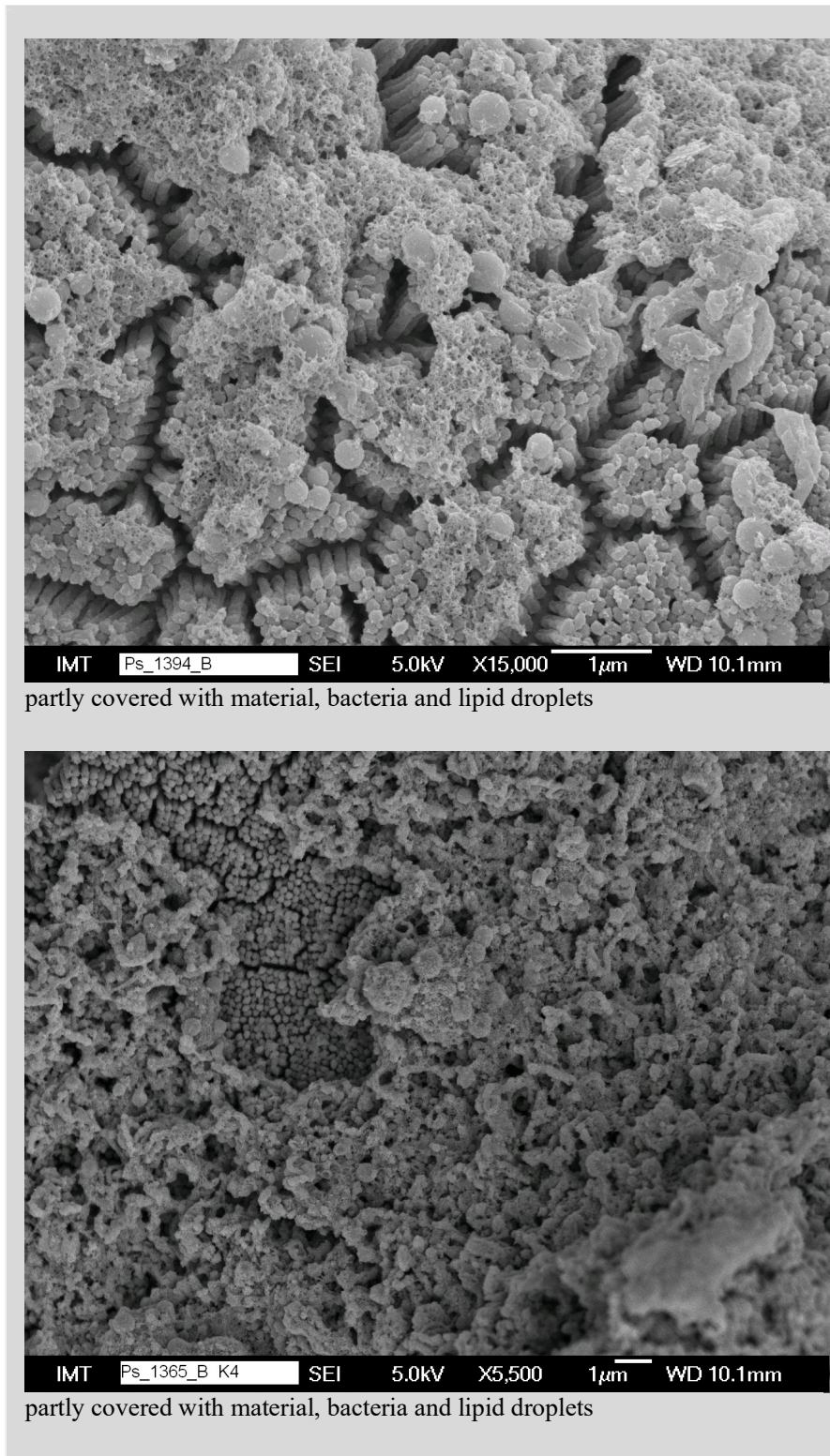


Figure 24.a: Presence of lipid droplets in the cells of digestive gland epithelium (hepatopanceras)- extrusion of the lipid droplets.

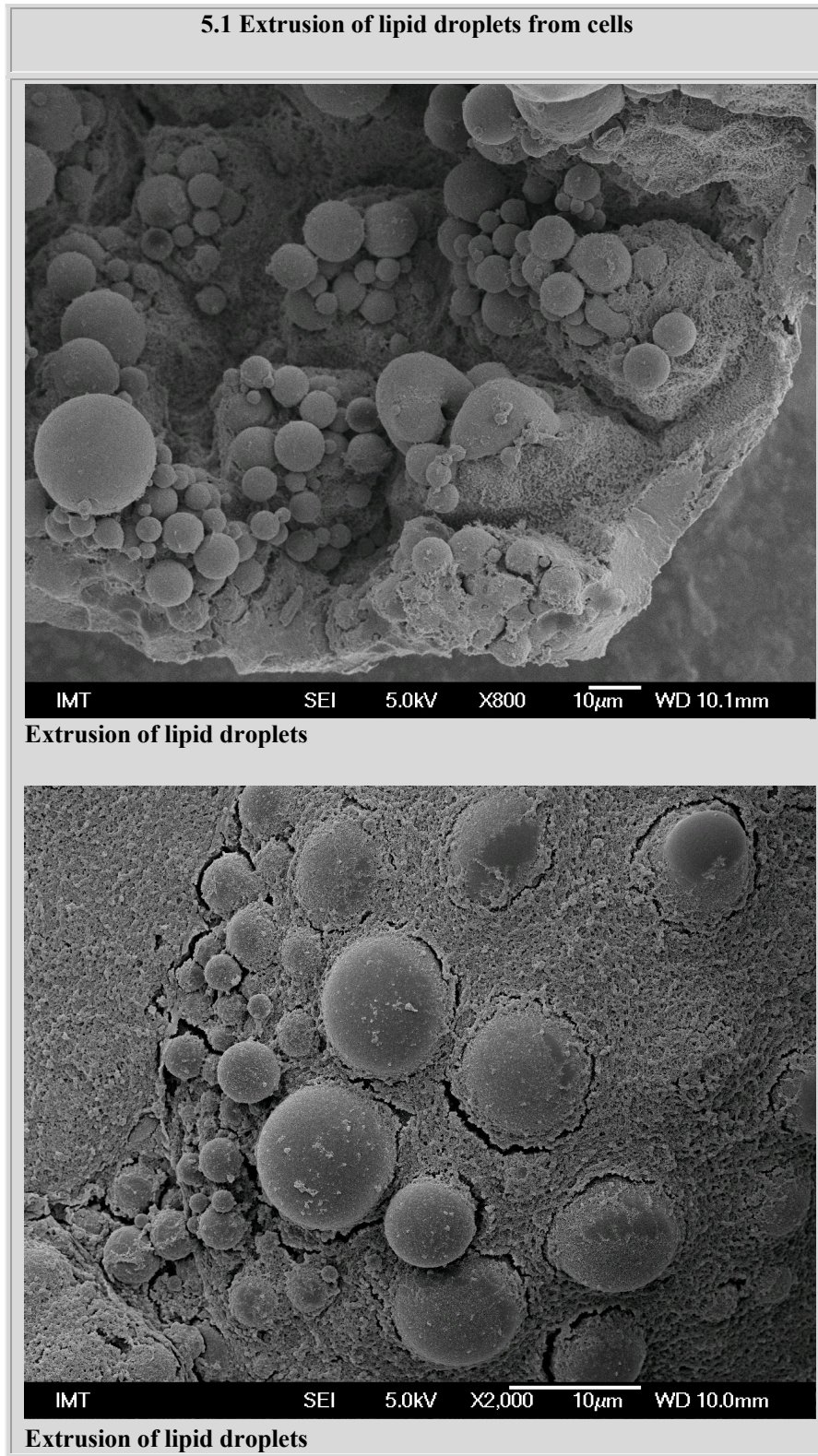
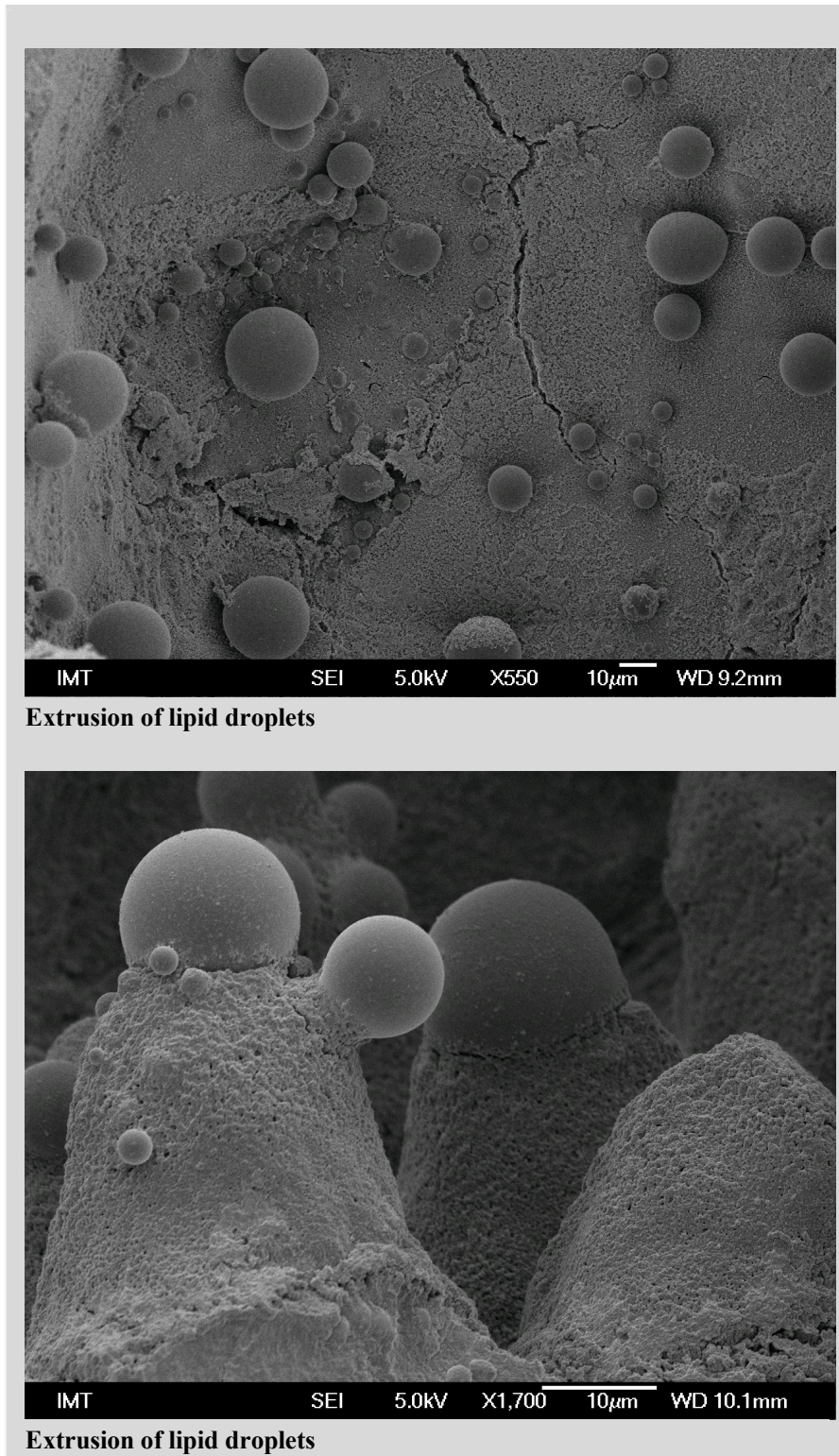


Figure 24.b: Presence of lipid droplets in the cells of digestive gland epithelium (hepatopanceras)-extrusion of the lipid droplets.



The hepatopancrease is the mainly organ for storing the lipid droplets. The thickness of the lipid droplets on epithelium are different and depend from the conditions in which is the organism. The thickness of lipid droplets in epithelium is very high in animals which are not under the stress and the opposite is very low if the animals are in stress conditions (Leser et al, 2008).

In different area of the hepatopancreas tubes are observed the extrusion of lipid droplets. The size and number of lipid droplets in cells of various tissues vary markedly in different physiological and pathological situations (Ghadially, 1997, Leser at al, 2008). The absence or reduction of the number of lipid droplets in hepatopancreatic cells of isopod crustaceans was described in starved animals (Storch, 1984; Strus, 1987) and in postmoult *P. scaber* (Szyfter, 1966).

Figure 25.a: Presence and shape of cellular protrusions in the digestive gland epithelium (hepatopancreas)- different shape and size.

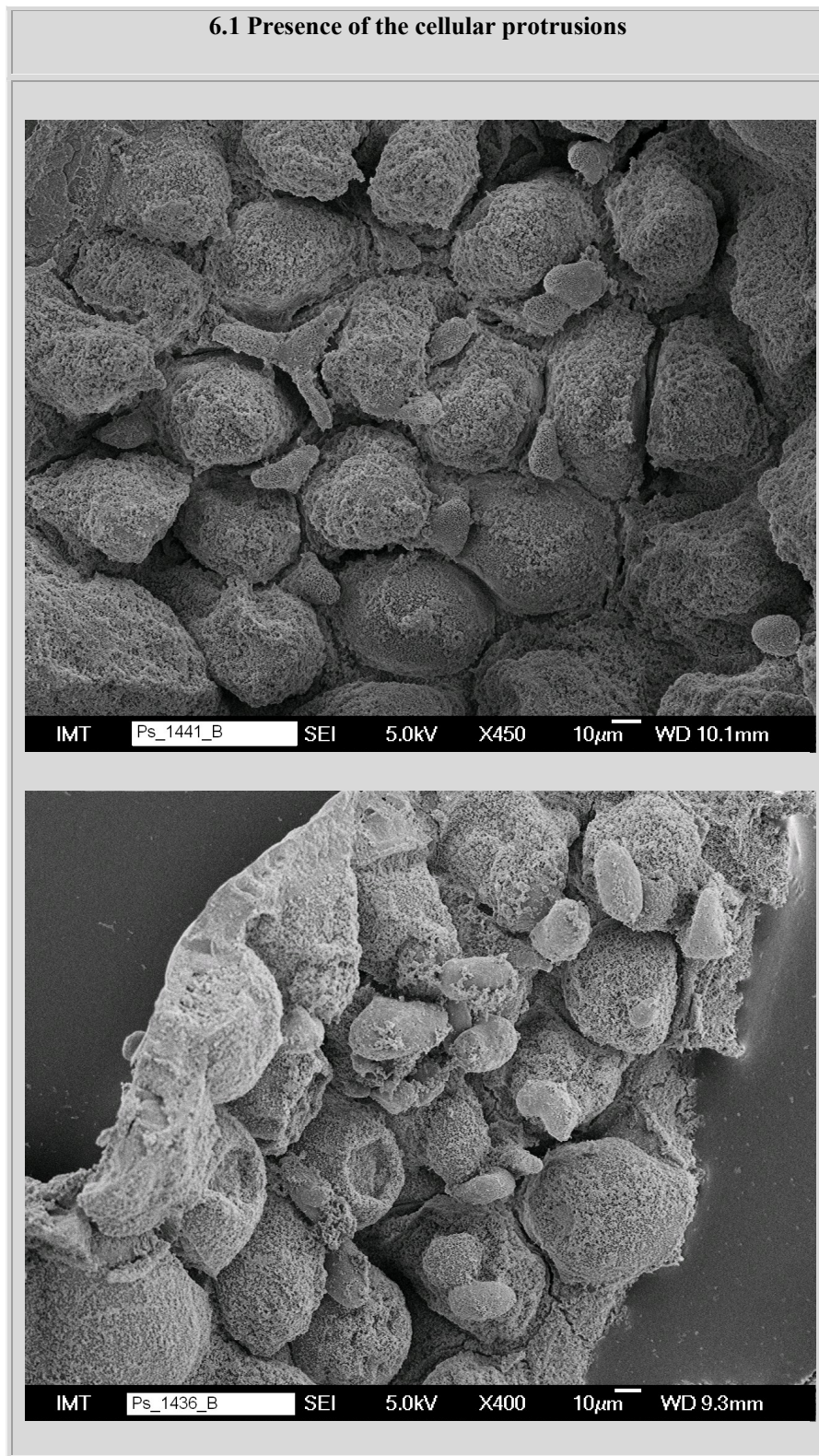
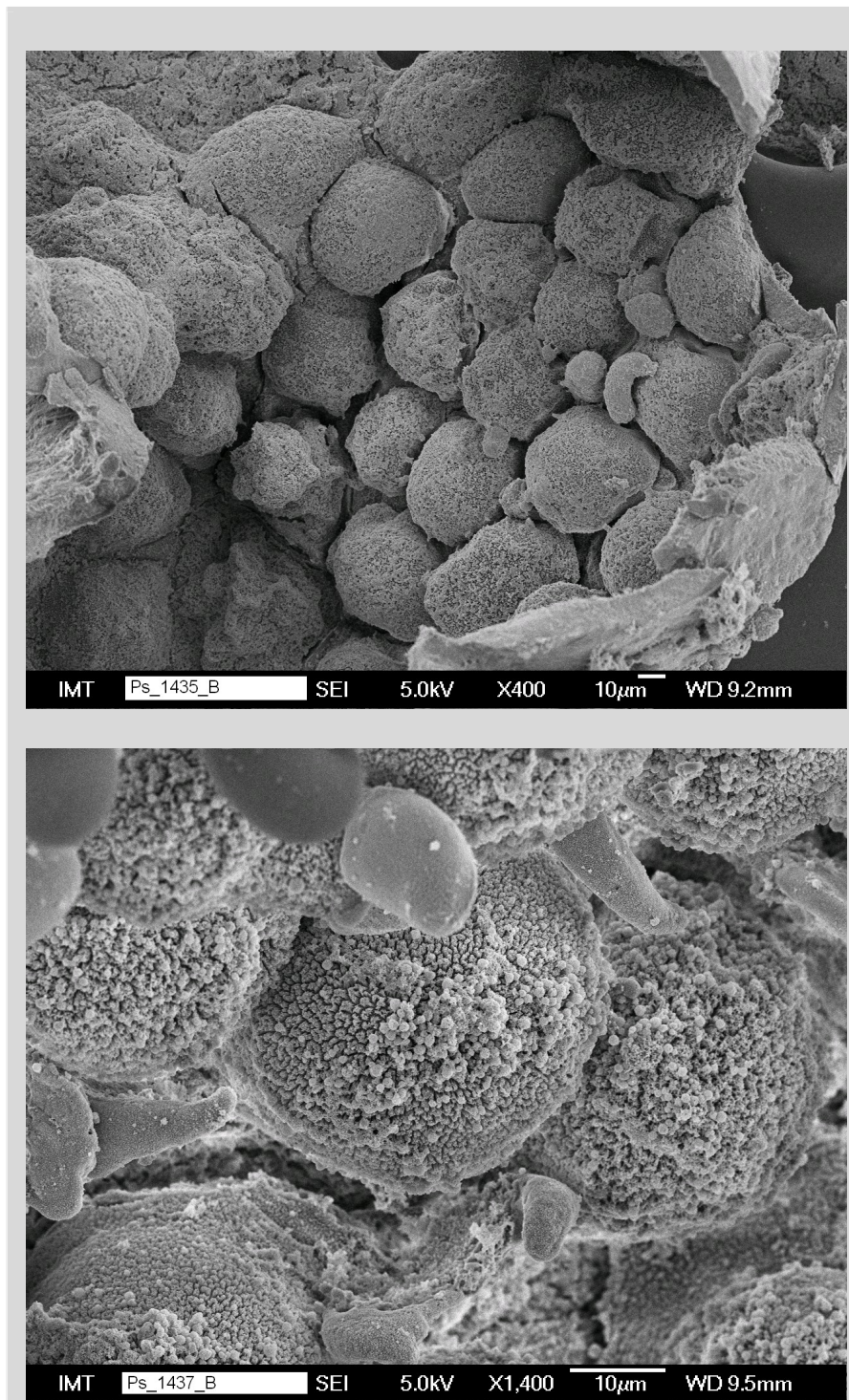


Figure 25.b: **Presence and shape of cellular protrusions in the digestive gland epithelium (hepatopancreas)- different shape and size.**



The presence of different shape and size of cellular protrusions are detected in the hepatopancreas of animals which are treated with the tungsten nanofiber and silver nanoparticles. This appearance is encountered only on animals under the stress conditions (Drobne et al,1998).

Figure 26.a: Tungsten nanofibers effects in surface of digestive gland epithelium cells.

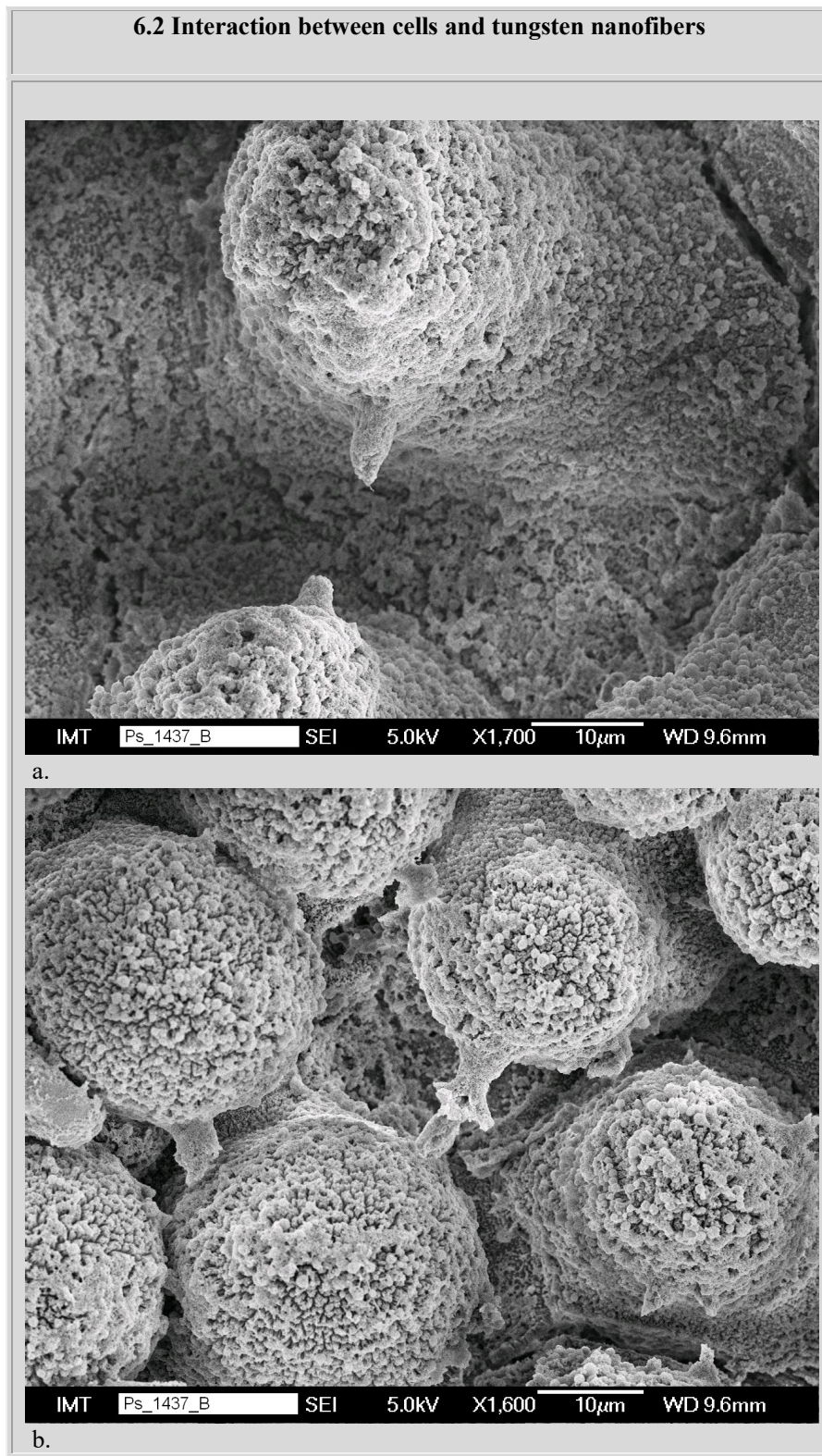


Figure 26.b: Tungsten nanofibers effects in surface of digestive gland epithelium cells.

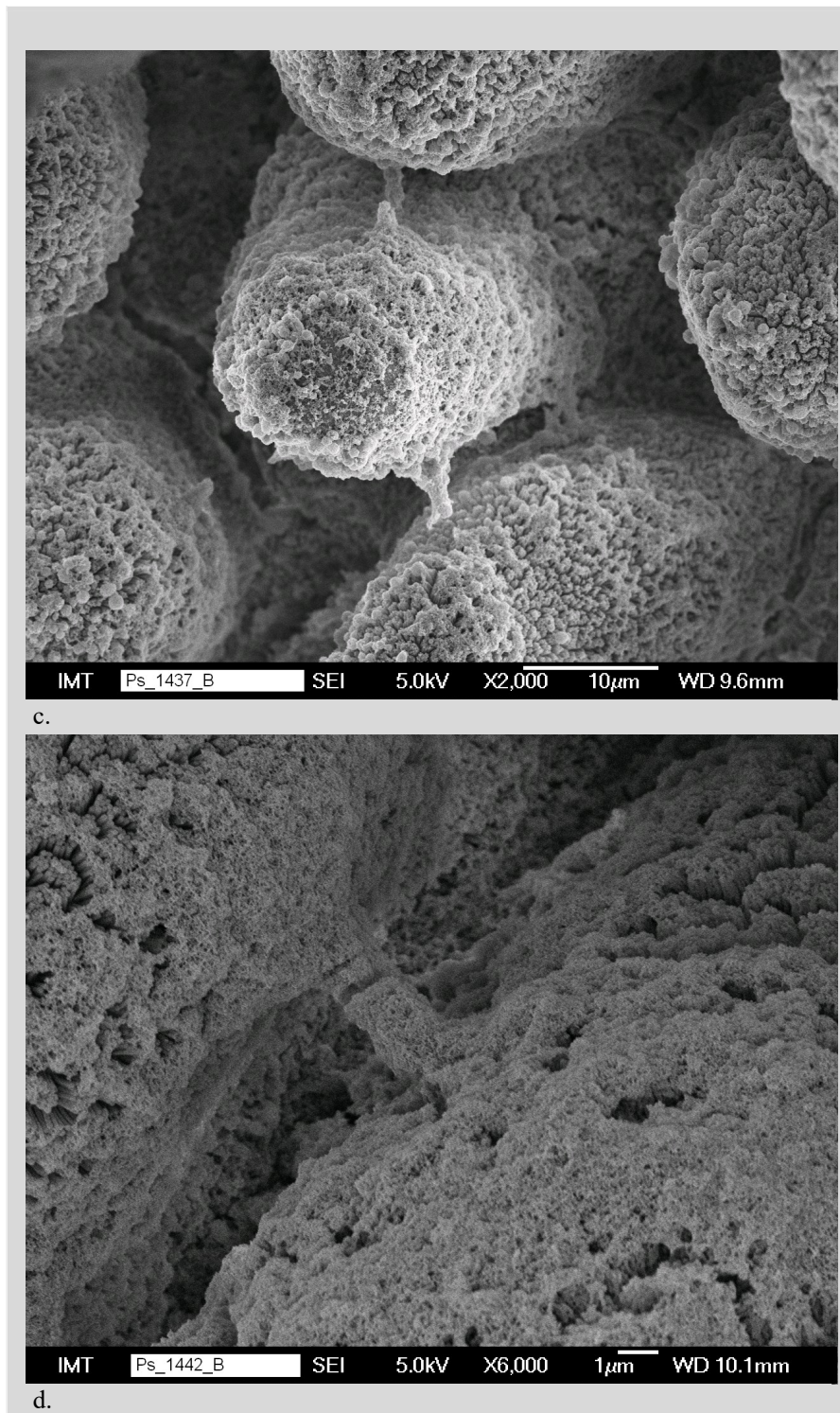
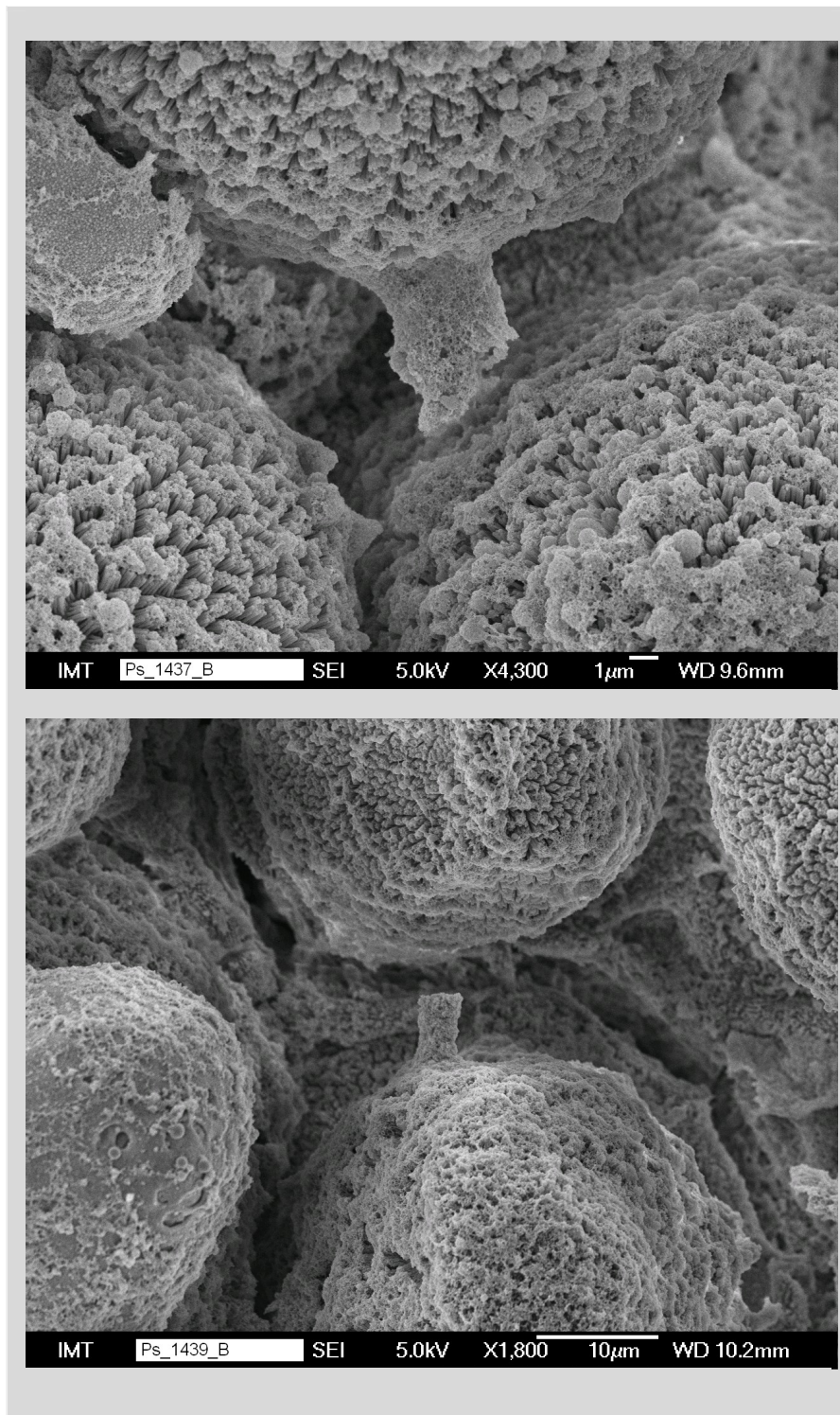


Figure 26.c: Tungsten nanofibers effects in surface of digestive gland epithelium cells.



We detected the following morphological changes of digestive gland epithelium in the treated animals with the tungsten as are presented in figure 26.a, 26.b and 26.c. The interaction between tungsten nanofibers and surface of cells is detected only in some small area of treated animal with the wolfram. After two weeks such interaction can be

visible in the digestive gland epithelium with scanning electron microscopy. The nanofibers can penetrate through the membrane of cells and destroy the cells, in some case they will cross the cell membranes and hold in to the cells. This phenomena is more common in the bottom part of the digestive tube and not in top part. The interactions begin when the nanaoparticle penetrate with the food in digestive gland epithelium and during the contractions (peristaltic of gut) of the tube the nanofibers can move in the direction of cells by some neighbor cells.

A big role in this reaction play all so the shape and size of the nanofibers, if they are large the possibility for attacking is much higher.

The cell membrane, mitochondria and cell nucleus are considered as major cell compartments relevant for possible nanoparticle-induced toxicity (Unfried et al. 2007). When nanoparticles interact with cell membranes, they cause defects such as physical disruptions, formation of holes and thinned regions. It was reported that cationic nano-objects pass through cell membranes by generating transient holes, a process undoubtedly associated with cytotoxicity (Verma et al. 2008). It is known that a range of nanofibres and nanotubes affects in in vitro exposure systems the phagocytic ability of the cells (Brown et al. 2007).

Chemical analysis

To be sure if the organisms eat the food which is prepared with the nanofibers we have measured the presence of the tungsten in fecal pallets as is presented in the table 11. We found the presence of tungsten in treated organisms three times more than in control organisms or outspoken in percentage 0.003 % in fecal of treated animals and 0.001 % in control animals.

The aim of this analyze was also to have data if the nanaofibers are released from the body with the fecal pallets and are not accumulated in the body for a long period.

Table 11: Chemical analyze of tungsten presence in fecal pallets.

Nr	Sample	Id. Code	Date of analyze	Weight % of W
1	Control	K6	28.05.2010	0.001
2	Control	K7	28.05.2010	0.001
3	Control	K8	28.05.2010	0.001
4	Control	K9	28.05.2010	0.001
5	WO _x 1000	WO ₃ 26	28.05.2010	0.003
6	WO _x 1000	WO ₃ 29	28.05.2010	0.003
7	WO _x 1000	WO ₃ 29	28.05.2010	0.003

0.001 W in control samples

0.003 W in exposed samples

Chemical analysis conformed 0.001 % W in control animals samples and 0.003 % W in exposed animals samples that means that real contend of tungsten in animals was 0.002 % (IMT chemical laboratory).

To get complete figure about the behavior of tungsten oxide nanofiber in test animals we performed chemical analyze of the hepatopancreas, gut, rest and food. The data confirmed that tungsten was present in test animals but quantity of hepatopancreas and rest on disposal were to small for chemical analysis.

Table 12: Chemical analyze of tungsten presence in hepatopancrease, gut, rest and in food.

Nr	Sample	Date of analyze	% of W
1	Control	24.06.2010	0.000
2	hepatopancreas	24.06.2010	*
3	Gut	24.06.2010	*
4	Rest	24.06.2010	0.009
5	Food K1R	24.06.2010	0.008
6	Food K1H	24.06.2010	0.000

* Not enough samples for analyzing (IMT chemical laboratory).

Histological analysis

Histological analyses represented in table 13 are in agreement with the observations of the samples performed in SEM.

Under better physiological conditions the epithelium range of animals is higher, and also the number of lipids and granules is higher at the digestive gland epithelium compared to the animals under stress. Based on the data from previous authors (Leser et al, 2008) the higher the range of the epithelium, lipids, and granules, the more normal the epithelium cells are, and vice versa.

Table 13: Histological analyzes of cross section of digestive gland tubes.

Number of animals	Internal code	Epithelium range	lipids range	granular range
1457	K4	4	2	4
1458	15 (1000)	4	4	2
1459	28 (5000)	4	4	3
1460	K5	2	1	4
1461	K6	3	3	4
1462	K7	3	3	3
1463	K8	4	2	3
1464	18 (1000)	/	/	3
1465	19 (1000)	5	3	4
1466	20 (1000)	5	4	3
1468	31 (5000)	4	2	3
1469	32 (5000)	4	4	2
1470	33 (5000)	5	4	3

Figure 27.a Histological analysis of digestive gland epithelium from exposed animals to WOx (light microscopy)

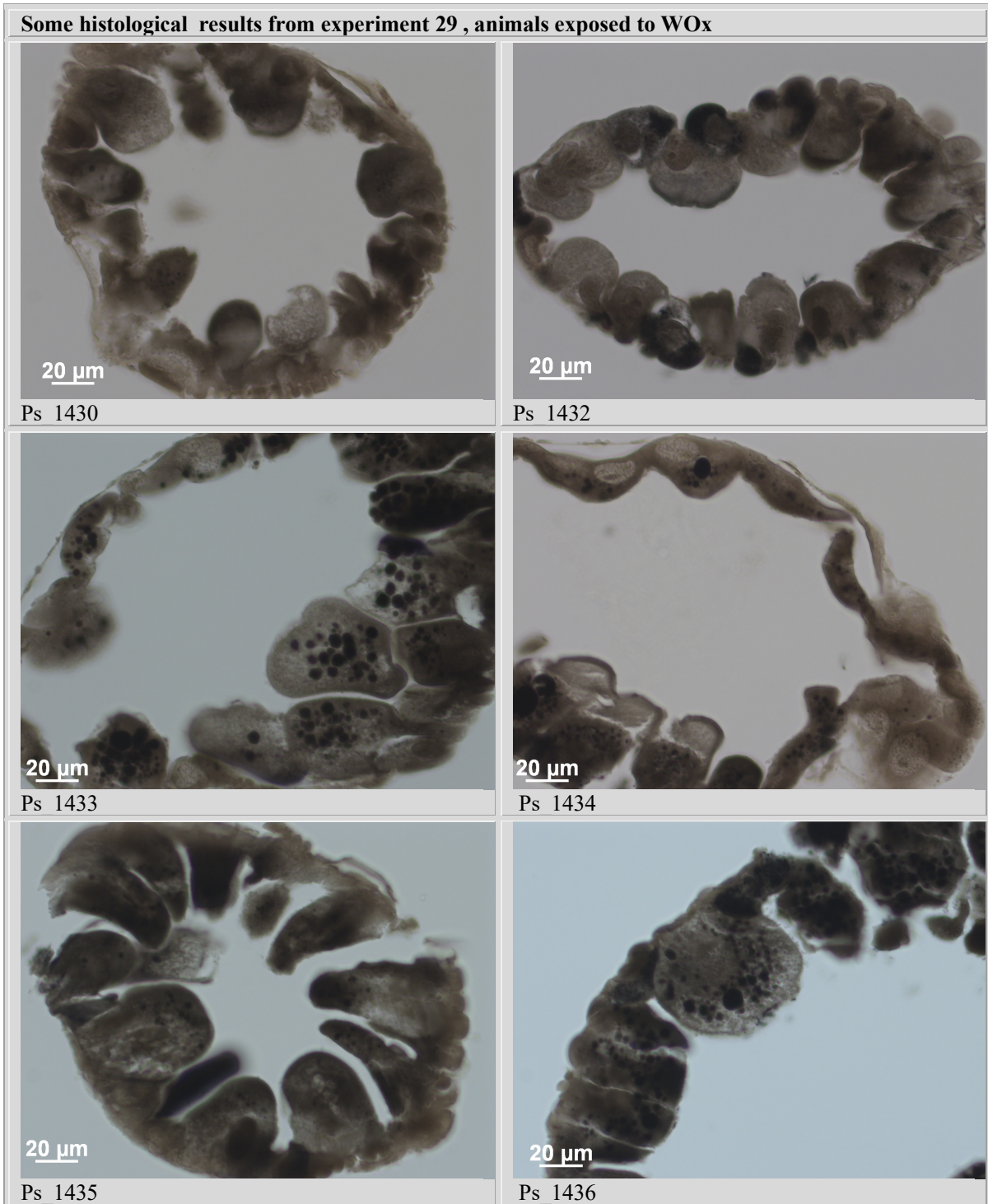
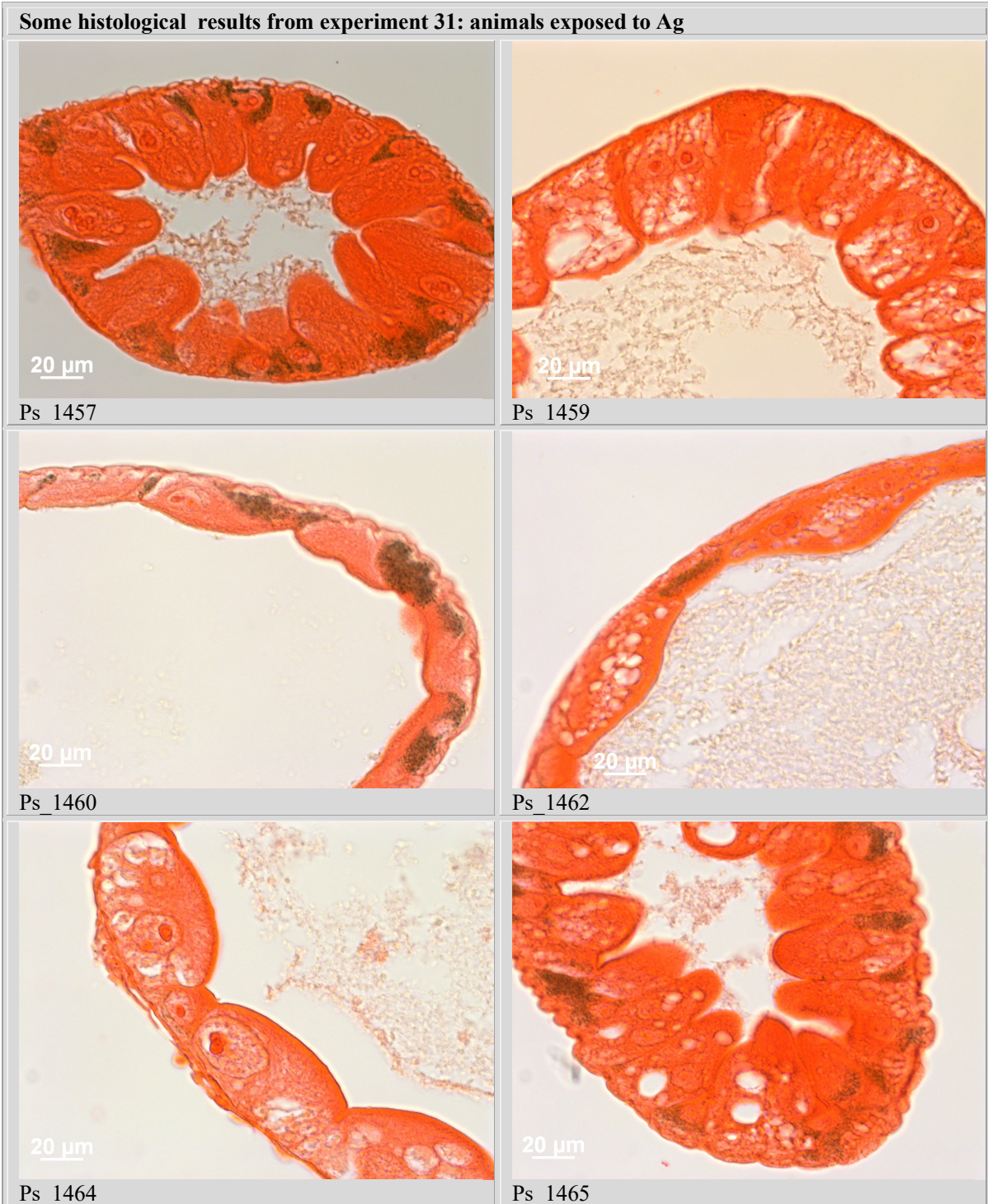


Figure 27.b Histological analysis of digestive gland epithelium from exposed animals to Ag (light microscopy)



5. Conclusions

After investigation about effects of ingested nanofibers and nanoparticles in test organism *Porcelio scaber* for two weeks, we are able to conclude:

In the digestive gland tube of animals fed with nanofibers we observed in some areas some unusual shapes of the cell membrane which is not observed in the control animals. The cell membrane was pierced by nanofibers and they are seen in areas between two cells (connecting them like a “bridge”) or sometimes the “bridge” is broken but the rest of the nanofiber is still parallel between two cells (figure 26. a, b, c).

A small number of these phenomena (exposed samples two weeks) shown that the nanofibers can not enter through the cells without external force that occurs during contractions of the digestive glands tube. To enter into the cell membrane the nanofibers should be at the proper time and proper position in the gland between two cells. With the help of the force during the contraction of digestive tube they can be pushed through the cell membrane. During the first contraction the nanofibers enter the cell membrane and after that they are covered with organic envelope. The nanofibers that reacted with cells can be broken during the next contraction (figure 26, b and d). In the same places similar forms were observed. The middle part of the fibers was broken during contraction and had fallen away and only a small part remained in the cell membrane (figure 26 a, e, d).

After two weeks of feeding with nanofibers, such interactions can be visible in the digestive gland epithelium with scanning electron microscopy. The nanofibers can penetrate through the membranes of cells and destroy the cells. In some cases they will cross the cell membrane and remain into the cells (figure 26. a,b,c).

The phenomena are observed almost close to the bottom of the tube and not in the top part of the tube. We suppose that: this phenomena is possible because of the high specific weight of WOx nanofibers compared to the other organic biomass. They always will fall down in the bottom of the tube where is a higher possibility to interact with the hepatopancreas cells exists.

Experimental limitations do not allow analyzing these details or the internal part of the phenomena through EDS because of the sensitivity of the method and the small amount of the nanofibers. But we observed also some other specifics regarding the shape of the cells and precipitation of the lipid droplets. These phenomena can neither be observed through histological analysis, due to the fact that this type of analysis is not appropriate because the dissections can not be made exactly to the small areas where the interaction takes place.

In the experiment with silver nanoparticles we found out that 70 % of microvilli were attacked. We can confirm that because they have lost their normal shape and size. The size of microvilli normally is from 400- 500 nm length and 100 nm width. In our investigation in the exposed animals we observed that these dimensions were different, the microvilli shrunked, and even in some parts they are absent.

The results of the PhD research work were published in a renowned international journal with impact factor (Appendix 1). An additional paper is in preparation for publication with the results which are found now. The finding of this work has been presented at international scientific conference with oral and poster presentation (Appendix 2)

6. Acknowledgements

I'd like to express my gratitude to these people:

Doc. Dr Matjaz Torkar, as supervisor from the Institute of Metals and Technology for his help during the time of study and aid provided during the research work and preparation of this thesis.

Prof. Dr Damjana Drobne as co supervisor from the Department of Biology, University of Ljubljana for her help and strong support during research work and writing of the thesis.

Prof. Dr Monika Jenko, Director of the Institute of Metals and technology for her support during my study.

Dr. Vladka Leser and M. Sc Ziva Pipan Kalec from Department of Biology -University of Ljubljana, for their help with sample preparation.

Other colleagues from the Institute of Metals and Technology for the assistance provided during the experimental work and research.

A special thanks to my parents and my family for moral and spiritual support that I got at any time.

7. References

- Becker, L.; Bada, J.L.; Winans, R.E.; Hunt, J.E.; Bunch, T.E.; French, B.M. Fullerenes in the 1.85-billion-year-old Sudbury impact structure. *Science*, **265**, 642 (1994).
- Boxall, A.B.A.; Tiede, K.; Chaudhry, M.Q. Engineered Nanomaterials in Soils and Water: How do They Behave and Could They Pose a Risk to Human Health?. *Nanomedicine*. **2**, 919-927 (2007).
- Brown, D.M.; Kinloch, I.A.; Bangert, U.; Windle, A.H.; Walter, D.M.; Walker, G.S.; Scotchford, C.A.; Donaldson, K.; Stone, V. An in vitro study of the potential of carbon nanotubes and nanofibres to induce inflammatory mediators and frustrated phagocytosis. *CARBON* **45**, 1743-1756 (2007).
- Donaldson, K. Biological activity of respirable industrial fibres treated to mimic residence in the lung. *Toxicol Letters* **72**, 299–305(1994).
- Donaldson, K.; Brown, G.M.; Brown, D.M.; Bolton, R.E.; Davis, J.M.G. The inflammatory generating potential of long and short fibre amosite asbestos samples. *British Journal of Industrial Medicine* **46**, 271–276 (1989).
- Drobne D.; Štrus, J.; Žnidaršič, N.; Zidar, P. Morphological description of bacterial infection of digestive glands in the terrestrial isopod *Porcellio scaber* (Isopoda, Crustacea). *Journal of Invertebrate Pathology* **73**, 113–119 (1999).
- Drobne, D.; Milani, M.; Leser, V.; Tatti, F. Surfacedamageinduced by FIB milling and imaging of biological samples is controllable. *Microscopy Research and Technique* . **70**, 895–903 (2007).
- Drobne, D., Terrestrial isopods – a good choice for toxicity testing of pollutants in the terrestrial environment. *Environmental Toxicology and Chemistry*. **16**, 1159–1164. (1997).
- Drobne, D.; Hopkin, S. P.. The toxicity of zinc in a “standard” laboratory test. *Ecotoxicology and Environmental Safety* **31**, 1–6. (1995).
- Drobne,D.; Milani, M.; Lesera, V.; Tatti, F.; Zrimec, A.; Znidarsica, N.; Rok Kostanjsek,R.; Strusa, J. Imaging of intracellular spherical lamellar structures and tissue gross morphology by a focused ion eam/scanning electron microscope (FIB/SEM). *Ultramicroscopy* **108** 663–670(2008).
- Drobne, D.; Jemec, A.; Pipan Tkalec, Ž. In vivo screening to determine hazards of nanoparticles: Nanosized TiO₂. *Environmental Pollution* **157**, 1157-1164 (2009).
- Drobne, D.; Strus, J. The effect of Zn on the digestive gland epithelium of *Porcellio scaber* (Isopoda, Crustacea). *Pflugers Archive – European Journal of Physiology*. **431**, R247–R248. (1996).
- EPA, Nanotechnology White Paper. U.S. Environmental Protection Agency Report EPA 100/B-07/001, Washington DC 20460, USA (2007).
- Ghadially, F.N. *Ultrastructural Pathology of the Cell and Matrix*. Butterworth-Heinemann, Boston, Oxford, Johannesburg, Melbourne, New Delhi, Singapore, p. 1414 (1997).
- Hames, C.A.C.; Hopkin, S.P. The structure and function of the digestive system of terrestrial isopods. *Journal of Zoology*. **217**, 599-627 (1989).

- Hames, C.A.C.; Hopkin, S.P. A daily cycle of apocrine secretion by the B cells in the hepatopancreas of terrestrial isopods. *Canadian Journal of Zoology* **69**, 1931-1937 (1991).
- Hart, G.A.; Kathman, L.M.; Hesterberg, T.W. In vitro cytotoxicity of asbestos and man-made vitreous fibres: roles of fibre length, diameter and composition. *Carcinogenesis* **15**, 971-977 (1994).
- Hassall, M.; Turner, J.G.; Rands, M.R.W. Effects of terrestrial isopods on the decomposition of woodland leaf litter. *Oecologia* **72**, 597-604 (1987).
- Hassall, M.; Zimmer, M.; Loureiro, S. Questions and possible new directions for research into the biology of terrestrial isopods. *European Journal of Soil Biology*. **41**, 57-61 (2005).
- Hayat, M.A. *Principles and Techniques of Electron Microscopy: Biological Applications*. Cambridge University Press (Cambridge,2000).
- Hopkin, S.P. Critical concentrations, pathways of detoxification and cellular ecotoxicology of metals in terrestrial arthropods. *Functional Ecology* **4**, 321-327(1990).
- Hopkin, S.P. *Ecophysiology of metals in Terrestrial Invertebrates*. Elsevier, London, New York, p. 366. (1989).
- Hopkin, S.P.; Martin, M.H. The distribution of zing, candium, led and coper within the hepatopancreas of a woodlouse. *Tissue & Cell* **14**, 703-715 (1982).
- Hyung, H.; Fortner, J.D.; Hughes, J.B.; Kim, J.H. Natural organic matter stabilizes carbon nanotubes in the aqueous phase. *Environmental Science and Technology* **41**, 179-84 (2007).
- Jemec, A.; Drobne, D.; Remškar, M.; Sepčič, K.; Tišler, T. Effects of ingested nano- sized titanium dioxide on terrestrial isopods Porcellio scaber. *Environ. Toxicol* **27**, 1904- 1914 (2008).
- Jiang, J.; Oberdörster, G.; Biswas, P. Characterization of size, surface charge, and agglomeration state of nanoparticle dispersions for toxicological studies. *Nanopart. Journal of Nanoparticle Research*. 11-77 (2009).
- Kennett, D.J.; Kennett, J.P.; West, A.; Mercer, C.; Hee, S.S.Q.; Bement, L.; Bunch, T.E.; Sellers, M.; Wolbach, W.S. Nanodiamonds in the Younger Dryas Boundary Sediment Layer. *Science* **323**,94 (2009).
- Kohler, H.R.; Huttenrauch, K.; Berkus, M.; Gräff, S.; Alberti, G. Cellular hepatopancreatic reactions in Porcellio scaber (Isopoda) as biomarkers for the evaluation of heavy metal toxicity in soils. *Applied Soil ecology* **3**, 1-15 (1996).
- Kostanjšek, R.; Štrus, J.; Avguštin, G. Genetic diversity of bacteria associated with the hindgut of the terrestrial crustacean Porcellio scaber (Crustacea: Isopoda) *FEMS Microbiology Ecology* **40** 171-179 (2002).
- Lešer, V.; Drobne, D.; Pipan, Z.; Milani, M.; Tatti, F. Comparison of different preparation methods of biological samples for FIB milling and SEM investigation. *Journal of Microscopy-Oxford* . **233**, 309-319 (2009).
- Lešer, V.; Drobne, D.; Vilhar, B.; Kladnik, A.; Žnidaršič, N.; Štrus, J. Epithelial thickness and lipid droplets in the hepatopancreas of *Porcellio scaber* (Crustacea: Isopoda) in different physiological conditions. *Zoology* **111**,419-432 (2008).
- Lok, C.N.; Ho, C.M.; Chen, R.; He, Q.Y.; Yu, W.Y.; Sun, H.Z.; Tam, P.K.H.; Chiu, J.F.; Che, C.M. Proteomic analysis of the mode of antibacterial action of silver nanoparticles. *Journal of Proteome Research*. **5**, 916-924 (2006).
- Moore, M.N. Do nanoparticles present ecotoxicological risks for the health of the aquatic environment? *Environment International* **32**, 967e976. (2006).

- Mueller, N.C.; Nowack, B. Exposure modeling of engineered nanoparticles in the environment. *Environmental Science and Technology* **2**, 4447-53(2008).
- Murr, L.E.; Esquivel, E.V.; Bang, J.J.; de la Rosa, G.; Gardea-Torresdey, J.L. Chemistry and nanoparticulate compositions of a 10,000 year-old ice core melt water. *Water Research* **38**, 4282-4296 (2004).
- NANO Risk Framework, Environmental Defense – DuPont Nano Partnership, DuPont, Wilmington, DE. http://www.edf.org/documents/6496_Nano%20Risk%20Framework.pdf. (2007).
- Oberdörster, E.; Oberdörster, J.; 2005. Nanotoxicology: an emerging discipline evolving from studies of ultrafine particles. *Environmental Health Perspect.* **113**, 823-839(2005).
- Paoletti, M.G.; Hassall, M. Woodlice (Isopoda: Oniscidea): their potential for assessing sustainability and use as bioindicators. *Agriculture Ecosystem and Environment*. **74**, 157–165. (1999).
- Pawert, M.; Triebkorn, R.; Graff, S.; Berkus, M.; Schulz, J.; Kohler, H.R. Cellular alterations in collembolan midgut cells as a marker of heavy metal exposure: ultrastructure and intracellular metal distribution. *Science of the Total Environment* **181**, 187-200 (1996).
- Perez, S.; Farre, M.; Barcelo, D. Analysis, behavior and ecotoxicity of carbon-based nanomaterials in the aquatic environment. *Trends in Analytical Chemistry* **28** No. 6, (2009).
- Prosi, F.; Dallinger, R. Heavy metals in the terrestrial isopod *Porcellio scaber* Latreille. Histochemical and ultrastructural characterization of metal-containing lysosomes. *Cell Biology and Toxicology* **4**, 81-95 (1988).
- REACH, Regulation (EC) No 1907/2006 of the European parliament and of the Council of 18 December 2006 concerning the registration, evaluation, authorization and restriction of chemicals. http://ec.europa.eu/environment/chemicals/reach/reach_intro.htm. (2006).
- Renwick, L.; Brown, D.; Clouter, A.; Donaldson, K. Increased inflammation and altered macrophage chemotactic responses caused by two ultrafine particle types. *Occup Environ Med* **61**, 442–447(2004).
- Scenihr, Scientific committee on emerging and newly identified health risks. Opinion on the appropriateness of the risk assessment methodology in accordance with the technical guidance documents for new and existing substances for assessing the risks of nanomaterials. European Commission; Health & Consumer Protection Directorate-General. http://ec.europa.eu/health/ph_risk/committees/04_scenihr/docs/scenihr_o_010.pdf. (21–22 June 2007).
- Segner, M., Braunbeck, T. Cellular response profile to chemical stress. In: Schürmann, G., Markert, B. (Eds.), *Ecotoxicology*. Wiley, *Spektrum Akademischer Verlag*, pp. 521–569.(1998).
- Smith, C.J.; Shaw, B.J.; Handy, R.D. Toxicity of single walled carbon nanotubes to rainbow trout, (*Oncorhynchus mykiss*): respiratory toxicity, organ pathologies, and other physiological effects. *Aquatic Toxicology* **82**, 94-109. (2007).
- Sondi, I.; Salopek-Sondi, B. Silver nanoparticles as antimicrobial agent: a case study on *E. coli* as a model for Gram-negative bacteria. *J. Colloid Interface Science* **275**, 177-182. (2004).
- Storch, V. The influence of nutritional stress on the ultrastructure of terrestrial isopods. *Symposia of the Zoological Society* **53**, 167-184 (1984).
- Štrus, J. The effects of starvation on the structure and function of the hepatopancreas in the isopod *Ligia italica*. *Investigacion Pesquera* **51**, 505-514 (1987).

Štrus, J.; Blejec, A. Microscopic anatomy of the integument and digestive system during the molt cycle in *Ligia italica* (Oniscidea). In: Kensley, B., Brusca, R.C. (Eds.), *Isopod Systematics and Evolution*. Crustacean Issues 13. A.A. Balkema, *Rotterdam Brookfield*, pp. 343–352. (2001).

Szyfter, Z. The correlation of moulting and changes occurring in the hepatopancreas of *Porcellio scaber* Latr. (Crustacea, Isopoda). *Bulletin de la Societe des amis des sciences et des lettres de Poznan*. **7**, 95-114(1966).

TGD Document, Technical guidance document on risk assessment, part II. European Commission. <http://europa.eu.int> (2003).

The World Market for Carbon Nanotubes, Carbon Nanofibers, Fullerenes, POSS and Graphene . www.futuremarketsinc.com © Future Markets, Inc. (2010).

Tiede, K.; Boxall, A.B.A.; Tear, S.P.; Lewis, J.; David, H.; Hasselov, M. Detection and characterisation of engineered nanoparticles in food and the environment. *Food Additives and Contaminants* **25** , 795-821 (2008).

Unfried, K.; Albrecht, C.; Klotz, L.O.; Von Mikecz, A.; Grether-Beck, S.; Schins R.P.F. Cellular responses to nanoparticles: Target structures and mechanisms. *Nanotoxicology* **1**, 52-71. (2007).

Verma, A.; Uzun, O.; Hu, Y.H.; Hu, Y.; Han, H.S.; Watson, N.; Chen, S.L.; Irvine, D.J.; Stellacci, F. Surface-structure-regulated cell-membrane penetration by monolayer-protected nanoparticles. *Nature Materials* **7**, 588-595 (2008).

Vogt, G. Monitoring of environmental pollutants such as pesticides in prawn aquaculture by histological diagnosis. *Aquaculture* **67**, 157_ 164. (1987).

Wägele, J-W.; Harrison, F.W.; Humes, A.G. *Microscopic Anatomy of Invertebrates. Crustacea*, Wiley-Liss, New York **9**, 529-617 (1992).

Wang, Y.; Stingl, U.; Anton-Erxleben, F.; Geisler, S.; Brune, A.; Zimmer, M. "Candidatus *Hepatoplasma crinochetorum*," a new, stalk-forming lineage of Mollicutes colonizing the midgut glands of a terrestrial isopod. *Applied and Environmental Microbiology* **70**, 61-66 (2004 a).

Wang, Y.; Stingl, U.; Anton-Erxleben, F.; Geisler, S.; Brune, A.; Zimmer, M. 'Candidatus *Hepaticola porcellionum*' a new, stalk-forming lineage of Rickettsiales colonizing the midgut glands of a terrestrial isopod . *Archives Microbiology* **181**, 299-304 (2004 b).

Warheit, D.B.; Hoke, R.A.; Finlay, C.; Donner, E.M.; Reed, K.L.; Sayes, C.M., Development of a base set toxicity tests using ultrafine TiO₂ particles as a component of nanoparticle risk management. *Toxicology Letters* **171**, 99–110. (2007).

Zidar, P., Zinc and cadmium toxicity testing on test organism (*Porcellio scaber* , Isopoda, Crustacea). Master of science thesis, University of Ljubljana, Biotechnical faculty, Department of Biology, p. **56**. (1998).

Žnidaršič, N.; Štrus, J.; Drobne, D. Ultrastructural alterations of the hepatopancreas in *Porcellio scaber* under stress. *Environmental Toxicology and Pharmacology* **13**, 161-174 (2003).

Index of Figures

Figure 1: Main markets for carbon nanotubes, carbon nanofibers, fullerenes, POSS and graphene, by Revenues 2009, presented by Future Markets, Inc.....	2
Figure 2: Main markets for carbon nanotubes, carbon nanofibers, fullerenes, POSS and graphene, by revenues 2015, presented by Future Markets, Inc.....	3
Figure 3: The fate of nanomaterials in the environment. Spreading in the environment of NMs produced in intentional or non intentional ways.....	4
Figure 4.a Nanofibers tested in the experiment number 26 and 29: tungsten three oxides nanofibers. numbers 39, 48, are code from producer Josef Stefan Institute (JSI).....	11
Figure 4.b: Nanofibers and nanaoparticles tested in the experiment number 26, 29 and 31. Tungsten three oxides nanofibers and silver nanoparticles. Number 39, 48, 65 are code from producer Josef Stefan Institute (JSI).....	12
Figure 5: Field Emission Scanning Electron Microscope JEOL JMS- 6500 F (manufactured JEOL Ltd. Japan) at Institute of Metals and Technology, Ljubljana.....	16
Figure 6: a) Porcellio scaber, adult ,b) Scheme of digestive system of porcellio scaber 1. Stomach 2.Gut 3. Hepatopancreas 4. Sphincter 5. Rectum. c) Boxes with the samples in holders, d) Desiccators with box of samples, e) Precision etching coating system Gatan Model 68215.....	17
Figure 7: Scheme of digestive glands preparation methods for observation with focused ion beam/scanning electron microscopy and transmission electron microscopy TEM.....	18
Figure 8: Inductively coupled plasma optical emission spectrometry (ICP-OES), model: PERKINELMER Optima 3100 RL (IMT, Laboratory for chemistry).....	23
Figure 9.a: Shape of cells in digestive gland epithelium (hepatopancreas)- normal appearance	39
Figure 9.b: Shape of cells in digestive gland epithelium (hepatopancreas)- normal appearance	40
Figure 10.a: Shape of the cells in digestive gland epithelium (hepatopancreas)- abnormal appearance.....	41
Figure 10.b: Shape of the cells in digestive gland epithelium (hepatopancreas)- abnormal appearance	42
Figure 11.a: Shape of the cells in digestive gland epithelium (hepatopancreas)- partly flat appearance	43

Figure 11.b: Shape of the cells in digestive gland epithelium (hepatopancreas)- partly flat appearance	44
Figure 12.a: Shape of the cells in digestive gland epithelium (hepatopancreas)- flat appearance	45
Figure 12.b: Shape of the cells in digestive gland epithelium (hepatopancreas)- flat appearance	46
Figure 13.a: Morphological characteristics of digestive gland epithelium (hepatopancrease)- predominantly (Dome shaped)	47
Figure 13.b: Morphological characteristics of digestive gland epithelium (hepatopancrease)- predominantly (Dome shaped)	48
Figure 14.a: Morphological characteristics of digestive gland epithelium (hepatopancrease)- abnormal appearance	50
Figure 14.b: Morphological characteristics of digestive gland epithelium (hepatopancrease)- abnormal appearance	51
Figure 15.a: Morphological characteristics of digestive gland epithelium (hepatopancrease)- Partly flat epithelium (less than 50 %)	52
Figure 15.b Morphological characteristics of digestive gland epithelium (hepatopancrease)- Partly flat epithelium (less than 50 %)	53
Figure 16.a: Morphological characteristics of digestive gland epithelium (hepatopancrease)- predominant flat epithelium (more than 50 %).....	54
Figure 16.b: Morphological characteristics of digestive gland epithelium (hepatopancrease)- predominant flat epithelium (more than 50 %)	55
Figure 17.a: Presence of the bacteria in cells surface of digestive tube (hepatopancreas) – same and different bacteria on surface	56
Figure 17.b: Presence and shape of the bacteria in cells surface of digestive tube (hepatopancreas) – same and different bacteria on surface	57
Figure 18.a: Presence of the bacteria in cells surface of digestive tube (hepatopancreas) – densely colonized	58
Figure 18.b: Presence of the bacteria in cells surface of digestive tube (hepatopancreas) – densely colonized	59
Figure 19.a: Presence of the bacteria in cells surface of digestive tube (hepatopancreas) – low amount	60
Figure 19.b: Presence of the bacteria in cells surface of digestive tube (hepatopancreas) – low amount	61
Figure 20.a: Presence and shape of microvilli in cells surface - normal appearance	62
Figure 20.b: Presence and shape of microvilli in cells surface - normal appearance	63

Figure 21.a: Presence and shape of microvilli in cells surface - abnormal appearance	64
Figure 21.b: Presence and shape of microvilli in cells surface - abnormal appearance	65
Figure 22.a Presence and shape of microvilli on cells surface - abnormal appearance	66
Figure 22.b: Presence and shape of microvilli in cells surface –abnormal appearance	67
Figure 23.a: Presence and shape of microvilli in cells surface - partly covered with material	68
Figure 23.b: Presence and shape of microvilli in cells surface - partly covered with material	69
Figure 24.a: Presence of lipid droplets in the cells of digestive gland epithelium (hepatopancreas)- extrusion of the lipid droplets	70
Figure 24.b: Presence of lipid droplets in the cells of digestive gland epithelium (hepatopancreas)- extrusion of the lipid droplets	71
Figure 25.a: Presence and shape of cellular protrusions in the digestive gland epithelium (hepatopancreas)- different shape and size	73
Figure 25.b: Presence and shape of cellular protrusions in the digestive gland epithelium (hepatopancreas)- different shape and size	74
Figure 26.a: Tungsten nanofibers effects in surface of digestive gland epithelium cells	75
Figure 26.b: Tungsten nanofibers effects in surface of digestive gland epithelium cells	76
Figure 26.c: Tungsten nanofibers effects in surface of digestive gland epithelium cells	77
Figure 27.a Histological analysis of digestive gland epithelium from exposed animals to WOx (light microscopy).....	80
Figure 27.b Histological analysis of digestive gland epithelium from exposed animals to Ag (light microscopy)	81

Index of Tables

Table 1: Framework of experiment: Total number of control and treated animals, experiment number and test, sample preparation, date of SEM investigation.....	19
Table 2: Method for sample preparation for scanning electron microscopy-SEM -	21
Table 3: Experiment nr.26 – Control samples.....	30
Table 4: Experiment nr.26 – Exposed samples to WO _x	31
Table 5: Experiment nr.29 – Control samples.....	32
Table 6: Experiment nr.29 – Exposed samples to WO _x	33
Table 7: Experiment nr.31 – Control samples.....	34
Table 8: Experiment nr.31 –Exposed samples to Ag (1000 ppm)	35
Table 9: Experiment nr.31 –Exposed samples to Ag (5000 ppm).....	36
Table 10: Schematic presentation of digestive gland epithelium characteristics.....	37
Table 11: Chemical analyze of tungsten presence in fecal pallets.....	78
Table 12: Chemical analyze of tungsten presence in hepatopancrease, gut, rest and in the food.	79
Table 13: Histological analyzes of cross section of digestive gland tubes.....	79

Appendix 1: Publications

Scientific paper:

Surface characteristics of isopod digestive gland epithelium studied by SEM.

Protoplasma
DOI 10.1007/s00709-010-0110-3

ORIGINAL ARTICLE

Surface characteristics of isopod digestive gland epithelium studied by SEM

Agron Millaku · Vladka Lešer · Damjana Drobne · Matjaz Godec · Matjaz Torkar · Monika Jenko · Marziale Milani · Francesco Tatti

Received: 12 November 2009 / Accepted: 13 January 2010
© Springer-Verlag 2010

Abstract The structure of the digestive gland epithelium of a terrestrial isopod *Porcellio scaber* has been investigated by conventional scanning electron microscopy (SEM), focused ion beam-scanning electron microscopy (FIB/SEM), and light microscopy in order to provide evidence on morphology of the gland epithelial surface in animals from a stock culture. We investigated the shape of cells, extrusion of lipid droplets, shape and distribution of microvilli, and the presence of bacteria on the cell surface. A total of 22 animals were investigated and we found some variability in the appearance of the gland epithelial surface. Seventeen of the animals had dome-shaped digestive gland “normal” epithelial cells, which were densely and homogeneously covered by microvilli and varying proportions of which extruded lipid droplets. On the surface of microvilli we routinely observed sparsely distributed bacteria of different shapes. Five of the 22 animals had “abnormal” epithelial cells with a significantly altered shape. In three of these animals, the cells were much smaller, partly or completely flat or sometimes pyramid-like. A thick layer

of bacteria was detected on the microvillous border, and in places, the shape and size of microvilli were altered. In two animals, hypertrophic cells containing large vacuoles were observed indicating a characteristic intracellular infection. The potential of SEM in morphological investigations of epithelial surfaces is discussed.

Keywords Scanning electron microscopy · Focused ion beam · Digestive gland epithelium · Hepatopancreas · Isopoda · Crustacea

Introduction

The digestive gland epithelium of the terrestrial isopod *Porcellio scaber* (Isopoda, Crustacea) has been thoroughly investigated by many authors (Štrus 1987; Hames and Hopkin 1989; Lešer et al. 2008). Significant alterations in their morphological characteristics were observed to be related to physiological condition (Hames and Hopkin 1989, 1991; Lešer et al. 2008). Additionally, there are also reports of differences in abundance and morphology of bacteria present on the surface of gland epithelium (Wood and Griffith 1988). However, to date no systematic investigation of gland surface characteristics using conventional scanning electron microscopy (SEM) has been conducted.

In terrestrial isopods, the hepatopancreas is composed of four blind-ending tubes, which lie freely in the body cavity. The hepatopancreatic epithelium contains two cell types, the large B cells that project into the lumen of the hepatopancreas and the wedge-shaped S cells that lie between the B cells. The B cells are secretory and absorptive; they usually contain many lipid droplets and glycogen, and they store some metal ions in granules (Hopkin and Martin 1982; Wägele et al. 1992). The S cells accumulate large amounts of metals such as calcium, and uric acid salts (Wägele et al. 1992). Morphological

A. Millaku · M. Godec · M. Torkar · M. Jenko
Institute of Metals and Technology,
Ljubljana, Slovenia

V. Lešer · D. Drobne (✉)
Biotechnical Faculty, Department of Biology,
University of Ljubljana,
Ljubljana, Slovenia
e-mail: damjana.drobne@bf.uni-lj.si

M. Milani
Materials Science Department and Laboratory FIB/SEM
“Bombay”, University of Milano-Bicocca,
Via Cozzi 53,
20125 Milan, Italy

F. Tatti
FEI Italia,
Viale Bianca Maria 21,
20122 Milan, Italy

Published online: 14 February 2010

 Springer

changes of B cells were attributed to the 24-h digestive cycle (Hames and Hopkin 1991) and recently evidence was presented that B cells have a constant shape and size under normal physiological conditions (Lešer et al. 2008). However, when the animals are subjected to stress, the response is reflected in changes of shape, size, and lipid droplet content of B cells (Köhler et al. 1996; Odendaal and Reinecke 2003; Žnidaršič et al. 2003; Lapanje et al. 2008; Lešer et al. 2008). So far, however, no systematic approach was used to reveal the morphological variability of this epithelium of non-stressed animals.

It is interesting that SEM is rarely selected as a principal method for structural investigation of epithelial morphological characteristics in general. There are many reasons for the paucity of SEM investigations in biology. The development of both transmission electron microscopy (TEM) and SEM began in the 1930s, but TEM reached its full potential for biological imaging almost 30 years earlier than SEM (Pawley 1997). An important reason for this may be that the early SEMs required users to operate with a much higher beam voltage than was necessary to produce low-resolution images of biological samples, and this stimulated the search for alternative microscopy techniques. These were in many cases less suitable than optimized SEM for study of biological samples.

Currently, the focused ion beam-scanning electron microscope (FIB/SEM) system, which has an electron column and an ion column embedded in the same specimen chamber, has opened new and attractive possibilities in biological sample research. A major strength of the application of the FIB/SEM system to investigations of biological samples is its ability to conduct *in situ* site-specific manipulation of a specimen and imaging in a wide range of magnifications (Drobne et al. 2007, 2008).

One aim of this study was to use the potential of SEM for morphological investigation of the digestive gland epithelium surface. Another was to describe morphological characteristics of gland epithelium surface in a population of normal, unstressed animals and so to provide basic morphological characteristics of non-stressed animals, a benchmark for future physiological or (eco)toxicological research. Our objective was a systematic study of the epithelial surface by conventional scanning electron microscopy combined with FIB/SEM and light microscopy.

Materials and methods

Experimental animals and laboratory culture

Terrestrial isopods, *P. scaber* Latreille, 1804 (Crustacea: Isopoda), were collected in gardens under concrete blocks, pieces of decaying wood, or other organic waste. The stock

cultures were kept in the laboratory for some weeks to allow animals to acclimatize and they were then analyzed by means of scanning electron microscopy or light microscopy.

The surface morphology of the hepatopancreatic epithelium was analyzed in 22 animals. In 11 of these, the digestive glands were investigated by both, light microscopy and SEM. In some selected animals, FIB/SEM was also used.

Scanning electron microscopy and FIB/SEM

The isolated digestive gland tubes were transferred into 1.0% glutaraldehyde and 0.4% paraformaldehyde in 0.1 M sodium cacodylate buffer (pH 7.2) for 2.5 h at room temperature. The chemically fixed samples were either directly dehydrated in a graded series of ethanol solutions or processed by the OTOTO method with OsO₄/thiocarbohydrazide/OsO₄/thiocarbohydrazide/OsO₄ (Lešer et al. 2009) and then dehydrated in a graded series of ethanol solutions. The samples were then dried at the critical point (Balzers Critical Point Dryer 030, Liechtenstein) and fastened onto mounts with silver paint (SPI) and gold sputtered (Sputter coater SCD 050, BAL-TEC, Germany). Before SEM or FIB/SEM investigation, the tubes were mechanically opened in two or three regions in order to expose the surface of gland epithelial cells.

Digestive gland tubes were investigated with a field emission scanning electron microscope (Jeol JSM-6500F, at the Institute of Metals and Technology, Ljubljana, Slovenia) or by a focused ion beam/scanning electron microscope (FEI Strata DB 235 M, at the University of Modena, Modena, Italy).

The FIB system was used to expose the subsurface structures by ion milling. After rough milling, the sample cross-section was polished. Rough milling conditions to open a trench employed beam currents of 5 to 7 nA, at 30 kV. Lower beam currents of 100 to 300 pA were used to polish the cross-section. The spot size produced by rough milling was approximately 100–150 nm in diameter, and for polishing it ranged from 20 to 35 nm in diameter. The dwell time for milling was 1 μs and the overlap was 50%. In some samples, a 1–2 μm thick protective platinum strip was deposited on the sample prior to milling.

Light microscopy

For light microscopy, the isolated digestive gland tubes were transferred to the Carnoy-B fixative for 2.5 h at room temperature. This is a standard fixative in our histological and histopathological research and provides good results. After fixation samples were dehydrated in absolute alcohol,

Characteristics of isopod digestive gland epithelium studied by SEM

transferred to xylene, and embedded in Paraplast Plus wax (Sigma). Cross-sections (8 μm thick; Reichert-Jung 2040 rotatory microtome, Austria) of the entire tube were cut, stained with eosin or hematoxylin and eosin and inspected with a light microscope (Axioskop 2 MOT, Carl Zeiss, Germany at Department of Biology, Biotechnical Faculty, University of Ljubljana).

Results

In digestive gland cells of 22 terrestrial isopods from the stock culture, we investigated the shape of B cells,

extrusion of lipid droplets, shape and distribution of microvilli, presence of bacteria on the cell surface, or intracellular infection.

On the basis of these morphological characteristics, the digestive glands were divided into two groups. In the first group, B cells were regularly dome-shaped along the entire gland tube reaching up to 80 μm in height (Fig. 1a–e). In the second group, cells had significantly altered shape and were either much smaller or dome- or pyramid-shaped, or partly, even completely flat (Fig. 2a–e). Sometimes they were significantly hypertrophic (Fig. 3a–e). We refer to those in the first group as *animals with regularly shaped digestive gland epithelium cells*, while members of the

Fig. 1 a–e Normal appearance of digestive gland epithelium. **a** Some cells extrude lipid droplets, others do not. **b** Cells are covered by microvilli where bacteria are found. **c** FIB milling revealed that lipid droplets appear as vesicles filled with homogenous material. **d** If lipids are washed out during the preparation procedure, FIB milling revealed the empty voids where lipids were originally deposited. **e** If lipids are washed out during the preparation procedure for light microscopy, empty regions are seen where lipids were originally deposited. **Bc** B cells, **B** bacteria, **H** holes, **L** lipid droplets, **Mi** microvilli

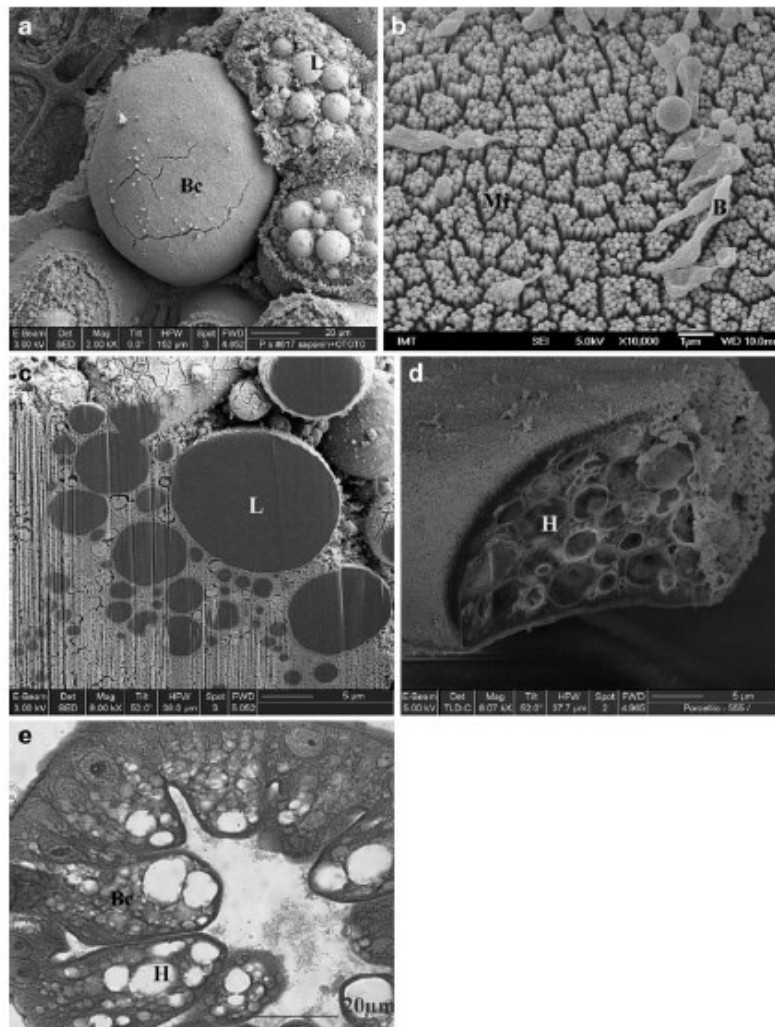
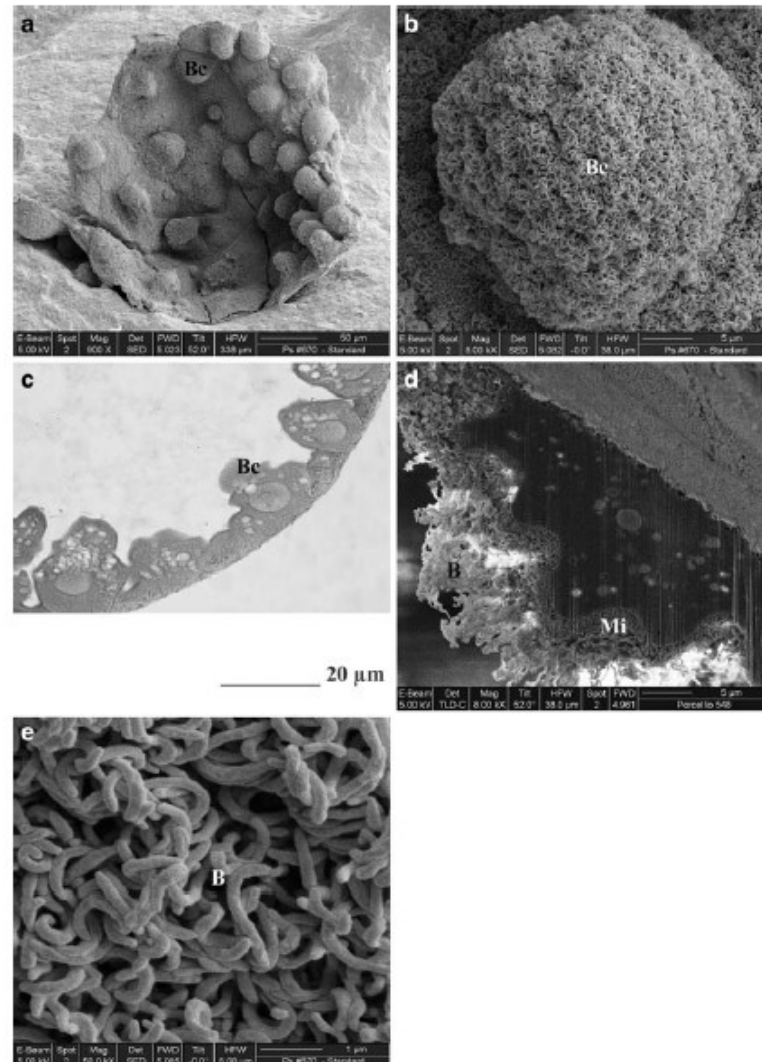


Fig. 2 a–e Abnormal appearance of digestive gland epithelium. **a, c, d** Cells are flattened or pyramid-shaped. **c** The cell surface is sometimes folded. **b, d, e** Cell surfaces are covered by a thick layer of bacteria. *Bc* B cells, *B* bacteria, *Mi* microvilli



second group are designated as *animals with irregularly shaped digestive gland epithelium cells*.

a. Regularly shaped digestive gland epithelial cells

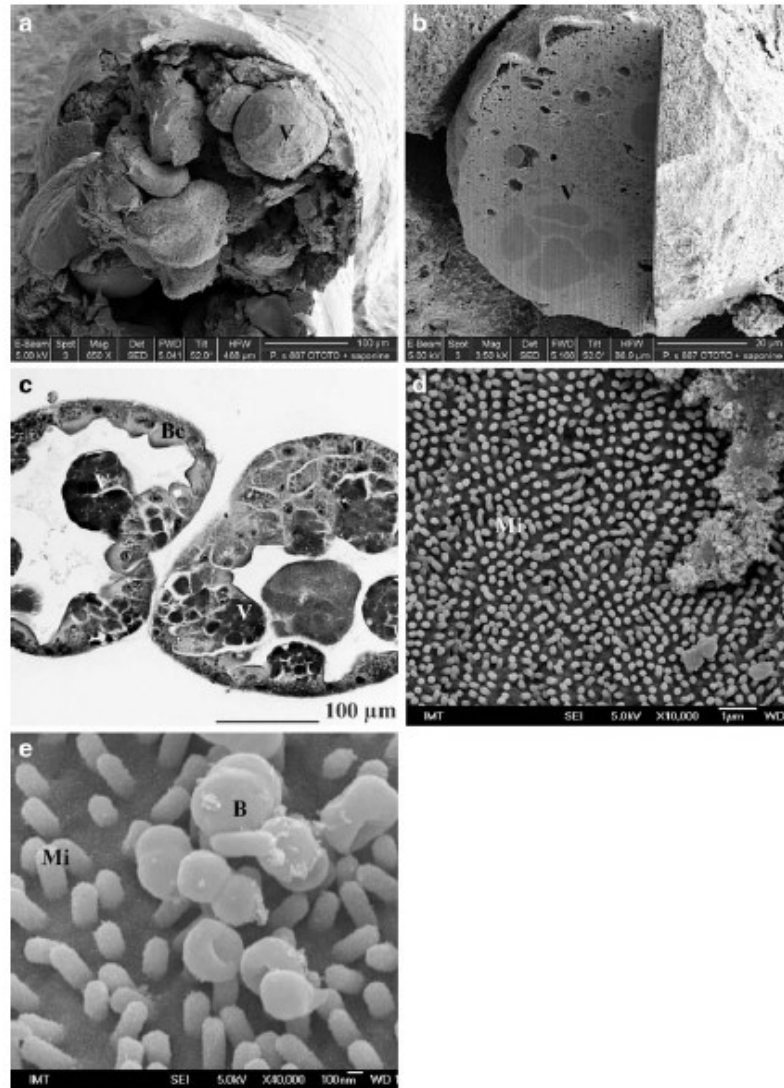
In the 17 or the 22 animals investigated, the cells were dome-shaped and some of them extruded lipid droplets into the lumen of the gland tube (Fig. 1a, c). These epithelia varied in the proportion of epithelial cells which were extruding lipid droplets. In some glands, a majority of cells were extruding lipid droplets while in others, none of the cells did so. The apical parts of cells which are extruding

lipid droplets appeared to be decayed. Other cells were evenly covered by microvilli (Fig. 1b). Here, we regularly observed single bacterial cells lying on the surface of microvillous border. They were sparsely distributed along the tube and had different shapes. They were spherical, quasi-cubic, or shaped like curved or spiral rods. Usually bacteria of similar shapes were detected in a single animal.

We indirectly confirmed the lipid content of extruded material by using a tissue preparation method which dissolves lipids. For this purpose, one tube of the same animal was prepared with the OTOTO preparation proce-

Characteristics of isopod digestive gland epithelium studied by SEM

Fig. 3 a–e Abnormal appearance of digestive gland epithelium. **a, b, c** Some cells are hypertrophic. **b** FIB milling revealed that the vacuoles are not filled with homogenous material. **c** Light micrographs confirm that cells are not filled with lipids. **d** Cell surfaces are in spots covered with microvilli of altered shape or **e** spherical-shaped bacteria. *Bc*: B cells, *B* bacteria, *Mi* microvilli, *V* vacuoles



ture, which preserves lipids (Fig. 1a, c). The other tube was neither postfixed nor conductively stained therefore lipids were washed out (Fig. 1d). The third tube was prepared for light microscopy following a procedure which also washes out lipids (Fig. 1e).

In addition, FIB milling revealed that OTOTO prepared cells are filled with homogenous material (Fig. 1c), while in those from which lipids were deliberately washed out, holes remained where originally lipids had been deposited (Fig. 1d). The same was confirmed by light microscopy

which showed empty regions remaining after lipids were washed out during the preparation (Fig. 1e).

b. Irregularly shaped digestive gland epithelial cells

In three of the 22 animals, the apical and lateral cell surfaces were densely colonized by bacteria (Fig. 2a–e), and a thick layer of bacteria covers the entire epithelial surface. However, cells in distal parts of a gland tube were less densely colonized. In regions of epithelium with a high density of bacteria, alteration in the shape of the cells was

detected, the epithelium becoming flat with pyramidal shaped cells (Fig. 2a, c, d). Cell surfaces were often found to have an irregularly folded appearance (Fig. 2c, d). Where the bacterial coverage was less dense, we also observed changes in shape, size, and density of microvilli. In some regions, microvilli were absent.

In two of 22 animals, cells were hypertrophic, sometimes even more than 150 μm in diameter (Fig. 3a–c). They were filled with large vacuoles, which were not washed out during sample preparation as the lipids were. In cells opened by FIB milling it appeared that the vacuoles were filled with heterogeneous material (Fig. 3b). Similar observations resulted from light microscopy (Fig. 3c). In some cells, microvilli still retained their usual appearance, while in other cells they were short, sparsely distributed or even absent (Fig. 3d). Here we observed single bacterial cells lying on the surface of microvilli (Fig. 3e).

Discussion

This is the first systematic report on an investigation by SEM of the morphological characteristics of digestive gland epithelium of non-stressed terrestrial isopod *P. scaber*.

Our results are in agreement with findings of Lešer et al. (2008) who report that animals in good physiological condition have digestive glands with thick epithelia and B cells filled with lipid droplets. Animals in poor condition, for example starved or chemically stressed animals, have partly or entirely flat digestive gland epithelia with less lipid droplets. The SEM micrographs also reveal that the thinner digestive gland epithelium is related to dense bacterial colonization of cell surfaces. If thinner digestive gland epithelium is linked to stress and poor physiological condition of *P. scaber*, the dense bacterial coverage indicate that these animals are in suboptimal physiological condition. This is not in agreement with some other reports where the authors describe dense bacterial population as symbionts, which as such, play a crucial role in animals' digestion (Wang et al. 2004a, 2004b).

Furthermore, our results are in agreement with reported morphological characteristics of intracellular bacterial infection of hepatopancreas of *P. scaber* (Drobne et al. 1999). The most prominent sign of this infection are white spots between 100 and 200 μm in diameter along the entire gland visible by a naked eye. Previous TEM studies confirmed that these spots are aggregations of vacuoles in the cells that are densely filled with bacteria (Drobne et al. 1999).

Many authors provided scanning electron images of digestive glands of *P. scaber* where rod-shaped bacteria, slightly curved rods, or comma-shaped and spiral-shaped bacteria were observed (Hames and Hopkin 1989, 1991; Storch 1984; Wood and Griffith 1988). Some authors report

the variation in their occurrence between sampling sites, collection dates, and substrate they were feeding upon (Wood and Griffith 1988; Lapanje et al. 2008). These reports are consistent with our findings.

In the study presented here, we have confirmed the potential of SEM in morphological investigation of epithelia to provide evidence which could not be obtained by other microscopies. SEM allows navigation through a large area of the sample and subsequently zooming into the area of interest.

Systematic SEM investigation of morphological characteristics of the digestive gland epithelium of the terrestrial isopod *P. scaber* provides a variety of information related to metabolism, nutritional status, and bacterial colonization of gland tubes. The results presented here show that SEM will provide biological structural evidence that contributes to complete morphological information at the tissue level.

Acknowledgments We thank FEI Italy for the access to Strata DB235 M at the University of Modena e Reggio Emilia, Italy. This work was supported by the Slovenian Ministry of Higher Education, Science, and Technology (J1-9475). We thank Bill Milne for English editing.

Conflicts of interest The authors declare that they have no conflict of interest.

References

- Drobne D, Štrus J, Žnidaršič N, Zidar P (1999) Morphological description of bacterial infection of digestive glands in the terrestrial isopod *Porcellio scaber* (Isopoda, Crustacea). *J Invertebr Pathol* 73:113–119. doi:10.1006/jipa.1998.4818
- Drobne D, Milani M, Lešer V, Tati F (2007) Surface damage induced by FIB milling and imaging of biological samples is controllable. *Microsc Res Tech* 70:895–903. doi:10.1002/jemt.20494
- Drobne D, Milani M, Leser V, Zrimec A, Žnidaršič, Kostanjšek R, Štrus J (2008) Imaging of intracellular spherical lamellar structures and tissue gross morphology by a focused ion beam/scanning electron microscope (FIB/SEM). *Ultramicroscopy* 108:663–670. doi:10.1016/j.ultramicro.2007.10.010
- Hames CAC, Hopkin SP (1989) The structure and function of the digestive system of terrestrial isopods. *J Zool* 217:599–627
- Hames CAC, Hopkin SP (1991) A daily cycle of apocrine secretion by the B cells in the hepatopancreas of terrestrial isopods. *Can J Zool* 69:1931–1937
- Hopkin SP, Martin MH (1982) The distribution of zing, cadmium, lead and copper within the hepatopancreas of a woodlouse. *Tissue Cell* 14:703–715
- Kohler HR, Huttenrauch K, Berlas M, Graff S, Alberti G (1996) Cellular hepatopancreatic reactions in *Porcellio scaber* (Isopoda) as biomarkers for the evaluation of heavy metal toxicity in soils. *Applied Soil Ecology* 3:1–15. doi:10.1016/0929-1393(95)00073-9
- Lapanje A, Drobne D, Nolde N, Valant J, Muscet B, Leser V, Rupnik M (2008) Long-term Hg pollution induced Hg tolerance in terrestrial isopod *Porcellio scaber* (Isopoda, Crustacea). *Environ Pollut* 153:537–547. doi:10.1016/j.envpol.2007.09.016
- Lešer V, Drobne D, Vilhar B, Kladnik A, Žnidaršič N, Štrus J (2008) Epithelial thickness and lipid droplets in the hepatopancreas of

Characteristics of isopod digestive gland epithelium studied by SEM

- Porcellio scaber* (Crustacea: Isopoda) in different physiological conditions. *Zoology* 111:419–432. doi:10.1016/j.zool.2007.10.007
- Lešer V, Drobne D, Pipan Z, Milani M, Tatti F (2009) Comparison of different preparation methods of biological samples for FTB milling and SEM investigation. *Journal of Microscopy-Oxford* 233:309–319. doi:10.1111/j.1365-2818.2009.03121
- Odendaal JP, Reinecke AJ (2003) Quantifying histopathological alterations in the hepatopancreas of the woodlouse *Porcellio laevis* (Isopoda) as a biomarker of cadmium exposure. *Ecotoxicol Environ Saf* 56:319–325. doi:10.1016/S0147-6513(02)00163-X
- Pawley J (1997) The development of field-emission scanning electron microscopy for imaging biological surfaces. *Scanning* 19:324–336
- Storch V (1984) The influence of nutritional stress on the ultrastructure of terrestrial isopods. *Symp Zool Soc* 53:167–184
- Štrus J (1987) The effects of starvation on the structure and function of the hepatopancreas in the isopod *Ligia italica*. *Investig Pesq* 51:505–514
- Wägele J-W, Harrison FW, Humes AG (1992) *Microscopic anatomy of invertebrates. Crustacea*, Wiley-Liss, New York 9:529–617
- Wood S, Griffith BS (1988) Bacteria associated with the hepatopancreas of the woodlice *Oniscus asellus* and *Porcellio scaber* (Crustacea, Isopoda). *Pedobiologia* 31:89–94
- Wang Y, Stingl U, Anton-Erxleben F, Geisler S, Brune A, Zimmer M (2004a) “*Candidatus Hepatoplasma crinochetorum*,” a new, stalk-forming lineage of Mollicutes colonizing the midgut glands of a terrestrial isopod. *Appl Environ Microbiol* 70:61–66. doi:10.1128/AEM.70.10.6166-6172.2004
- Wang Y, Stingl U, Anton-Erxleben F, Geisler S, Brune A, Zimmer M (2004b) ‘*Candidatus Hepatocola porcellionum*’ a new, stalk-forming lineage of Rickettsiales colonizing the midgut glands of a terrestrial isopod. *Arch Microbiol* 181:299–304. doi:10.1007/s00203-004-0655-7
- Žnidaršič N, Štrus J, Drobne D (2003) Ultrastructural alterations of the hepatopancreas in *Porcellio scaber* under stress. *Environ Toxicol Pharmacol* 13:161–174. doi:10.1016/S1382-6689(02)00158-8

THE MICROFLORA AND PHYSICO-CHEMICAL PROPERTIES OF LIGNITE FROM THE MIRASH MINE, NEAR KASTRIOT

MIKROFLORA IN FIZIKALNO-KEMIJSKE LASTNOSTI LIGNITA IZ RUDNIKA MIRASH PRI KASTRIOTU

Fatime Plakolli¹, Luljeta P. Beqiri², Agron Millaku³

¹Faculty of Education, Rr. Agim Ramadani 10000 Pristine, Kosovo
²University of Pristine, Faculty of Mine and Metallurgy, Mitrovica, Kosovo
³Ministry of Environment and Spatial Planning, Rilindja K3, Kosovo
fatimekoka2008@hotmail.com

Prejem rokopisa – received: 2010-03-08; sprejem za objavo – accepted for publication: 2010-04-29

Coal, as an important source of energy, is very often the subject of study for scientists from the areas of chemistry, physics, technology, and biology, etc. In Kosovo, large deposits of coal, in the form of lignite, can be found. Lignite is mostly used to produce electrical energy; however, the interest of the country of Kosovo is to study many of the aspects of lignite.

In this paper an analysis of the microflora of lignite from the mine in the locality of Mirash, near Kastriot, is presented. With modern microbiological methods, the density, assortment, and some of the morphological and physiological characteristics of bacteria (heterotrophic, proteolytic, amilolytic, lypolytic and celulolytic) were determined and aerobic bacteria and fungi (yeasts and moulds) were investigated also. The samples of lignite were analyzed for physico-chemical attributes, for example, a determination of ash, and of C, O, H, N, S, carbonates, silicates, etc. The biomass of the isolated microflora from lignite was submitted for a chemical analysis and an astounding number of bacterial microflora and fungal was found. A composition chemical link between the coal and the microbial biomass was observed: the values of C, O, N, and H were found to be approximately similar in the coal and the bacterial mass.

Key words: coal, lignite, bacterial and fungal microflora, energy, carbonates, silicates, biomass

Premog kot pomemben vir energije je pogosto predmet študija znanstvenikov s področja kemije, fizike, tehnologije, biologije in drugih ved. Na Kosovu so velike količine premoga v obliki lignita. Največ lignita se uporablja za proizvodnjo električne energije, zato je razumljiv interes kosovske družbe in znanosti za njegovo vsestransko preučevanje. V tem prispevku je predstavljena analiza mikroflore lignita iz rudnika Mirash pri Kastriotu. Z modernimi mikrobiološkimi metodami so bile določene gostota, razvrstitev, morfološke in fiziološke značilnosti bakterij (heterotrofnih, proteolitičnih, alilolitičnih, lipolitičnih in celulolitičnih). Istočasno so bile preiskane tudi aerobne bakterije in glive (kvasovke in plesni). Vzorci lignita so bili analizirani in določene so bile fizikalno-kemične lastnosti, kot so: vsebnost pepela, vsebnosti C, O, H, N, S, karbonatov, silikatov in podobnega. Biomasa izolirane mikroflore iz lignita je bila kemijsko analizirana. Najdeno je osupljivo veliko število bakterijske mikroflore in gliv v lignitu in opažena je bila povezava med kemijsko sestavo premoga in biomaso mikrobov. Vsebnosti C, O, N in H so bile približno enake v premogu in v masi bakterij.

Ključne besede: premog, lignit, mikroflora bakterij in gliv, energija, karbonati, silikati, biomasa

1 INTRODUCTION

Coal is considered to be a very important source of energy, and it has been used since the earliest times (before the new era). The economic development of society during the past 1000 years was based on coal as a source of energy (1). Oil and its derivatives are also an important source of energy, and by the beginning of the second half of the 20th Century it had achieved primacy as a source of energy. Nowadays, an interest in coal has once again emerged, because 80 % of fossil fuel reserves are coal as compared to 18 % for oil.

Actually, 45 % of the globally generated energy is generated with coal, as compared to 30 % from oil and 14 % from natural gas (2). Coal is a fossil fuel; it is an organic sedimentary rock; and it is formed by the accumulation of organic matter (plant debris).

This process usually takes place in waterlogged environments (water basins, lakes, marshes, swamps) (3).

Coalification covers a number of geological periods, which can be used to determine the geological history of the Earth's crust (4). For this reason, the process of coal formation took place as a result of a number of different factors (pressure, humidity, lack of air, microbiological reactions, physical and chemical reactions, etc.). The best way to describe this complex process, which took place over millions of years, is the accumulation of dead organic (plant) matter that subsequently forms coal. The composition of coal is very complex; however, it consists mainly of carbon (between 60 % and 95 %). Thus, it has a very wide range of uses and a characteristic structure. Coal contains the following biogenic elements: carbon, hydrogen, oxygen and sulfur. From the biochemical point of view coal contains the same elements as did the tropical plants from which it was formed: oils, resins, etc. It ranges in color between black and brownish-black. Its strength is between 0.5 kg/cm² and 2.5 kg/cm² and its specific weight is 1–1.7.

F. PLAKOLLI et al.: THE MICROFLORA AND PHYSICO-CHEMICAL PROPERTIES OF LIGNITE ...

Coals are divided into humic (formed by the degradation of land plants) and sapropelic (algae and fungi) (5) and it is found in the form of sedimentary rocks. After the fossilization the organic matter was submitted to degradation and in specific circumstances a new matter was formed, which served as the skeleton for the formation of coal. The following can be found in plant cells: cellulose, hemicellulose, lignin, proteins, oils, waxes, resins, cutin, etc. Through the interaction of micro-biological, physical and chemical, as well as geological factors, the organic matter turns into a mass called torv (peat), lignite and other kinds of coal. The coalification process has two phases: humification and carbonization. During the process of humification, organic materials, under the influence of the above-mentioned factors, turn into torv (peat) – humus. The peat is then degraded by microorganisms. Bacteria are known to degrade organic matter and cellulose, on which occasion enzymes and biocatalyzers are produced and affect the oxidoreduction process, as well. Microorganisms affect the inorganic matter by increasing the mineral solubility (7).

According to several authors (8, 9, 10), upon the degradation of peat, microorganisms reduce their activity as a consequence of the formation of antiseptic substances, such as phenols (8).

During the second phase, torv or sapropel will turn into anthracite, lignite, coal, etc (9).

In aerobic conditions, 80 % of the organic matter is lost, whereas in anaerobic conditions only 5 % of the organic matter is lost (10). During the degradation of the organic matter proteolytic microorganisms degrade proteins. Then the degradation of the oils by lipolytic microorganisms and that of cellulose by cellulolytic microorganisms follows and afterwards, the degradation of hemicellulose, lignin, cutin and eventually resins, occurs.

The influence of physical and chemical factors in the formation of coal is characterized by increased pressure and the catalytic influence of minerals and gases together with water, temperature and pH. From the petrographic point of view lignite is xylitic. Geological data show that the Kosovo Coal Basin dates back to the Pliocene (approximately 2.5 million years ago). This tectonic basin was formed during the Oligocene (other layers were sedimented on top of it during the late Tertiary Period). Its reserves are estimated to 2.2 billion tons and could be as high as 10 billion tons. According to (11), the ecoregions in the Kosovo basin during the Pliocene consisted of wetlands, hills and mountains. Based on the ecological conditions, in which certain groups of plants lived, the following wetland vegetation zones existed (12):

- 1) Submerged aquatic plants (Myriophyllum)
 - a) floating plants
 - b) emergent plants (Graminea and Cyperaceae)
- 2) Mountain vegetation zone (Taxodiaceae)

- 3) Shrub zone (Polipodiaceae)
- 4) Dry forest zone (Sequoia forests) (14)

II. Hilly region

Forest zone: Salix, Alnus, Populus (15)
Deciduous forest zone: Quercus, Fagus, Carpinus, Tilia, Castanea, Acer, etc.

III. Mountainous region: Pinus, Picea, Abies, Laryx (16).

From these groups of plants the coal was formed. According to several references, coal and different microorganisms co-existed since the time the deposit was formed, around 2.5 million years ago. They have survived in a latent or dormant state, which slowed down their metabolism in order to survive the unfavorable conditions. The other form is called spores or endospores, and many scientific papers have dealt with coal and microorganisms.

It was established that certain species of bacteria can clean coal and improve its quality, e.g., leptospirillum, ferroxidans and thiobacillus ferroxidans. These species have been bred to use phenol as their only source of food (17) and pseudomonas and arthrobacter have degraded coal molecules by "eating" sulfur and other contaminants.

Bacteria increase the intensity of methane degradation (attested in the labs of the US Energy Department). The digestive system of the above-mentioned bacteria eliminates harmful pollutants and helps the production of clean coal (18). Certain strains (Pseudomonas) can degrade or ferment, coal derivatives (fenatren) producing CO₂ and H₂O: Fenatren – 1 – hydroxyl 2 – naphtoic acid – salicylic acid – catechol – CO₂+H₂O (19). The bacteria digest the carbon in the rocks and produce natural gas for a period of about 10–1000 years (21) and lock methane at the bottom of the sea in anaerobic conditions. The aim of this study was to determine the presence of the bacterial and fungal microflora in the lignite from the Mirashi-Kastrioti Coal Mine. The presence of heterotrophic, proteolytic, amilolytic, lipolytic, cellulolytic, aerobic bacteria and fungi was studied in order to get an idea about the existing microflora at the time when the lignite was formed.

Furthermore, the aim of this study was to determine the composition of the ash, biogens and bacterial biomass in the lignite from the Mirashi Coal Mine. The authors were motivated by the claim (6) that hopanoids, the compounds in the membranes of prokaryotic cells (as well as bacteria), can be found in great abundance here (as well as by the data on the amount of carbon in the coal of the Kosova basin). It must be stressed that hopanoids are the main constituents of coal (90 %). Scientific data show that the membranes of prokaryotic cells (bacteria, cyanobacteria) have the most hopanoids.

Since the organic material (in coal) consists largely of bacteria in the form of kerogen, which is the organic precursor of petroleum, it becomes obvious that hoba-

noids or bacterioplanetrol are isolated from kerogen. In order to verify the relation between the accumulation of kerogens and bacterial activity, the authors (20, 23) have demonstrated the importance of bacteria in the formation of fossil fuels and the degradation of organic matter.

2 MATERIAL AND METHODS

Lignite samples from the Mirashi Coal Mine in the vicinity of Kastriot were used as study material and samples of dry and wet coal were examined. For the physico-chemical analysis of the coal (lignite), gravimetric, chromatographic and spectrophotometric methods were used. The following parameters were determined: moisture, ash, combustible volatile matter, lower calorific value, fixed carbon, total sulfur, organic sulfur, inorganic sulfur, SiO₂, Al₂O₃, Fe₂O₃, CaO, magnesium oxide and sulfur oxide.

A lump of coal was first examined. Later it was subjected to grinding and mixed with sterilized tap water in order to determine the presence of microflora on its

surface and interior. Modern methods were applied to determine the presence of microflora (Standard Methods for the Examination of Water and Wastewater, APHA – last edition). The presence of biogens was determined using a sophisticated apparatus (VARIO MACRO CHNS). Initially, wet coal was dried at a temperature of 105 °C for 2 h. A sample of coal with a weight of 75 mg to 125 mg was used. The minimum weight for a reliable analysis was 40 mg. First, the content of biogens present in the lignite, the ratio between C and N, C and H as well as C and S were determined. Then the presence and the amount of biogens in the bacterial biomass isolated from the lignite were determined using the same apparatus.

3 RESULT WITH DISCUSSION

3.1 Microbiological analysis of lignite

The microbiological, physical and chemical results were obtained in the three-month period of March, April and May. The results represent the arithmetical average of three measurements. Wet coal was used due to the fact that it had a higher density of microorganisms.

Table 1: Heterotrophic bacteria and physiological groups isolated from lignite

Tabela 1: Heterotrofne bakterije in fiziološke skupine, izolirane iz lignita

Bacterial group	Unit	Number	x/%
Heterotrophic bacteria (saprophytic)	mL	28,855,000	100
Proteolytic	mL	3,375,000	11.49
Amilolytic	mL	4,900,000	16.98
Lipolytic	mL	2,380,000	8.24
Cellulolytic	mL	3,200,000	11.08
Sporogenic (microaerophilic)	mL	15,000,000	51.98
Total		28,855,000	99.97

(The amount of substance fraction, x%)

Table 2: Fungal microflora isolated from the lignite of the Mirashi Coal Mine.

Tabela 2: Mikroflora gliv, izoliranih iz lignita iz premogovnika Mirashi

Fungi type	Unit	Number	x/%
Mold	mL	16,000,000	66.66 %
Yeast	mL	8,000,000	33.33 %
Total		24,000,000	99.99

Table 3: Some physical parameters of the lignite from the Mirashi Coal Mine (March, April and May 2008)

Tabela 3: Nekaj fizikalnih parametrov lignita iz premogovnika Mirashi (marec, april in maj 2008)

Month	w(M)/%	w(A)/%	w(Vm)/%	Hu/(MJ/kg)
March	41.30	12.84	41.27	8.563
	44.64	16.49	38.87	7.809
	42.35	18.9	35.94	6.889
April	41.30	19.20	37.35	7.332
	42.20	15.1	39.37	7.966
	41.25	15.15	38.95	7.834
May	42.40	12.80	39.31	7.947
	42.32	17.79	35.67	6.804
	42.30	19.60	36.88	7.184
	40.28	13.74	36.82	7.165
Average value	42.03	16.16	38.04	7.549

Legend: M – moisture content, A – ash content, Vm – volatile matter, Hu/(MJ/kg) – lower calorific value.

F. PLAKOLLI et al.: THE MICROFLORA AND PHYSICO-CHEMICAL PROPERTIES OF LIGNITE ...

The data show that the sporogenic bacteria (51.98 %) dominate the microflora, followed by the proteolytic bacteria (11.49 %) and amilolytic (16.98 %). The results of the analysis prove that the physiological groups listed in **Table 1** were present in the plant matter from which the lignite was formed. Based on the results in **Table 1** (according to which a single group may contain up to 28,855,000 bacteria), we can conclude that 1 t of lignite contains about $28.8 \cdot 10^{12}$ microorganisms, as was stated by other authors as well (6).

According to **Table 2**, just 1 g of lignite with moisture content contains 16 million mold cells (66.6 %). The remaining 33.33 % are yeast cells.

3.2 Physical and chemical analysis

The above-mentioned lump of coal was used to determine the content of moisture and ash, combustible volatile matter as well as the lower calorific value of the coal (**Table 3**).

The lower calorific value of lignite present in **Table 4** was 8027 MJ.

CaO and SiO₂ are the main components in the ash of the coal from the Mirashi Coal Mine. The large concentration of CaO shows that it originates from limestone sedimentary rock. The large presence of SiO₂ shows that the lignite originates from silica algae (silica rich soil) (**Table 5**).

Table 4: Content of components important for the calorific value of lignite (Mirashi Coal Mine March, April and May 2008)

Tabela 4: Vsebnost komponent pomembnih za kalorično vrednost lignita (premogovnik Mirashi, marec, april in maj 2008)

No	Analyzed parameters	Content, w/%
1	Coke	34.06
2	Fixed carbon	18
3	Vaporizing matter	20.2
4	Volatile matter	39.64
5	Total sulfur	0.78
6	Other	7.52

Table 5: Chemical composition of ash of lignite from the Mirashi Coal Mine (March, April and May 2008)

Tabela 5: Kemijska sestava pepela v lignitu iz premogovnika Mirashi (marec, april in maj 2008)

Components Content, w/%	
SiO ₂	27.48
Al ₂ O ₃	11.82
Fe ₂ O ₃	7.46
CaO	37.33
MgO	3.2
SO ₂	9.6
Other	3.11

Table 6: Content of biogens (C, N, S, H) in lignite from the Mirashi Coal Mine

Tabela 6: Vsebnost biogenov (C, N, S, H) v lignitu iz premogovnika Mirashi

First measurement	Sample weight	Unit	Sample	m(C)/m(N) ratio	Content, w/%
	40.4	mg	lignite	43.06	w(N) = 1.096 w(C) = 47.19 w(S) = 1.268 w(H) = 4.383
Second measurement	40.0	mg	lignite	45.55	w(N) = 1.032 w(C) = 47 w(S) = 1.347 w(H) = 4.392
Third measurement	40.8	mg	lignite	49.23	w(N) = 1.055 w(C) = 51.92 w(S) = 1.381 w(H) = 4.405
Average value				45.94	w(N) = 1.061 w(C) = 48.73 w(S) = 1.332 w(H) = 4.36

Table 7: Presence of biogens (C, N, S, H) in the microbial biomass isolated from lignite of the Mirashi Coal Mine

Tabela 7: Prisotnost biogenov (C, N, S, H) v biomasi mikrobov, izoliranih iz lignita iz premogovnika Mirashi

Measurement	Sample weight m/mg	Sample	C/N ratio w(C)/w(N)	Content, w/%
First measurement	84-95	Microbial biomass w(C)/w(N) = 2.07	N: C: S: H:	21.34 44.36 0.77 7.18
Second measurement	84-95	w(C)/w(N) = 2.07	N: C: S: H:	21.53 44.75 0.72 7.31
Third measurement	84-95	w(C)/w(N) = 2.08	N: C: S: H:	21.42 44.68 0.70 7.24
w(AV)/w(N) = 21.43; w(C) = 44.59; w(S) = 0.73; w(H) = 7.24				

3.3 The presence of biogens (C, N, S, H) in the analyzed coal and in the microbial biomass isolated from the same

Data in **Table 6** show that carbon is the main component in biogenic coal (48.73). The average value of $m(C)/m(N)$ ratio is 45.94.

The data in **Table 7** confirm, once again, the domination of carbon in the microbial biomass isolated from the lignite of the Mirashi Coal Mine. The results show that there is a resemblance in the constitution of the biogens in the coal and those in the bacterial biomass. It has been confirmed that during the Pliocene the vegetation in the Kosovo basin consisted of 132 different types of plants with numerous sub-types, grasses, aquatic plants, trees, etc. A number of authors (11, 12, 13, 14, 15) have reconstructed the vegetation of that period by comparing the fossil pollen grains and spores from the Pliocene with those from the present day. The same plants can nowadays be found in the area of the Kosovo coal basin.

4 CONCLUSION

Based on the investigations performed, the following conclusions can be drawn:

- The lignite from the coal mine in Mirash (Kastriot) has a high density of microorganisms, i.e., 28,855,000 microorganisms per gram or $28 \cdot 10^{12}$ microorganisms per ton.
- Among the isolated microorganisms we have determined the presence of bacteria, molds and yeasts (gram positive, negative and variable). The most common shapes were rods, spheres and spirals.
- Forty pure cultures were isolated (with typical representatives).
- Due to its physical and chemical characteristics the lignite from the Kosovo basin is of a better quality than that of other basins in the region.
- The presence of biogens (C, N, H, S) in the coal and the microbial biomass provides evidence of their functional interaction during the process of coal formation.
- The number of microorganisms in 1 g of lignite is evidence that most of the microorganisms are deposits of hopanoids, respectively carbon.
- The fossil pollen grains and spores found in different horizontal and vertical layers of the Kosovo coal

basin give us a picture of the vegetation of the area from which the lignite was formed.

5 REFERENCES

- ¹ M. Berisha: Studij distribucije nekih elemenata u substance Kosovskog uglja. Doctor's Thesis. Prirodno matematički fakultet. PMF, Prishtina, 1982, p. 7-9
- ² L.I. Munro: Chemistry in engineering, Prentice Hall. (Inc), 1964
- ³ P. Nikolić, D. Dimitrijević: Monografija savremena administracija. Beograd, (3, 9, 13, 175) 1980
- ⁴ A. Towle: Modern biology, Rinehard Winston, 1990, 221, 353-354
- ⁵ Z. i J. Aljančić: Ugalj kao izvoz energije, Naučna knjiga, Beograd, 1951
- ⁶ L. Prescott, J. Harley, D. Klein: Microbiology. Fourth ed. McGraw-Hill, 1999, 41-42
- ⁷ C. L. Brierly: Microbiological minig. Science American, 247 (1982) 2, 44-53
- ⁸ P. Atlas: Microorganisms and petroleum pollutants. BioScience, 28 (1978) 6, 378-391
- ⁹ D. Allen: Coal. Abana (Appalachian Blacksmiths), 2003
- ¹⁰ H. H. Lowry, F. Wily: Chemistry of coal utilization, 1963, 208
- ¹¹ V. Nikolić: Proučavanje spora i polena iz pliocenskog lignita Kosovskog basena sa osvrtom na današnji izgled vegetacije Kosova. Prirodnački muzeum u Beogradu, 1966
- ¹² M. Atanacković: Pliocen Kosovskog basena. Geološko paleontološka studija. Zavod za geološka istraživanja C. Gore. Knj. III. Titograd, 1959
- ¹³ E. Nagy: Polynoloische Untersuchung der am Fusse des Matra-Gebirges galagenten ober panonischen, 1952
- ¹⁴ M. Janković: Fitoekologija sa osnovama Fitocenologije i pregledom tipova vegetacija na Zemlji. Naučna knjiga, Beograd, 1963
- ¹⁵ I. Horvat: Sistematski odnosi termofilnih hrastova i borovih šuma jugoistočne Evrope. Biocai glasnik, 12 (1959), 1-2
- ¹⁶ N. Pantić: Paleobotanika, Naučna knjiga, Beograd, 1960
- ¹⁷ M. Plakolli: Examination of phenolic degrading ability of bacterial cultures isolated from phenolic waste water of the place drying of the plant "Kosova" Acta Biol. Med. Exp., 10 (1985), 5-12
- ¹⁸ M. Lin, E. Premuzić: Coal - purifying bacteria, Brookhaven National Laboratory, New York, 2001
- ¹⁹ M. Rogoff, I. Wender: Bacterial oxidation of phenanthrene, Bureau de Mines, U.S Department of Interior Region V Bruceton, Pennsylvania, 1956
- ²⁰ Ourisson et al: The microbial origin of fossil fuels. Sci. Am. 251 (1984) 2, 44-51
- ²¹ A. Martini: Green Car Congress Ecology. University of Massachusetts, 2008
- ²² D. Valentine: Bacteria keep undersea methane out of the atmosphere. Santa Barbara, California USA, 2007
- ²³ P. Luger et al: The crystal structure of Hop-17 (21)-en-3B-y1 acetate of *Pluchea pteropoda* Hemsl. Vietnam. Cryst. Res. Technol. 35 (2002) 3, 355-362

UDK 669.1.782
Professional article/Strokovni članek

ISSN 1580-2949
MTAEC9, 44(5)289(2010)

RECYCLING OF STEEL CHIPS RECIKLIRANJE JEKLENIH OSTRUŽKOV

Matjaž Torkar, Martin Lamut, Agron Millaku

Institute of Metals and Technology, Lepi pot 11, SI-1000 Ljubljana, Slovenia
matjaz.torkar@imt.si

Prejem rokopisa – received: 2010-05-17; sprejem za objavo – accepted for publication: 2010-06-20

The recycling of waste metallic materials and the use of scrap are important for the economic production of a steelworks. Here, we investigate the technology of remelting steel chips. It was confirmed that the main problems with using chips in an electric arc furnace were the chips' large specific surface and the high losses due to the chips' oxidation. To overcome both problems the compaction and remelting of the chips were tested. The investigation revealed that a major problem for the recycling ecology of steel chips was the safe removal of cutting fluids and oils from the chips' surface. The chemical analysis of the remelted chips confirmed that stainless-steel chips can be an acceptable source of the alloying elements chromium, nickel and molybdenum.

Key words: steel chips, magnetic separation, cold compaction, remelting

Recikliranje odpadnih kovinskih materialov in uporaba starega železa sta pomembna za ekonomiko železarne. Tehnologija proizvodnje jekla s pretaljevanjem starega železa v elektro obločni peči je primerna tudi za jeklene ostružke. Preizkušena je bila tehnologija pretaljevanja jeklenih ostružkov. Glavni ugotovljeni problemi pri uporabi ostružkov v elektro obločni peči so velika specifična površina in velike talilne izgube zaradi oksidacije ostružkov. Zato je bilo preizkušeno stiskanje ostružkov in njihovo pretaljevanje. Predstavljeni so rezultati teh preizkusov. Ti so pokazali, da je bila glavna težava pri ekološkem recikliranju jeklenih ostružkov odstranitev rezilne tekočine in olj z njihove površine brez kontaminacije zraka. Kemijska analiza pretaljenih ostružkov je potrdila, da so ostružki nerjavnega jekla koristen vir legiranih elementov, kot so krom, nikelj in molibden.

Ključne besede: jekleni ostružki, magnetno ločevanje, hladno stiskanje, pretaljevanje

1 INTRODUCTION

Wastes that were traditionally discarded from industrial production are nowadays recycled.¹ The discarding of waste materials has a negative environmental impact and is a waste of time and money for the manufacturer of steel or machine parts.² Steel chips are a by-product of the mechanical working of steel parts in the metal industry and their quantity is considerable. The quantities of steel chips recorded by years in Slovenia are shown in **Table 1**.

Table 1: Quantity of steel chips in Slovenia

Tabela 1: Količina ostružkov železa v Sloveniji

Year Leto	Classification number/Klasifikacijska številka: 120101 Quantity of filings and turnings of steel/ Količina opilkov in ostružkov železa (t)
2002	58 120
2003	33 111
2004	48 828
2005	43 991
2006	53 180
2007	93 381

Source: Statistical Office of the Republic of Slovenia

Steel production in the Republic of Slovenia is based on the remelting of scrap. From the data in **Table 1** it is evident that steel chips could be an important source of iron and other elements for steel producers.

With the prices of nickel and chromium currently high, and on the rise in recent years, the production of steel is becoming increasingly more expensive, and with the prices rising, the recycling of steel chips is beginning to look more appealing for steel companies.^{2,3,4,5} For better productivity during metal working the cutting tools are cooled and lubricated with special cooling liquids consisting of lubrication, cooling and anti-corrosion agents. However, the chips are contaminated with these substances and need to be cleaned before any further processing. It is important to note that discarded coolants from the manufacturing of steel have a more harmful impact on the environment than dry chip processing.⁴ This means that the coolants have to be removed in order to obtain more environmentally friendly waste from the chips generated in the processing of the steel. The discarding of metallic chips is harmful to the environment, regardless of whether they are contaminated or not, and these chips should not end up in landfills, thereby losing their potential for reuse. In the near future the recycling of these chips will actually cost less than disposing of them in a landfill.

The first step during the recycling of chips is usually the separation of the cooling liquid and the oil with a centrifuge.^{3,4} It is also possible to remove the lubricant by washing them in an organic solvent that dissolves the organic contaminants from the chips' surface. The latter possibility is less acceptable because most organic solvents are carcinogenic and harmful to the environment, and their use and removal are regulated by the law.

Vacuum separation² is also used, by heating the chips in a vacuum chamber up to 270 °C. The low pressure in the chamber accelerates the evaporation of volatile components that are pumped out, cooled in a condenser at appropriate temperatures and the oils and water are separated. After regeneration, the oil is reused for machining.

The best quality of regenerated oil is obtained with a treatment involving supercritical CO₂ gas at a pressure of 100 bar.² However, when compared to other methods, this method is too expensive for the cleaning of chips.

After the chips of structural steel are cleaned they are separated from the chips of stainless steel using magnetic separation.⁶

Steel chips have a high specific volume and a low density that makes the remelting more difficult and with a low yield. For this reason, compacting with a cold press or briquetting, which increase the density of the chips, makes possible a more effective melting process.

The content of chromium in stainless steel is greater than that of nickel, but the price of nickel makes it more costly overall than chromium in the production of stainless steel.

The cost of nickel is so high that the price of stainless steel is directly related to the price of nickel, which has increased six fold from 2002 to 2006.³ The price of ferrochrome has more than doubled in the past four years (2002 to 2005)³, but the increase in the chromium price is still lower than the increase in the nickel price. For this reason, any source of chromium and nickel is cost attractive for stainless-steel producers.

For the producer of stainless steel in Slovenia an evaluation of the mixture of chips with respect to the content of chromium, nickel and molybdenum, as a possible additional source of alloying elements, was made.

2 EXPERIMENTAL

Magnetic tests showed the chips, declared as stainless-steel chips, were in reality a mixture of carbon steel and stainless steel. After the magnetic separation, however, only the stainless-steel chips were processed further.

Two methods of degreasing the chips were tested: heating in a laboratory furnace up to 400 °C and burning the volatile gases, and washing the chips in a waste organic solvent, trichloroethylene. Using both methods, dry and clean chips were obtained.

The degreased chips were cold pressed into cylindrical compacts, more suitable for remelting because of their higher density and lower volume. For the cold pressing a manually driven screw press was applied. The chips were charged in a hollow, slightly conical tool and repeatedly added and pressed until the tool was full. The pressed chips were then pressed out of the tool from the opposite site.

The compacts were then melted in a 20-kg induction-melting furnace using a premelt of known

composition. The compacted chips were added to the primary melt and after remelting a sample of the melt was submitted to chemical analysis and the contents of nickel, chromium and molybdenum in the chips were calculated. The chemical analysis was performed with optical emission spectrometry ARL and controlled with



Figure 1: Mixture of steel chips
Slika 1: Mešanica jeklenih ostružkov

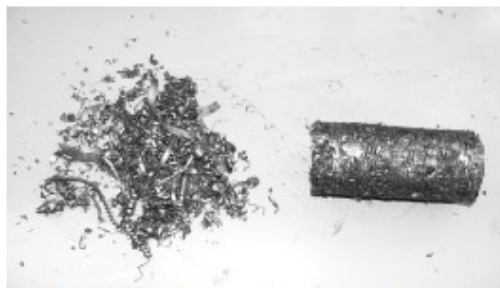


Figure 2: Separated stainless steel chips and compacted, cold pressed chips
Slika 2: Ločeni ostružki nerjavnega jekla, hladno stisnjeni ostružki



Figure 3: Compacts of stainless steel chips after cold pressing
Slika 3: Stisnjeni ostružki nerjavnega jekla po hladnem stiskanju



Figure 4: Charging of compact into melt
Slika 4: Dodajanje stisnjencev v talino



Figure 5: Casting of sample for chemical analysis
Slika 5: Ulivanje vzorca za kemijsko analizo

wet chemical analysis. The quantity and composition of the slag were not taken into account.

3 RESULTS AND DISCUSSION

The magnetic separation revealed that the investigated sample consisted of a mixture of 1/3 of stainless steel and 2/3 of carbon steels, but for further processing only the chips of stainless steel were used.

Two methods for removal of the cooling fluid were tested. First, degreasing in trichloroethylene, which is an effective solvent for greases and a variety of organic materials. Its use is harmful because it is carcinogenic and it is suitable only for applications in laboratory-controlled conditions, whereas it is not suitable for industrial processing.

The second method was heating the chips to 400 °C in an electric furnace, when the water and oil evaporated, and clean and dry chips were obtained. The heating smoke was burned to CO₂ and H₂O by introducing it into a flame.

M. TORKAR et al.: RECYCLING OF STEEL CHIPS



Figure 6: Ingots composed of basic steel and added compacts
Slika 6: Ingota, sestavljena iz osnovnega jekla in dodanih stisnjencev

On an industrial level, it is also possible to charge oil-contaminated chips with scrap directly. In this case the organic impurities would be burned out at high temperatures and the formed gases would escape through the filters for furnace exhaust gases. In the case of a too low temperature, the evaporation of oils and their collection in filters may reduce the filters' efficiency.

3.1 Compacting the chips

The direct melting of the chips in the 20-kg induction furnace was not possible. Because of the low density, the chips in the furnace would only be heated to a temperature below the melting point. For the melting it was necessary to prepare chips in a compacted form and for this reason, the chips were cold pressed into a cylindrical form with a pressure of 1765.8 kPa. For comparison the pressing of contaminated and degreased chips was tested. In both cases the product was compacted into a round, cylindrical form with a diameter of 55 mm and length of 120 mm, and with a density of between 3 kg/dm³ and 4 kg/dm³. The pressed forms were of round section and had a diameter of 55 mm and a length of 120 mm. The size of the forms was limited by the dimensions and the height of the pressing-tool cavity.

3.2 Remelting the chips

An induction-melting furnace requires a minimal density of charge, and the density of the compacts was still too low for direct melting in an induction furnace. The compacts were only heated and their temperature did not reach the melting point. To master the melting a primary melt with known composition was prepared and then the compacts were charged into the molten steel. First, 7 kg of mild steel was melted in the 20-kg induction furnace and its chemical composition was determined. The mass of the molten steel was reduced by 765 g to 6 235 g, 13 000 g of compacts added and a total melt mass of 19 235 g was achieved. The slag was

Table 2: Chemical composition of primary melt, after the addition of chips and calculated composition of chips. All in mass fractions, w/%
Tabela 2: Kemijska sestava primarne taline, po dodatku ostružkov in izračunana sestava ostružkov. Vse v mas. deležih, w/%

Chemical composition		C	Si	Mn	Ni	Cr	Mo	Cu	Fe
Primary melt w/%		0.14	0.25	0.19	0.04	0.03	0.05	0.11	99.30
Weight (g)	6235	8.73	15.59	11.85	2.49	1.87	3.12	6.86	6191.36
Mixture w/%		0.24	0.35	0.89	4.30	8.80	0.60	0.34	84.82
Weight (g)	19235	46.16	67.32	171.19	827.11	1692.68	115.41	65.40	16315.13
Chips w/%		0.29	0.40	1.23	6.34	13.01	0.86	0.45	77.88
Weight (g)	13000	37.44	51.74	159.35	824.61	1690.81	112.29	58.54	10065.23

removed from the melt and a sample for chemical analysis was taken. The rest of the melt was cast into ingots with a square cross-section. The weight of the as-cast sample for the chemical analysis and ingots together was 18 150 g. The difference between 1 085 g and 19 235 g is the material loss (slag, drops, remains in the melting furnace).

3.3 Determination of the composition of the chips

The basis for the calculation of the content of elements in the stainless-steel chips was the total mass of 19 235 g. This represents 13 000 g of chips of unknown composition diluted within 6 235 g of mild steel with known composition. A programme was prepared in Excel for the calculation of the chemical composition of the premelt, of the ingots and of the content of the individual elements in the chips. From the chemical composition of the premelt and of the composition of the ingot the content of elements in the chips in **Table 2** was calculated.

4 CONCLUSIONS

The recycling of steel chips with remelting in an induction-melting furnace was investigated. Based on the experimental results, the following conclusions can be drawn:

Tests with magnets revealed that the investigated chips were a mixture of 1/3 of non-magnetic fraction (stainless steel) and 2/3 of magnetic fraction (structural

steel). Both fractions of chips were successfully separated with magnetic separation and the following composition of the investigated chips was obtained: 13.01 % Cr, 6.34 % Ni, 0.86 % Mo and 0.45 % Cu.

The higher carbon content and the lower chromium content in the chips are probably due to the inaccuracy of magnetic separation method or the incomplete elimination during the burning of the oil contamination.

The investigations confirmed that the compaction of the chips is necessary for a better yield of material in the melting process and that stainless steel is a valuable source of alloying elements.

5 REFERENCES

- ¹ D. Janke, L. Savov, H.-J. Weddige, E. Schulz, Scrap-based steel production and recycling of steel, *Materiali in tehnologije* 34, (2000) 6, 387–399
- ² J. Bongardt, Technical Note: Reduction of waste from fabrication processes. *The Journal of The South African Institute of Mining and Metallurgy*, March/April 1997, pp 63–67
- ³ Sean Dyer, Bao Ngo, Kurt Wivagg, Chip Recycling: Recycling of chips from BZZ conditioning processes, Worcester Polytechnic Institute, A Major Qualifying Project for Degree of Bachelor of Science, www.wpi.edu/Pubs/E-project/Available/E-project-04267-151242/unrestricted/YR_SGMQP_05.pdf
- ⁴ V. A. Kurdyukov, A. A. Sergeev and A. A. Reznakov, Efficient methods of processing metal chips, *Metallurgist*, 41 (1997) 9–11, 331–335
- ⁵ S. I. Stepanov, Some laws on the hot and cold compression of steel chips, *Powder Metallurgy and Metal ceramics*, 5 (1966) 2, 99–102
- ⁶ William J. Bronkala, *Magnetic separation*, Wiley-VCH Verlag GmbH & Co. KGaA., DOI:10.1002/14356007.b02_19, June 15, 2000

Appendix 2: Personal bibliography for the period 2008-2010

COBISS Kooperativni online bibliografski sistem in servisi COBISS

AGRON MILLAKU [31394]

Osebna bibliografija za obdobje 2008-2010

ČLANKI IN DRUGI SESTAVNI DELI

1.01 Izvirni znanstveni članek

1. PLAKOLLI, Fatime, BEQIRI, Luljeta P., MILLAKU, Agron. The microflora and physico-chemical properties of lignite from the Mirash mine, near Kastriot = Mikroflora in fizikalno-kemijske lastnosti lignita iz rudnika Mirash pri Kastriotu. *Mater. tehnol.*, 2010, letn. 44, št. 5, str. 271-275, tabele. [COBISS.SI-ID [826282](#)]

2. MILLAKU, Agron, LEŠER, Vladka, DROBNE, Damjana, GODEC, Matjaž, TORKAR, Matjaž, JENKO, Monika, MILANI, Marziale, TATTI, Francesco. Surface characteristics of isopod digestive gland epithelium studied by SEM. *Protoplasma*, 2010, vol. 241, no. 1-4, str. 83-89. <http://dx.doi.org/10.1007/s00709-010-0110-3>, doi: [10.1007/s00709-010-0110-3](https://doi.org/10.1007/s00709-010-0110-3). [COBISS.SI-ID [6240377](#)]

1.04 Strokovni članek

3. TORKAR, Matjaž, LAMUT, Martin, MILLAKU, Agron. Recycling of steel chips = Recikliranje jeklenih ostružkov. *Mater. tehnol.*, 2010, letn. 44, št. 5, str. 289-292, ilustr. [COBISS.SI-ID [826026](#)]

1.08 Objavljeni znanstveni prispevek na konferenci

4. MILLAKU, Agron, PLAKOLLI, Mujë, VEHAJI, Idriz. The impact of biological chemical and physical pollution on the water quality in river Klina. V: Conference on water observation and information system to decision support, 27-31 May 2008, Ohrid Republic of Macedonia. *Balwois*. Skopje: Ministry of education and science of Republic of Macedonia, cop. 2008, str. 1/9-9/9. <http://balwois.org>. [COBISS.SI-ID [796842](#)]

1.12 Objavljeni povzetek znanstvenega prispevka na konferenci

5. MILLAKU, Agron, LEŠER, Vladka, DROBNE, Damjana, GODEC, Matjaž, TORKAR, Matjaž, JENKO, Monika, MARZIALE, Milani, TATTI, Francesco. Surface characteristics of digestive gland epithelium of a terrestrial isopoda porcellio scaber studied by SEM = Značilnosti površine epitelija prebavne žleze organizma porcellio scaber preiskovane s SEM. V: JENKO, Monika (ur.). 17. konferenca o materialih in tehnologijah, 16.-18. november 2009, Portorož, Slovenija = 17. konferenca o materialih in tehnologijah, 16.-18. november 2009, Portorož, Slovenija. *Program in knjiga povzetkov*. Ljubljana: Inštitut za kovinske materiale in tehnologije, 2009, str. 50. [COBISS.SI-ID [781738](#)]

6. MILLAKU, Agron, LEŠER, Vladka, DROBNE, Damjana, JENKO, Monika, TORKAR, Matjaž. Morphology of digestive gland epithelium of porcelio scaber studied by SEM. V: VESELÝ, Marian (ur.), VINCZE, Andrej (ur.), VÁVRA, Ivo (ur.). 13th Joint Vacuum Conference, June 20-24, 2010, Hotel Patria, Štrbské Pleso High Tatras, Slovak Republic. *Programme and book of abstracts*. Brno: Tribun EU s.r.o., 2010, str. 66. [COBISS.SI-ID [812202](#)]

7. MILLAKU, Agron, DROBNE, Damjana, TORKAR, Matjaž, JENKO, Monika. Normal and abnormal appearance of digestive gland epithelium surface of porcellio scaber studied by SEM. V: USKOKOVIĆ, Dragan (ur.). Twelfth Annual Conference YUCOMAT 2010, Herceg Novi, Montenegro, September 6-10, 2010. *Programme and the book of abstracts*. Belgrade: Institute of Technical Sciences of the Serbian Academy of Sciences & Arts, 2010, str. 172. [COBISS.SI-ID [825514](#)]

Zahteva za izpis bibliografije je bila poslana z računalnika: 193.2.15.1

Izpis bibliografskih enot: vse bibliografske enote

Izbrani format bibliografske enote: ISO 690

Vir bibliografskih zapisov: Vzajemna baza podatkov COBISS.SI/COBIB.SI, 22. 10. 2010